ZooKeys 710: 1–14 (2017)
doi: 10.3897/zookeys.710.20025
http://zookeys.pensoft.net

RESEARCH ARTICLE

A peer-reviewed open-access journal
ZooKeys
Launched to accelerate biodiversity research

Three new cavernicolous species of the millipede genus *Trichopeltis* Pocock, 1894 from southern China (Diplopoda, Polydesmida, Cryptodesmidae)

Weixin Liu[1], Sergei Golovatch[2], Mingyi Tian[1]

1 *Department of Entomology, College of Agriculture, South China Agricultural University, 483 Wushanlu, Guangzhou 510642, China* **2** *Institute for Problems of Ecology and Evolution, Russian Academy of Sciences, Leninsky pr. 33, Moscow 119071, Russia*

Corresponding authors: *Mingyi Tian* (mytian@scau.edu.cn); *Sergei Golovatch* (sgolovatch@yandex.ru)

Academic editor: *P. Stoev* | Received 4 August 2017 | Accepted 21 September 2017 | Published 19 October 2017

http://zoobank.org/35A124EC-7256-4881-B1D3-DDEE7128018B

Citation: Liu W, Golovatch S, Tian T (2017) Three new cavernicolous species of the millipede genus *Trichopeltis* Pocock, 1894 from southern China (Diplopoda, Polydesmida, Cryptodesmidae). ZooKeys 710: 1–14. https://doi.org/10.3897/zookeys.710.20025

Abstract

Three new species of *Trichopeltis* are described from caves in southern China: *T. bellus* **sp. n.**, *T. intricatus* **sp. n.**, and *T. reflexus* **sp. n.**, all presumed troglobites. The former two come from Yunnan Province, the latter one from Hunan Province. An updated key to all eleven currently known species of *Trichopeltis* is provided.

Keywords

Trichopeltis, new species, key, troglobite, southern China

Introduction

The Cryptodesmidae is a relatively small millipede family that globally encompasses approximately 40 genera and 130 species. It is distributed from Mexico to Argentina in the Americas, occurring also in tropical Africa and tropical to subtropical Asia to Papua New Guinea and Japan in the East (Enghoff et al. 2015). In tropical or subtropical Asia and Australasia, Cryptodesmidae currently comprise only 12 genera (including two that remain dubious) and 36 species.

At present, the Indo-Malayan genus *Trichopeltis* Pocock, 1894 is composed of eight species: *T. bicolor* (Pocock, 1894), the type species from Sumatra, Indonesia; *T. cavernicola* Golovatch, 2016 and *T. muratovi* Golovatch & VandenSpiegel, 2017, both from Laos; *T. doriae* Pocock, 1895 and *T. feae* Pocock, 1895, both from Myanmar; *T. kometis* (Attems, 1938) (= *T. deharvengi* Golovatch, Geoffroy, Mauriès & VandenSpiegel, 2010) from Vietnam, Laos and Cambodia; *T. latellai* Golovatch, Geoffroy, Mauriès & VandenSpiegel, 2010 from Guizhou Province, China; and *T. watsoni* Pocock, 1895 from Myanmar and Darjeeling District, India. *Trichopeltis latellai* is also the only genus and species of Cryptodesmidae reported so far from China (Golovatch and VandenSpiegel 2017).

Rather recently, *Trichopeltis* has been reviewed and a key provided to five of its species (Golovatch et al. 2010, Golovatch and Akkari 2016, and the references therein). The present paper records an additional three new species of *Trichopeltis*, all three of which are presumed to be troglobites from southern China.

Materials and methods

All specimens used in this study were collected by hand from caves in southern China and are preserved in 95% ethanol. The type material is deposited in the zoological collection of the South China Agricultural University, Guangzhou, China (SCAU).

Observations and dissections were performed using a Leica S8 APO stereo microscope. The line drawings were prepared with a Zeiss Imager Axioskop40 microscope and a camera lucida attached for the scope. Photographs were taken with a Canon EOS 40D camera, then focus-stacked with Z-stack software, or Keyence VHX-5000 digital microscope, and further edited using Adobe Photoshop CS5 and Illustrator CC software.

The terminology used here follows that of Golovatch et al. (2012) and Golovatch and VandenSpigel (2017).

Taxonomy

***Trichopeltis bellus* sp. n.**
http://zoobank.org/12B62C80-9542-458B-B5BC-7420F16729CA
Figs 1–3

Type material. Holotype ♂ (SCAU), China, Yunnan Province, Qujing City, Luoping County, Machang Village, Shuiyuan Dong Cave, 24°49'33"N, 104°21'48"E, 1530 m, 18.VI.2015, leg. Mingyi Tian, Weixin Liu, Xinhui Wang & Mingruo Tang.

Paratypes. 2 ♀ juv. (SCAU), same data as the holotype.

Etymology. To emphasize the very pretty appearance of this species; adjective.

Diagnosis. Differs from other species of the genus by the unusually elongate and densely setose gonopodal coxa. Superficially similar to *T. intricatus* sp. n., but distin-

Figure 1. *Trichopeltis bellus* sp. n., ♂ holotype. **A–B** habitus, dorsal and ventral views, respectively.

guished from the latter in the longer tergal setae (Fig. 1A), and gonopodal femorite with a large, club-shaped, mesoventral lobe (Fig. 3). See also Key below.

Description. Length of holotype *ca.* 16 mm, width of midbody pro- and metazonae 1.5 and 4.5 mm, respectively. Coloration in alcohol uniformly light yellow. Adults with 20 segments (Fig. 1). In width, head < collum < segment 2 < 3 < 4 < 5 < 7–16 < 6 (Figs 1A, 2A); following segment 16, body rapidly tapering towards telson (Fig. 1A).

Head: vertex densely pilose and microgranulate, clypeus clearly smooth (Fig. 2B), epicranial suture superficial. Labrum with three teeth. Antennae short and clavate, reaching behind segment 2 when stretched dorsally; in length, antennomere 6 > 3 > 2 > 5 = 4 > 1 > 7 (Fig. 2B).

Collum fan-shaped (Fig. 2A), incompletely covering the head from above, dorsal surface with six irregular transverse rows of small, round, setigerous tubercles (Fig. 2A). Marginal lobules on collum: 13+13 small, microvillose, setigerous, nearly sharp anteriorly and 6+6 similarly small, microvillose, but squarish laterally.

Mid-dorsal regions on segments 2–16 with five more or less regular, transverse rows of similarly small, setigerous tubercles, 6–8 + 6–8 per row (Fig. 2A). The tubercles extending onto paraterga, but each of the latter only with three or four irregular rows of similar tubercles (Fig. 1A). Following metaterga with 6–8 rows of smaller tubercles (Fig. 2E).

Paraterga very strongly developed (Figs 1–2), high, only slightly declivous, but never extending down below level of venter (Fig. 2C), each with 6–8 small, dentiform, lateral and 5–7 much larger, squarish caudolateral lobules, all evident, setigerous and

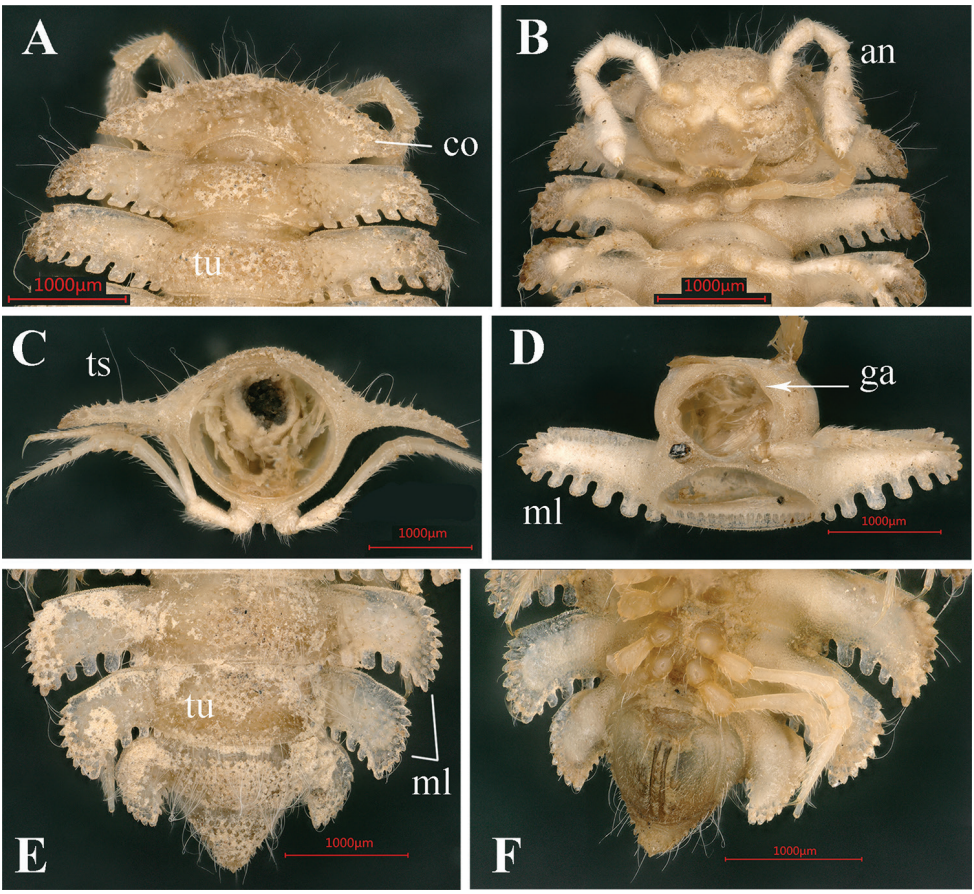

Figure 2. *Trichopeltis bellus* sp. n., ♂ holotype. **A** collum and segments 2–3, dorsal view **B** head and segments 1–4, ventral view **C** cross-section of segment 8, caudal view **D** segment 7, ventral views **E–F** segments 17–19 and telson, dorsal and ventral views, respectively. Abbreviations: an = antenna; co = collum; ga = gonopod aperture; ml = marginal lobules; ts = tergal seta; tu = tubercles.

microvillose (Figs 1–2). Caudolateral lobules on paraterga mostly oblong, relatively large, and well separated from one another (Figs 1–2). Caudolateral corner of paraterga projecting behind rear tergal margin only on segments 17–19 (Fig. 3E–F).

Integument clearly microgranulate throughout (Fig. 1A), prozonae finely alveolated. Limbus regularly crenulated. Stricture between pro- and metazonae broad, shallow and finely microgranulated. Tergal setae simple, very long and subfiliform (Fig. 1A). Ozopores invisible, pore formula untraceable.

Epiproct tip sharp, with four spinnerets apically (Fig. 2F). Hypoproct subtrapeziform, 1+1 caudal setigerous papillae clearly separated (Fig. 2F).

Pleurosternal carinae clearly present on segment 2 alone. Sterna modestly setose, cross-impressions moderate, clearly broadened between ♂ coxae 6, 7 and 9 (Figs 1B, 2D). Gonopod aperture rhomboid (Figs 1B, 2D).

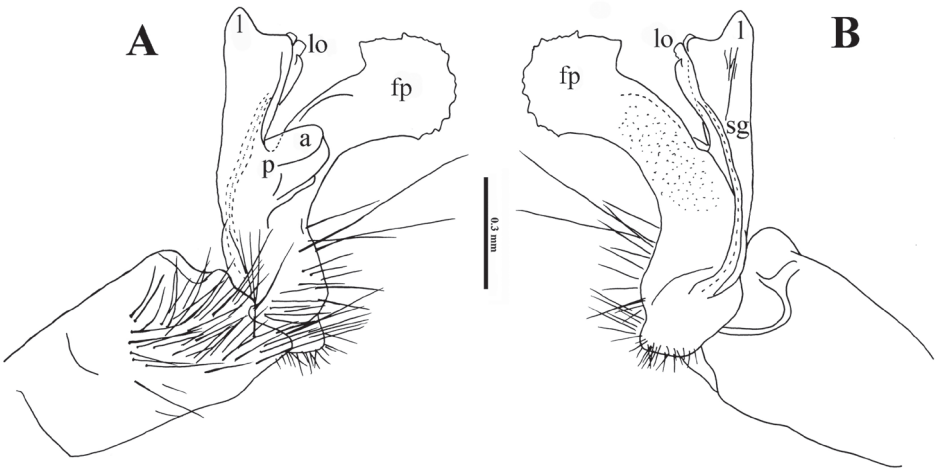

Figure 3. *Trichopeltis bellus* sp. n., ♂ holotype. **A–B** right gonopod, lateral and mesal views, respectively. Abbreviations: a = lobe on acropodital process; fp = femoral process; l = apical lobe; lo = lobules; p = acropodital process; sg = seminal groove.

Legs very long and slender, unmodified, produced beyond paratergal lateral margin (Figs 1B, 2C), about 1.8 times as long as midbody height.

Gonopods (Fig. 3) complex. Coxa subcylindrical, unusually long, and very densely setose on lateral side. Prefemora densely setose, with a few particularly long setae. Femorite composed of extremely strong mesoventral process (**fp**), the latter about as long as telopodite, slightly curved, club-shaped. Acropodite suberect, laterally with a smaller, parabasal, rounded process (**p**) supporting a still smaller lobe (**a**) apically. Acropodite with one evident apical lobe (**l**) and a few very small subapical lobules (**lo**). Seminal groove (**sg**) entirely mesal, terminating without pulvillus at **lo**, forming no distinct solenomere.

Remark. Based on the unpigmented body and long legs, this species is probably a troglobite.

***Trichopeltis intricatus* sp. n.**
http://zoobank.org/2CFBA46B-60D9-4798-B8A2-5C373BA620EF
Figs 4–6

Type material. Holotype ♂ (SCAU), China, Yunnan Province, Kunming City, Shilin County, Guishan Town, Haiyi I Dong Cave, 24°38'50"N, 103°32'49"E, 1890 m, 16.VI.2015, leg. Mingyi Tian, Weixin Liu, Xinhui Wang & Mingruo Tang.

Etymology. To emphasize the complex gonopods; adjective.

Diagnosis. Differs from all congeners except *T. bellus* sp. n. by the unusually densely setose gonopodal coxa, and from all species by the particularly complex gonopod which shows a number of peculiar processes and lobules (Fig. 4). See also the Key below.

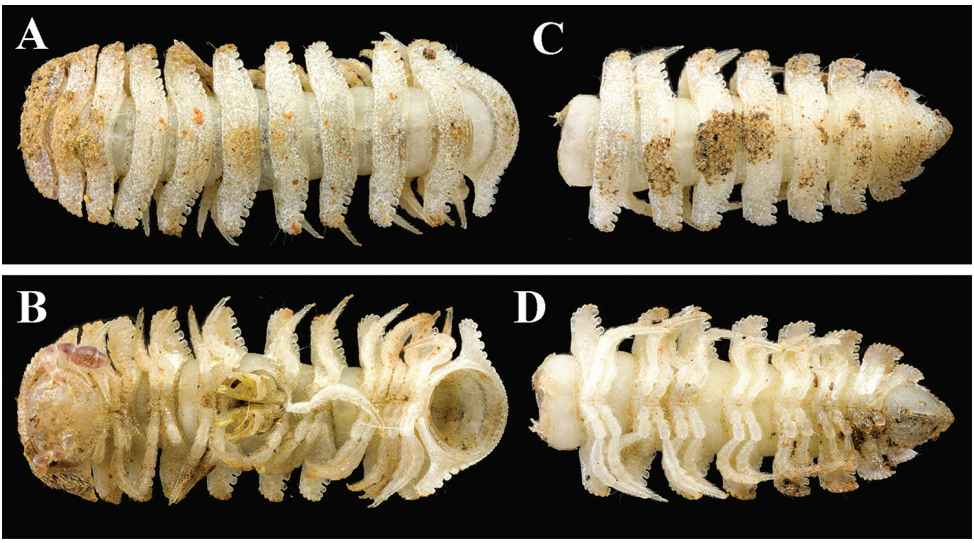

Figure 4. *Trichopeltis intricatus* sp. n., ♂ holotype. **A–B** anterior part of body **C–D** posterior part of body, dorsal and ventral views, respectively.

Description. Length of holotype *ca.* 10 mm, width of midbody pro- and metazonae 1.5 and 2.5 mm, respectively. Coloration in alcohol nearly pallid. Body with 20 segments (Fig. 4). All characters as in the previous species (Figs 1–3), except as follows. In width, head < collum < segment 2 < 3–4 < 5 < 6 < 7; thereafter body increasingly tapered towards telson (Fig. 4).

Head sparsely pilose. Antennae very short and clavate, reaching behind segment 2 when stretched dorsally; in length, antennomere 6 > 3 > 4 = 5 = 2 = 7 = 1 (Fig. 5B).

Collum fan-shaped, inverted subtrapeziform, incompletely covering the head from above, with five irregular transverse rows of small, round, setigerous tubercles (Fig. 5A). Marginal lobules on collum: 15+15 small, microvillose, nearly sharp anteriorly and 6+6 similarly small, but squarish laterally.

Mid-dorsal regions on segments 2–16 with five regular, transverse rows of about 15+15 similarly small, setigerous tubercles extending onto paraterga, in frontal and caudal rows smaller than others (Fig. 4A & C).

Paraterga 3–5 with 4–5 small, dentiform, lateral and 5–6 much larger, squarish, caudal lobules. Similarly, paraterga 2 and 6–16 with 6 lateral, 6–7 caudal lobules.

Tergal setae simple, very short and mostly abraded (Fig. 4A & C).

Epiproct short, conical (Fig. 5D).

Gonopod aperture subcordiform (Figs 4B, 5D).

Legs short and robust (Figs 4–5), produced beyond paratergal lateral margin, about 1.2 times as long as midbody height.

Gonopods (Fig. 6) very complex. Coxa short and squarish, but unusually densely setose laterally, much like in the previous species. Prefemora densely setose, but with more numerous longer setae. Femorite only slightly curved caudally at base with a

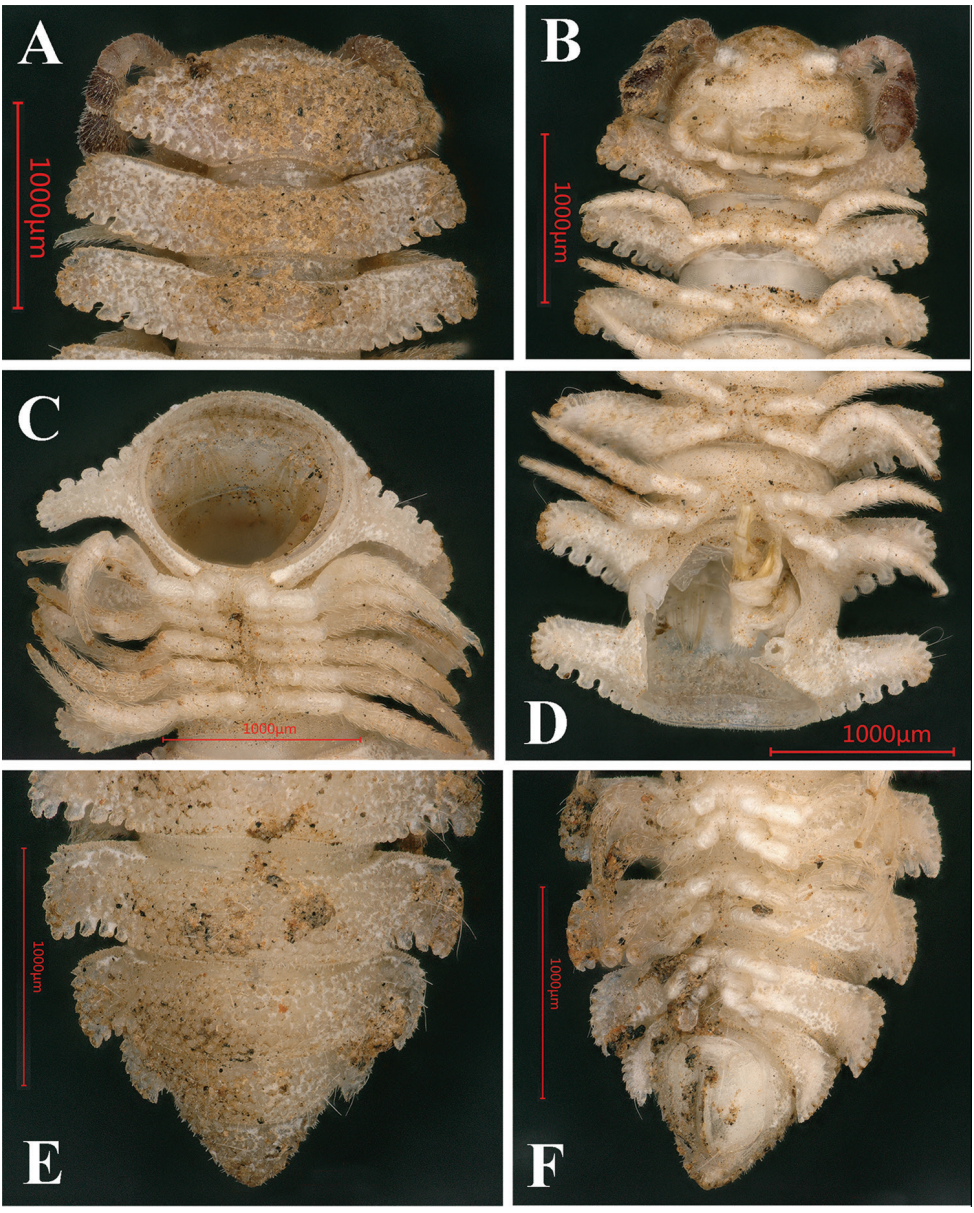

Figure 5. *Trichopeltis intricatus* sp. n., ♂ holotype. **A** collum and segments 2–3, dorsal view **B** head and segments 1–4, ventral view **C** cross-section of segment 10, caudal view **D** segment 5–7, ventral views **E–F** segments 16–19 and telson, dorsal and ventral views, respectively.

clearly tripartite femoral process (**p**), branches **p1** (mesal) and **p2** (lateral) being subequal, long and rounded at end, branch **p3** being basalmost slender and acuminate at end. Acropodite longer than **p**, at base with a long, slender, apically mushroom-shaped lobe (**m**) on lateral side, and an even longer, slender, finger-shaped, mesal,

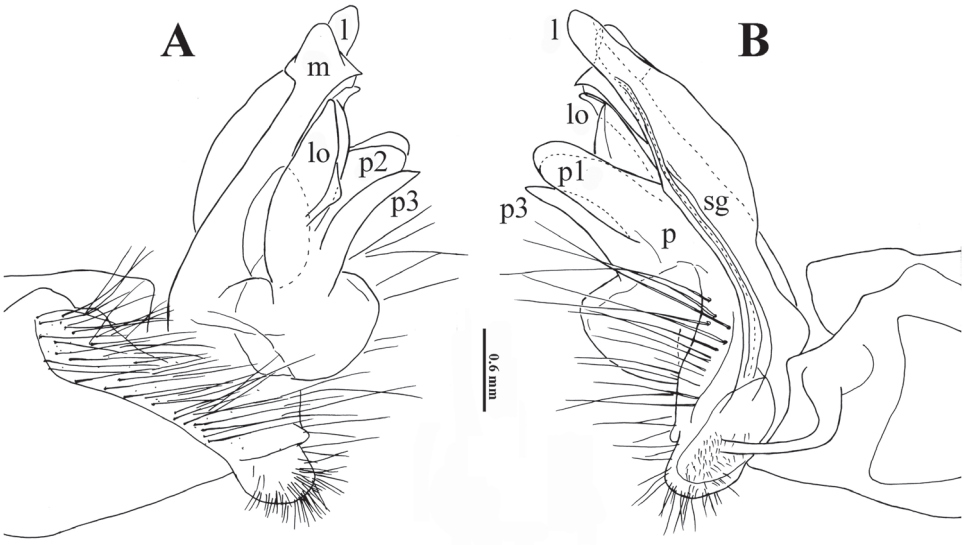

Figure 6. *Trichopeltis intricatus* sp. n., ♂ holotype. **A–B** right gonopod, lateral and mesal views, respectively. Abbreviations: l = apical lobe; lo = lobules; m = mushroom-shaped lobe; p = acropodital process; p1–3 = processes 1–3; sg = seminal groove.

apical lobe (**l**), as well as a group of lobules (**lo**) between **p** and **m**. Seminal groove (**sg**) entirely mesal, terminating without pulvillus near **lo**, forming no distinct solenomere.

Remark. Based on the pallid body, this species may be a troglobite.

Trichopeltis reflexus sp. n.

http://zoobank.org/63B2C168-31B7-4631-AD90-304AD18105B0
Figs 7–9

Type material. Holotype ♂ (SCAU), China, Hunan Province, Chenzhou City, Linwu County, Xianghualing Town, II Dong Cave, 19.VI.2009, leg. Mingyi Tian & Zhihong Xue (CHIhn09-LWX03).

Paratypes. 1 ♂, 3 ♀ (SCAU), same data as the holotype.

Etymology. To emphasize that most of the paraterga are upturned.

Diagnosis. Differs from all congeners except *T. cavernicola* Golovatch, 2016 by the clearly upturned paraterga, and from all congeners by the shapes of the various lobes which are all confined to the distal third of the gonopodal telopodite. Among congeners, only *T. latellai* Golovatch, Geoffroy, Mauriès & VandenSpiegel, 2010, from two caves in Guizhou Province (Golovatch et al. 2010) strongly resembles *T. reflexus* sp. n. in showing a similarly condensed apical third of the gonopodal telopodite, but that in the latter species is less strongly curved, untwisted and more elaborate. See also Key below.

Description. Length of both sexes *ca.* 10 mm, width of midbody pro- and metazonae 0.8 and 2.5 (♂) or 1.0 and 2.5 mm (♀), respectively. Coloration in alcohol nearly

Figure 7. *Trichopeltis reflexus* sp. n., ♂ paratype. **A–B** habitus, dorsal and ventral views, respectively.

pallid. Body with 20 segments (Fig. 7). All characters as in *T. bellus* sp. n. (Figs 1–3), except as follows. In width, head < collum < segment 2 < 4 < 3 = 5 < 6–15; thereafter body increasingly tapered towards telson (Fig. 7).

Collum with 3–4 irregular transverse rows of small and sharpened tubercles. Marginal lobules on collum: 13+13 small, setigerous, nearly sharp anteriorly and 3+3 similarly small, dentiform laterally (Fig. 8A–B).

Mid-dorsal regions on segments 2–16 with two regular, transverse rows of 3+3 and 4+4 tubercles similar to those on collum (Fig. 8A–B), extending onto paraterga, the latter with 2–3 similar tubercles; following metaterga with three rows of 3+3, 2+2 and 3+3 tubercles (Figs 7A, 8E–F). Caudal margin of mid-dorsal region of metaterga with 12–16 lobules (Fig. 8A–B, E).

Paraterga very strongly developed (Figs 7–8), lateral margin narrow and upturned, but still remaining below a regularly convex dorsum (Fig. 8D). Paraterga with 3–4 lateral and 4–6 caudal lobules (Figs 7–8).

Tergal setae simple and short, mostly abraded (Fig. 7A).

Epiproct short, conical (Fig. 8F).

Pleurosternal carinae poorly-developed, but present on segments 2 and 3.

Sterna clearly broadened only between ♂ coxae 9. Gonopod aperture suboval (Fig. 8C).

Legs short, but slender, about 1.2 times as long as midbody height (Figs 7–8).

Gonopods (Fig. 9) complex only in apical third of telopodite. Coxa as usual, short and squarish, with one long seta. Prefemoral part as usual, with only a few particularly

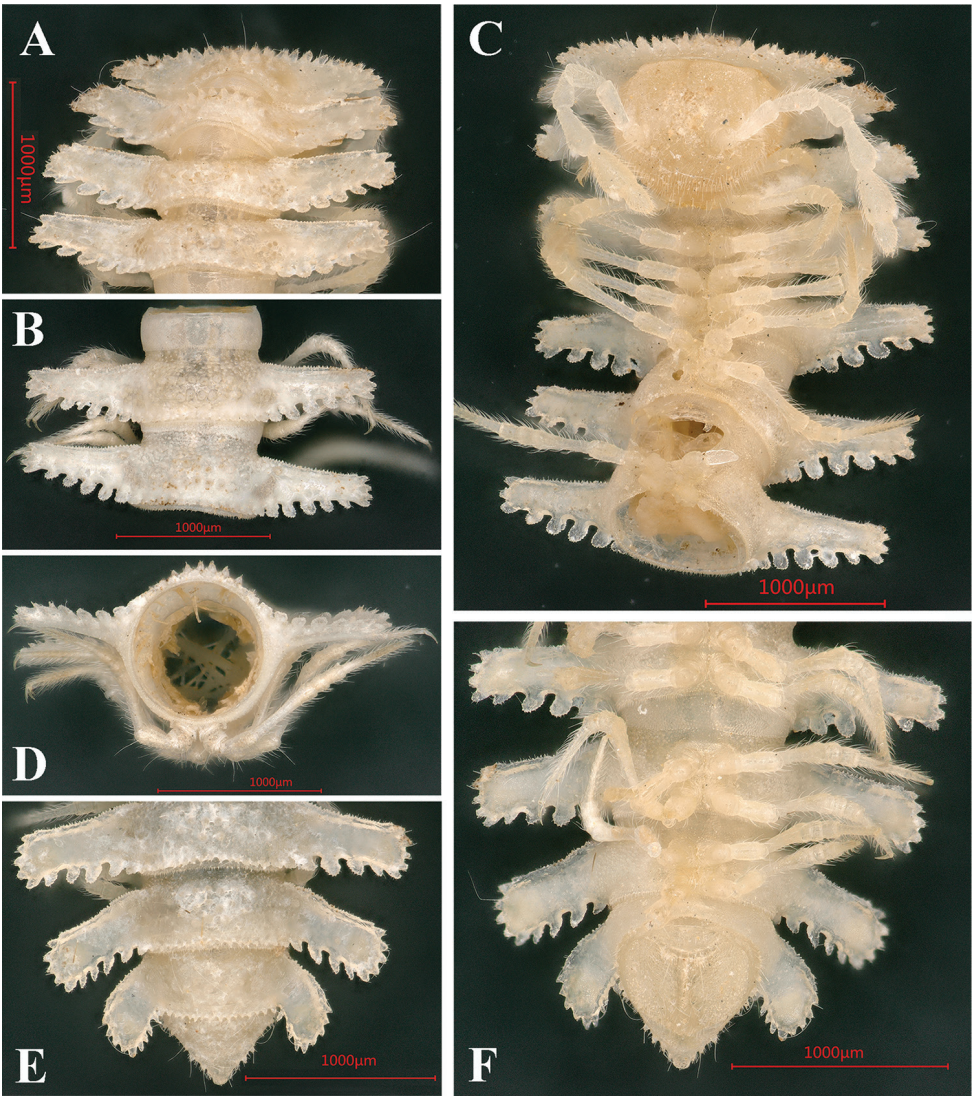

Figure 8. *Trichopeltis reflexus* sp. n., ♂ paratype. **A** collum, segments 2–4, dorsal view **B** segments 8–9, dorsal view **C** head and segments 1–7, ventral view **D** cross-section of segment 9, caudal view **E–F** segments 17 or 16–19 and telson, dorsal and ventral views, respectively.

long setae distally. Telopodite slightly curved caudally, without femoral processes at base. Acropodite strongly condensed, tripartite, with a large, subtriangular, more basal lobe (**b**) and a short, squarish, more distal lobe (**d**), both similar in size and lying on lateral side; caudal to both **b** and **d** with a few differently shaped lobules (**lo**); apical lobe (**l**) highest, acuminate, folded. Seminal groove (**sg**) entirely mesal, terminating without pulvillus near **lo**, forming no distinct solenomere.

Remark. Based on the pallid body and slender legs, this seems to be a troglobite.

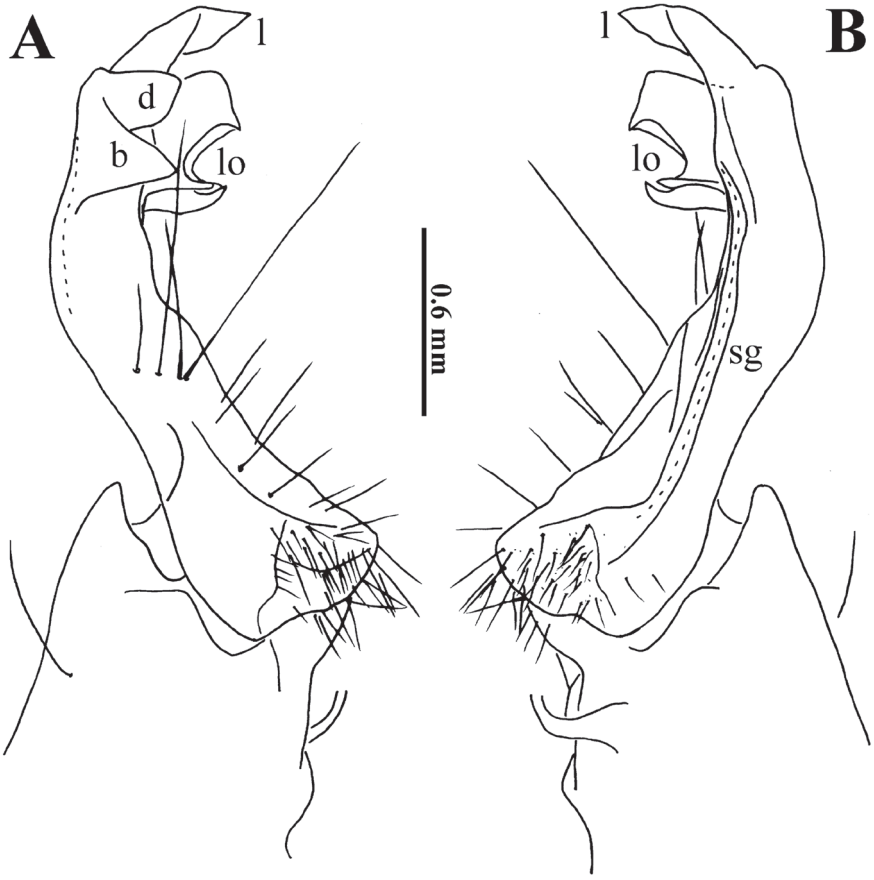

Figure 9. *Trichopeltis reflexus* sp. n., ♂ paratype. **A–B** right gonopod, lateral and mesal views, respectively. Abbreviations: b = acropodite basal lobe; d = acropodite distal lobe; l = apical lobe; lo = lobules; sg = seminal groove.

Key to species of *Trichopeltis*

(modified after Golovatch et al. 2010 to incorporate all five species described since the latest synopsis)

1 Tegument unpigmented, pallid to light yellowish; cavernicolous species **2**
– Tegument clearly pigmented, red- or grey-brown to blackish; epigean species **6**
2 Central parts of metaterga with 2–4 irregular transverse rows of setigerous tubercles; gonopodal coxa as usual, at most with only few setae **3**
– Central parts of metaterga with 5–6 irregular transverse rows of setigerous tubercles; gonopodal coxa unusually densely setose on lateral side (Figs 3, 6); Yunnan, China **5**

3 Paraterga declivous; tergal setae very long, about half as long as body diameter; gonopodal telopodite clearly twisted; Guizhou, China ..... ***T. latellai***
– Paraterga clearly upturned; tergal setae much shorter; gonopodal telopodite untwisted, seminal groove running entirely on mesal side **4**
4 Central parts of metaterga with 3–4 irregular transverse rows of setigerous tubercles; gonopodal telopodite with a pulvillus subapically; Laos..... ***T. cavernicola***
– Central parts of metaterga with 2–3 rather regular transverse rows of setigerous tubercles (Fig. 7A); gonopodal telopodite without pulvillus (Fig. 9); Hunan, China ..... ***T. reflexus* sp. n.**
5 Tergal setae very long (Figs 1–2); gonopods relatively simple (Fig. 3)..... ..... ***T. bellus* sp. n.**
– Tergal setae very short (Figs 4–5); gonopods especially elaborate..... ..... ***T. intricatus* sp. n.**
6 Central parts of metaterga with 4–6 irregular transverse rows of setigerous tubercles **7**
– Central parts of metaterga with 2–3 irregular transverse rows of setigerous tubercles **10**
7 Gonopodal telopodite clearly 3-branched, solenomere long and slender; Myanmar ..... ***T. doriae***
– Gonopodal telopodite without long branches, only more or less deeply notched apically; solenomere rudimentary, barely visible **8**
8 Central parts of metaterga with 4–5 rather regular transverse rows of setigerous tubercles; gonopodal telopodite with a conspicuous accessory seminal chamber and a pulvillus, but devoid of denticles laterally or mesally; Laos .... ***T. muratovi***
– Central parts of metaterga with 5–6 rather regular transverse rows of setigerous tubercles; gonopodal telopodite without accessory seminal chamber, but with a pulvillus, also abundantly denticulate either laterally or mesally **9**
9 Body *ca.* 12 mm long and 3.0 mm wide; gonopodal telopodite abundantly denticulate on lateral face. Vietnam, Laos and Cambodia and possibly endemic to the Indochina Peninsula..... ***T. kometis***
– Body *ca.* 16 mm long and 4.8 mm wide; gonopodal telopodite abundantly denticulate on mesal face. Sumatra, Indonesia ..... ***T. bicolor***
10 Frontal margin of paraterga abundantly lobulated. Solenomere lobe-shaped, tip nearly pointed ..... ***T. feae***
– Frontal margin of paraterga entire, not lobulated. Solenomere axe-shaped, tip pointed ..... ***T. watsoni***

Conclusions and discussion

The family Cryptodesmidae was hitherto known to encompass three presumed troglobiont species: *Peridontodesmella alba* Schubart, 1957, from Brazil (Trajano et al. 2000);

Trichopeltis latellai, from two caves in Guizhou, China (Golovatch et al. 2010); and *T. cavernicola*, from two caves in Laos (Golovatch 2016, Golovatch and VandenSpiegel 2017). The three new species described above show clear traits of troglomorphism, thereby considerably increasing the number of presumably troglobiont cryptodesmids known globally.

Almost all of southern China is blanketed by Earth's most extensive karsts (Deharveng and Bedos 2012). Some of them are known to be especially rich in biodiversity, while the Mulun and surrounding karsts in Guangxi Province host some of the richest cave fauna of China (Deharveng et al. 2008). This fauna encompasses millipedes as well (Golovatch 2015).

At present, most of the species of *Trichopeltis*, including both epigean and cavernicolous taxa, occur in Indo-Burma and Indochina. With the description of the above three new taxa, and with further explorations of southern China karst region, the southern part of the country will certainly become an important hotspot of *Trichopeltis* diversity. Due to a rapid discovery of new species, the previous key (Golovatch et al. 2010), which is only a few years old, is already out of date. The same is likely to occur with the new key provided above, as there is little doubt that new taxa will be found in the near future at least in southern China.

Acknowledgements

We are particularly grateful to the caving team of the South China Agricultural University, Guangzhou, China, for their assistance in the field. We also thank three reviewers and the academic editor Dr. Pavel Stoev for their corrections and useful suggestions that improved our manuscript. This study was sponsored by the Specialized Research Fund for the Doctoral Program of Higher Education of China (Grant no. 20134404110026).

References

Deharveng L, Bedos A (2012) Diversity patterns in the tropics. In: White WB, Culver DC (Eds) Encyclopedia of Caves. Academic Press, Chennai, 238–250. https://doi.org/10.1016/B978-0-12-383832-2.00032-3

Deharveng L, Bréhier F, Bedos A, Tian MY, Li YB, Zhang F, Qin WG, Tan XF (2008) Mulun and surrounding karsts (Guangxi) host the richest cave fauna of China. Subterranean Biology 6: 75–79.

Enghoff H, Golovatch SI, Short M, Stoev O, Wesener T (2015) Diplopoda – taxonomic overview. In: Minelli A (Ed.) Treatise on Zoology – Anatomy, Taxonomy, Biology. The Myriapoda 2(16): 363–453. https://doi.org/10.1163/9789004188273_017

Golovatch SI (2015) Cave Diplopoda of southern China with reference to millipede diversity in Southeast Asia. ZooKeys 510: 79–94. https://doi.org/10.3897/zookeys.510.8640

Golovatch SI (2016) The millipede family Cryptodesmidae in Indochina (Diplopoda, Polydesmida). ZooKeys 578: 33–43. https://doi.org/10.3897/zookeys.578.7994

Golovatch SI, Akkari N (2016) Identity of the millipede, *Pseudoniponiella kometis* (Attems, 1938) (Diplopoda: Polydesmida: Cryptodesmidae). Tropical Natural History 16(1): 1–6.

Golovatch SI, VandenSpiegel D (2017) One new and two little-known species of the millipede family Cryptodesmidae from Indochina (Diplopoda, Polydesmida). Zoologicheskii zhurnal 96(7): 757–767.

Golovatch SI, Geoffroy JJ, Mauriès JP, VandenSpiegel D (2010) Two new species of the millipede genus *Trichopeltis* Pocock, 1894 (Diplopoda: Polydesmida: Cryptodesmidae) from Vietnam and China. Arthropoda Selecta 19(2): 63–72.

Trajano E, Golovatch SI, Geoffroy JJ, PintodaRocha R, Fontanetti CS (2000) Synopsis of Brazilian cavedwelling millipedes (Diplopoda). Papéis Avulsos de Zoologia 41(18): 259–287.

ZooKeys 710: 15–32 (2017)
doi: 10.3897/zookeys.710.13941
http://zookeys.pensoft.net

RESEARCH ARTICLE

A peer-reviewed open-access journal
ZooKeys
Launched to accelerate biodiversity research

A new species of *Mongolodiaptomus* Kiefer, 1938 from northeast Thailand and a key to the species (Crustacea, Copepoda, Calanoida, Diaptomidae)

Santi Watiroyram[1], La-orsri Sanoamuang[2,3]

1 *Division of Biology, Faculty of Science, Nakhon Phanom University, Nakhon Phanom 48000, Thailand* **2** *Applied Taxonomic Research Center, Khon Kaen University, Khon Kaen 40002, Thailand* **3** *International College, Khon Kaen University, Khon Kaen 40002, Thailand*

Corresponding author: *Santi Watiroyram* (santi.watiroyram@npu.ac.th)

Academic editor: *D. Defaye* | Received 2 June 2017 | Accepted 20 September 2017 | Published 19 October 2017

http://zoobank.org/45F4587D-5F74-40A0-A7D7-8A89394506C7

Citation: Watiroyram S, Sanoamuang L (2017) A new species of *Mongolodiaptomus* Kiefer, 1938 from northeast Thailand and a key to the species (Crustacea, Copepoda, Calanoida, Diaptomidae). ZooKeys 710: 15–32. https://doi.org/10.3897/zookeys.710.13941

Abstract

This study describes the new species *Mongolodiaptomus loeiensis* **sp. n.** collected from a temporary pond nearby a cave located in Loei Province, in northeastern Thailand. *Mongolodiaptomus loeiensis* **sp. n.** is similar to *M. calcarus* (Shen & Tai, 1965) in the male but can be distinguished from its congeners by the following unique characteristics in the males: (1) the right caudal ramus has 3 ventral chitinous prominences; (2) intercoxal plate of P5 is produced into 2 spine-like lobes on distal margin; (3) the basis of right P5 has a subglobular chitinous prominence on mid-distal caudal surface; and (4) the principal lateral spine on the right Exp-2 P5 is extremely bent at its tip. The occurrence of diaptomid copepods in the study area is discussed and an identification key to worldwide species of the genus *Mongolodiaptomus* Kiefer, 1938 is presented herein.

Keywords

Copepoda, Diaptomidae, Loei Province, new record, rare species, southeast Asia, taxonomy

Introduction

The freshwater calanoid copepods have been intensively studied in Thailand especially in northeast Thailand. However, their study in the Loei Province in the upper northeast region has so far been largely neglected. According to Sanoamuang (2002), only three diaptomid species were previously recorded in Loei Province, namely *Mongolodiaptomus botulifer* (Kiefer, 1974), *M. calcarus* (Shen & Tai, 1965), and *Phyllodiaptomus praedictus* (Dumont & Reddy, 1994). During the years 2014–2016, the first author had led sampling surveys on planktonic and cave-dwelling copepods in the upper northeastern region in order to fill the gap of copepod richness and distribution in this region (Watiroyram et al. 2015, 2017). As results of this study, *Mongolodiaptomus loeiensis* sp. n. and other diaptomids were discovered in water bodies outside the caves.

The genus *Mongolodiaptomus* Kiefer, 1938 was defined by Kiefer (1938) by several characters, especially in the male fifth leg. Nevertheless, some of these characters are not useful for separating the species because they are shared by certain species of *Allodiaptomus* Kiefer, 1936 and *Neodiaptomus* Kiefer, 1932. After the revision of Reddy et al. (2000), the solution on diagnosis of problematic species was well defined on generic characters. Based on this revision, *Mongolodiaptomus* is characterized by the second exopod of the right male P5 having 3 spines and processes on its outer margin; one principal spine somewhat on middle of segment, and 1–2 spinous processes proximally or/and distally. As a result, nine species of *Allodiaptomus, Diaptomus* and *Neodiaptomus* were transferred into the genus *Mongolodiaptomus*; namely *M. birulai* (Rylov, 1922), *M. botulifer*, *M. calcarus*, *M. gladiolus* (Shen & Lee, 1963), *M. malaindosinensis* (Lai & Fernando, 1978), *M. mephistopheles* (Brehm, 1933), *M. pectinidactylus* (Shen & Tai, 1964), *M. rarus* (Reddy, Sanoamuang & Dumont, 1998), *M. uenoi* (Kikuchi, 1936) (for more details see Kiefer 1939; Reddy et al. 1998, 2000; Sanoamuang 1999, 2002; Luong et al. 2016).

To date, 37 diaptomid species are known from inland waters of Thailand (Sanoamuang 2002). Of these, seven species belong to the genus *Mongolodiaptomus*: *M. malaindosinensis*, *M. botulifer*, *M. calcarus*, *M. dumonti* Sanoamuang, 2001, *M. pectinidactylus*, *M. rarus,* and *M. uenoi*. *Mongolodiaptomus loeiensis* sp. n., the eighth species from Thailand, is illustrated and described herein together with a dichotomous key to the worldwide species of the genus *Mongolodiaptomus*. Additionally, the geographical distribution of the recorded diaptomids in Loei Province is briefly discussed.

Material and methods

Samples were collected using a plankton net with a mesh size of 60 μm. The copepod samples were transferred into 120 ml plastic bottles and preserved in 70% ethanol. In the laboratory, samples were selected for individual adults and placed in a mixture of glycerol and 70% ethanol (ratio ~ 1:10 v/v) under a stereomicroscope at 40× magnification.

Specimens were transferred to pure glycerol and dissected at 40–100-× magnification under an Olympus SZ51 stereomicroscope.

All appendages and body ornamentation were examined at1000-× magnification. All the drawings were made at the same magnification (1000-×), with a drawing tube mounted on an Olympus compound microscope (CX31). The final versions of the drawings were made using the CORELDRAW® 12.0 graphic program. For permanent slides, all body parts were put in a drop of glycerol on a microscope slide, covered by a cover glass, and sealed with nail polish.

Specimens for a scanning electron microscopy (SEM) were dehydrated in an ethanol series (50%, 70%, 80%, 90%, 95%, 100%, and 100%) for 15 min each concentration. After dehydration, specimens were dried in a critical point dryer using liquid carbon dioxide as the exchange medium. Dried specimens were mounted on stubs using adhesive tape under a stereomicroscope. Then, specimens were coated with gold in a sputter-coater. The SEM photographs were carried out using a scanning electron microscope (FEI Helios NanoLab G3 CX).

The following abbreviations are used throughout the text and figures

Enp	endopod;
Exp	exopod;
Exp/Enp-n	exopodal segment n/endopodal segment n;
P1–P5	swimming legs 1–5.

The nomenclature and descriptive terminology follow Huys and Boxshall (1991), including analysis of caudal setae (I–VII). Specimens were deposited at the Natural History Museum, London, United Kingdom (**NHMUK**) and at the Nakhon Phanom University, Faculty of Science, Thailand (**NPU**).

Taxonomic section

Order Calanoida Sars, 1903
Family Diaptomidae Baird, 1850
Genus *Mongolodiaptomus* Kiefer, 1938

***Mongolodiaptomus loeiensis* sp. n.**
http://zoobank.org/898BBF26-8F13-40B3-8A3F-EC36579FA3B1
Figs 1–7

Type locality. A temporary pond nearby the Prakaipetch Cave, Nadokkham Subdistrict, Na Duang District, Loei Province, northeastern Thailand; 17°54'23"N, 101°54'23"E; altitude: 420 m above sea level.

Holotype. One adult male, NHMUK 2017.134, dissected and mounted in glycerol on one slide: collected on 5 August 2015 by S. Watiroyram.

Allotype. One adult female, NHMUK 2017.135, dissected and mounted in glycerol on one slide: collected on same date by the same collector.

Paratypes. Ten adult females and males, NHMUK 2017.136–145, undissected and preserved in 70% ethanol in 1.5 ml microtube; 10 adult females and males, NPU 2017–001, undissected and preserved in 70% ethanol in 1.5 ml microtube: collected on same date by the same collector.

Differential diagnosis. The right P5 Exp-2 of male in *Mongolodiaptomus loeiensis* sp. n. with principal spine slightly posterior to mid-outer margin and one spinous process each proximally and distally, fits the diagnostic features of the genus *Mongolodiaptomus* sensu Reddy et al. (2000).

The male of new species is most similar to *M. calcarus* by the segment 20 of right antennule with serrated spine, and the armature of P5: on right P5 (1) the presence of strong and stout coxal spine, (2) Exp-2 with similar shape and size, and (3) Exp-2 with strong and bent principal lateral spine; on left P5 (1) basis with long and narrow hyaline membrane on inner margin, and (2) Exp-2 with row of strong spinules on inner margin at distal half of segment. However, *M. loeiensis* sp. n. differs from *M. calcarus* by following morphological characters: (1) the new species with three chitinous processes on ventral surface of the right caudal ramus while *M. calcarus* with only two chitinous processes, (2) intercoxal plate of the new species with outgrowth process into two-spine like lobes at distal margin while *M. calcarus* without any outgrowth process, (3) basis of right P5 in the new species with inner hyaline membrane and with sub-globular chitinous process on caudal surface while *M. calcarus* without hyaline membrane, and with spur-like chitinous process, (4) the new species with long and slender end claw while it is typical short and robust in *M. calcarus*. Additional differences occur in female characteristics as follows: (1) the genital somite of *M. loeiensis* sp. n. with bulges on proximal, sub-middle, and middle region at right margin while *M. calcarus* is slightly convex on those region, (2) the right side of genital somite with spine located on outgrowth process in *M. loeiensis* sp. n. but it is directly inserted on somite in *M. calcarus*, (3) the left side of genital somite with slightly proximal dilated and spine inserted on small prominence while *M. calcarus* with obviously proximal rounded lobe and spine directly inserted on its segment.

Description of adult female. Body length (Fig. 1A), measured from anterior margin of rostrum to posterior margin of caudal rami, 1.0–1.3 mm. Rostral spines (Figs 1B, 4B) with two teeth-like process in anterior margin. Prosome (Fig. 1A) ovoid, with cephalosome and 5 pedigers; pediger 4 and 5 fused, partly separated at lateral side. Pediger 5 (Figs 1C, 4A) with symmetrical postero-lateral wings, reaching proximal part of genital somite; each wing with one inner and one posterior spine on posterolateral margins (former spine smaller than later one). Urosome (Fig. 1A, D) consisting of 3-somites including genital somite, urosomite 2 and anal somite, approximately 1/2 as long as prosome. Genital somite (Figs 1C–F, 4A) exceeding in length urosomite 2, anal somite and caudal ramus combined. Right side: with dilated laterally in three

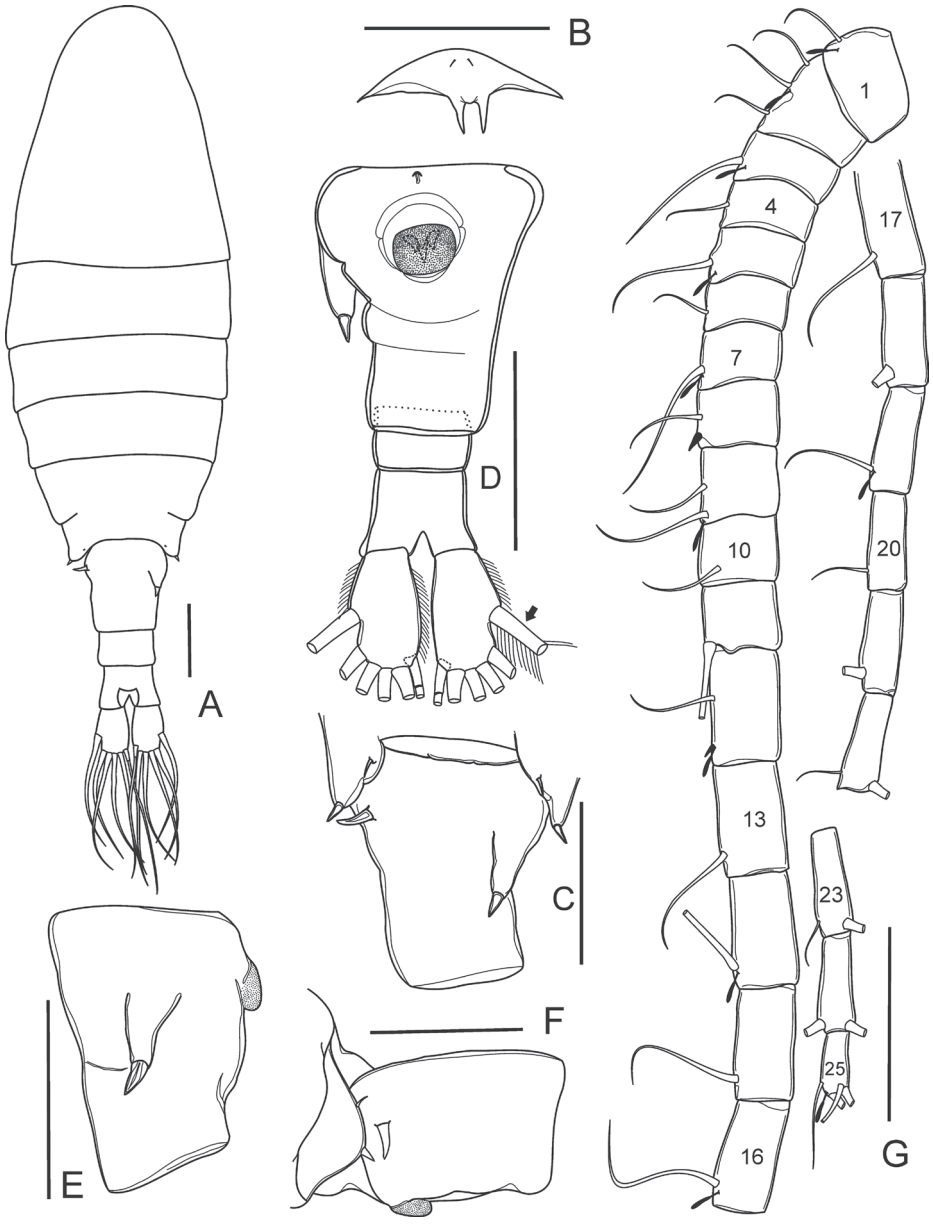

Figure 1. *Mongolodiaptomus loeiensis* sp. n. Female: **A** habitus, dorsal view **B** rostrum, frontal view **C** lateral wings on pediger 5 and genital somite, dorsal view **D** urosome, ventral view (black arrow points to smooth region of lateral seta) **E** genital somite, lateral view **F** lateral wing on pediger 5 and genital somite, lateral view **G** antennule. Scale bar 100 μm.

regions on proximal half of segment length; with postero-laterally directed outgrowth (sub-conical process), extended beyond half of somite; with a short and blunt posterior spine on respective outgrowth. Left side: with regular margin, with a spine on

dorso-lateral surface at proximal part, larger and sharper than the right spine. A pair of gonopores located beneath a genital operculum on mid-ventrally proximal part. Urosomite 2 symmetrical, shorter than latter somite. Anal somite (Figs 1A, D, 4C) slightly expanded at distal end, almost as long as caudal rami; anal operculum small and slightly concave on its posterior margin.

Caudal rami (Figs 1D, 4C) symmetrical, each ramus slightly expanded on distal end, about 1.6 times as long as wide; with a row of setules along inner and outer margins. Each ramus with six setae (seta II–VII): lateral (II) seta with smooth region on proximally outer margin; dorsal seta (VII) proximally jointed, bare, and longest.

Antennule (Fig. 1G) symmetrical, 25-segmented, reaching beyond the end of caudal setae. Setal formula starting from the first to the last segment (a = aesthetasc, s = spine): 1+a, 3+a, 1+a, 1, 1+a, 1, 1+a, 1+s, 2+a, 1, 1, 1+a+s, 1, 1+a, 1, 1+a, 1, 1, 1+a, 1, 1, 2, 2, 2, 4+a.

Antenna (Fig. 2A) 11-segmented. Coxa with one seta on distal corner. Basis with two inner setae on distal corner. Exp-1–6 with 1, 3, 1, 1, 1, and 1 inner seta, respectively. Exp-7 with one inner and three apical setae. Enp-1 with two inner setae. Enp-2 with nine inner and seven apical setae.

Mandible (Fig. 2B) with four strongly chitinized teeth and a single seta on gnathobase. Basis with four inner setae. Enp 2-segmented: Enp-1 with four inner setae, Enp-2 with nine apical setae plus tiny spinules along outer margin. Exp 4-segmented, with 1, 1, 1, and 3 setae, respectively.

Maxillule (Fig. 2C) with seven spines and six setae on praecoxal arthrite. Coxal endite and coxal epipodite with three and nine setae, respectively. Proximal and distal endites each with four setae; basal exite with one seta. Enp reduced, represented by eight apical setae. Exp with six setae plus a row of setules on median margin.

Maxilla (Fig. 2D) with three setae on proximal praecoxal and coxal endites, and distal praecoxal and coxal endites. Allobasis with three setae. Enp reduced to two segmented, each with three setae.

Maxilliped (Fig. 2E) with four endites on syncoxa: 1, 2, 3, 3 setae inserted on respective endites; endite 4 with tiny spinules on distal corner. Basis with three setae, ornamented with spinules on proximal half of segment. Enp 6-segmented, with 2, 3, 2, 2, 2, and 4 setae, respectively.

P1–P4 (Figs 3A–D), biramous, Exp longer than Enp. P1 with 3-segmented Exp and 2-segmented Enp, P2–P4 with 3-segmented Exp and Enp. Exp and Enp with longitudinal setules on inner and outer margin, respectively. Armature formula of P1–P4 as follows (legend: outer-inner seta/spine; outer-apical-inner; Arabic numerals represent setae, Roman numerals represent spines):

	Coxa	Basis	Exopod			Endopod		
			1	2	3	1	2	3
P1	0-1	0-0	I-1	0-1	I-3-2	0-1	1-2-3	----
P2	0-1	0-0	I-1	I-1	I-3-3	0-1	0-2	2-2-3
P3	0-1	0-0	I-1	I-1	I-3-3	0-1	0-2	2-2-3
P4	0-1	1-0	I-1	I-1	I-3-3	0-1	0-2	2-2-3

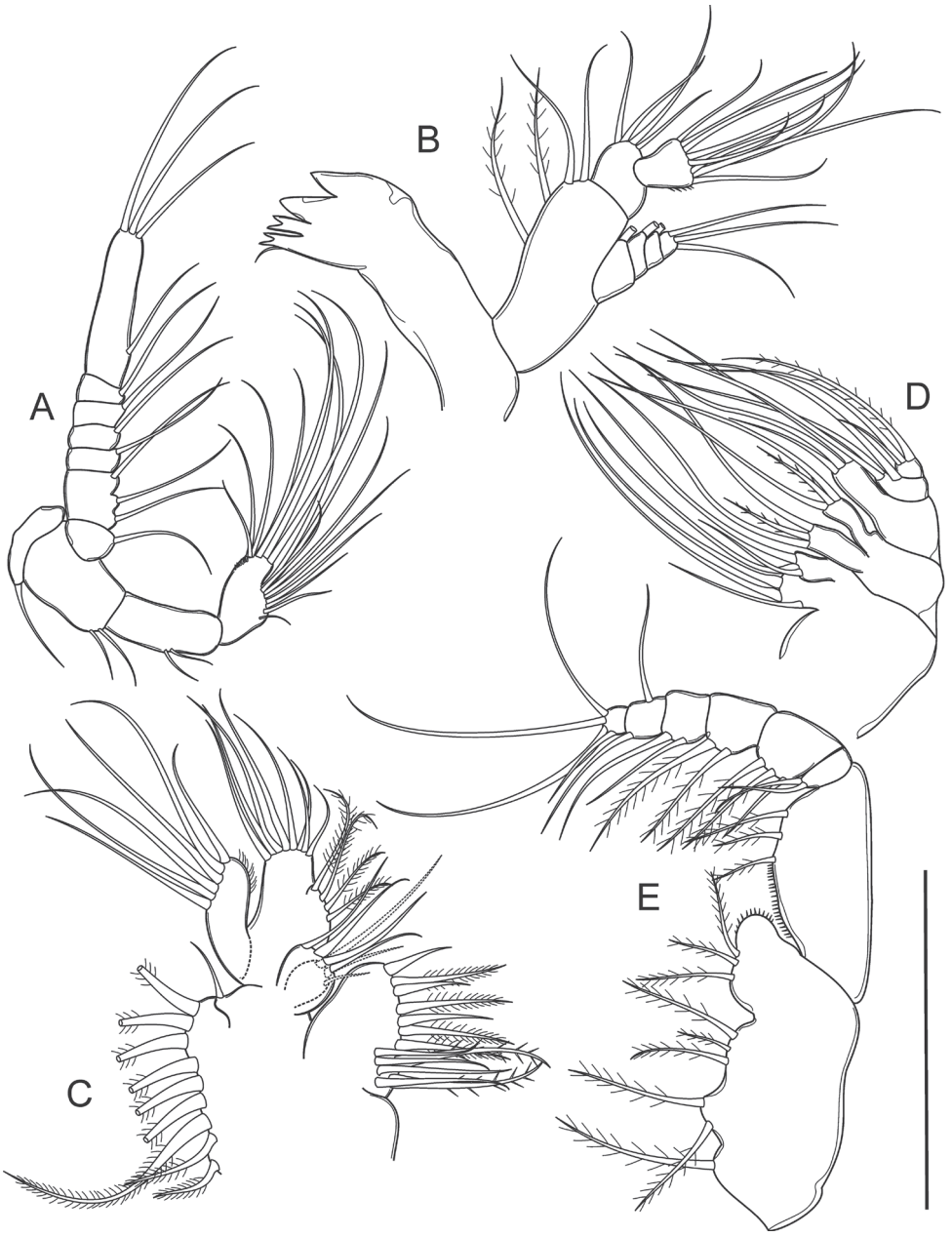

Figure 2. *Mongolodiaptomus loeiensis* sp. n. Female: **A** antenna **B** mandible **C** maxillule **D** maxilla **E** maxilliped. Scale bar 100 μm.

P5 (Figs 3E–F, 5F–I) symmetrical. Coxa with a blunt, stout spine on protuberance at distal outer corner on caudal surface. Basis with a thin, bare seta on outer margin, reaching middle of Exp-1. Exp 3-segmented and Enp 2-segmented. Exp-1 sub-rectangular, more than 2.0 times as long as wide, slightly longer than Enp. Exp-2 sub-trian-

gular, drawn out into claw-like, with a row of strong spinules along middle of both margins; with short and bare lateral spine. Exp-3 reduced into small prominence, with short lateral spine, and long apical seta. Enp subconical, Enp-1 rectangular, slightly shorter than wide. Enp-2 narrowed distally, with a circular row of spinules on distal end.

Additional ornamentation of P1–P5 as in Figs 3A–F, 5F–I.

Adult females with a single egg sac containing 8–10 eggs.

Description of adult male. Body length (Fig. 6A) measured from anterior margin of rostrum to posterior margin of caudal rami, 0.9 –1.1 mm (mean = 1.0 mm, n = 5), smaller than female. Prosome as in female but lateral wings not well developed compared to those in female, pediger 5 without inner spine inserted on dorso-posterior margin of each wing. Urosome (Figs 4D, 6B–C) 5-segmented and asymmetrical, oriented downward to right side. Genital somite (Fig. 6B) dilated postero-laterally on right side accompanied with a small seta on distal corner. Urosomites 2–3 (Figs 4D, 6C) with a field of long hairs ventrally along middle of segment. Urosomite 4 (Figs 4D–E, 6B) with posterolateral dilated on right side; dorso-posterior margin expanded beyond anal operculum. Anal somite (Figs 4D–E, 6B–D) similar to female but asymmetrical, right side located at lower position than opposite side. Caudal rami (Figs 4D–E, 6B–D) similar to female in setation but having different shape and ornamentation on right ramus. Ramus asymmetrical and cylindrical shaped: right ramus with three ventral chitinous prominences: two teeth-like on large bulge at proximal region (outer one small and with sharped tip; inner one large and with rounded tip), and one semi-circular ridge located above insertion of caudal seta IV and V.

Antennule (Figs 4F–G, 6E) asymmetrical, reaching beyond end of caudal setae. Right antennule 22-segmented, setal formula (a = aesthetasc, s = spine): 1+a, 3+a, 1+a, 1, 1+a, 1, 1+a, 1+s, 2+a, 1+s, 1+s, 1+a+s, 1+a+s, 2+a+s, 2+a+s, 2+a, 2+s, 1+s, 2, 3+s, 2, 4+a; geniculated between segment 18 and 19; segment 20 (antepenultimate) with comb-like spine (3–5 teeth).

Left antennule, antenna, mouthparts, and P1–P4 similar to those in female.

P5 (Figs 5A–E, 7) asymmetrical, right leg reaching beyond caudal setae. Intercoxal plate with two tooth-like lobes on distal margin, its tip bent forward to left leg. Right P5: coxa with strong and stout spine inserted on well-developed posterior lobe on caudal surface. Basis with long and narrow hyaline lamella at inner margin; small chitinous prominence (sub-globular in shape) located approximately mid-distal of segment on caudal surface; distal outer margin with short, thin seta on frontal surface. Exp 2-segmented: Exp-1 small and shorter than wide, approximately 0.6 times as long as wide; with two prominent knobs on caudal surface; distal outer corner produced. Exp-2 enlarged, approximately 2.0 times as long as wide; proximal and distal part enlarged in similar size, inner margin slightly convex and outer margin concave; with two minute knobs and one principal (lateral) spine at outer margin (knob-like projection located on proximal and distal region; lateral spine inserted slightly anterior to mid-outer margin of segment). Lateral spine strong, cylindrical, approximately 1/2 of segment length; its tip bent upward to posterolateral direction on caudal view. End claw sickle-shaped, strong and pointed tip; approximately 1.5 times as long as Exp-2, inner and outer margins smooth. Enp 1-segmented, conical,

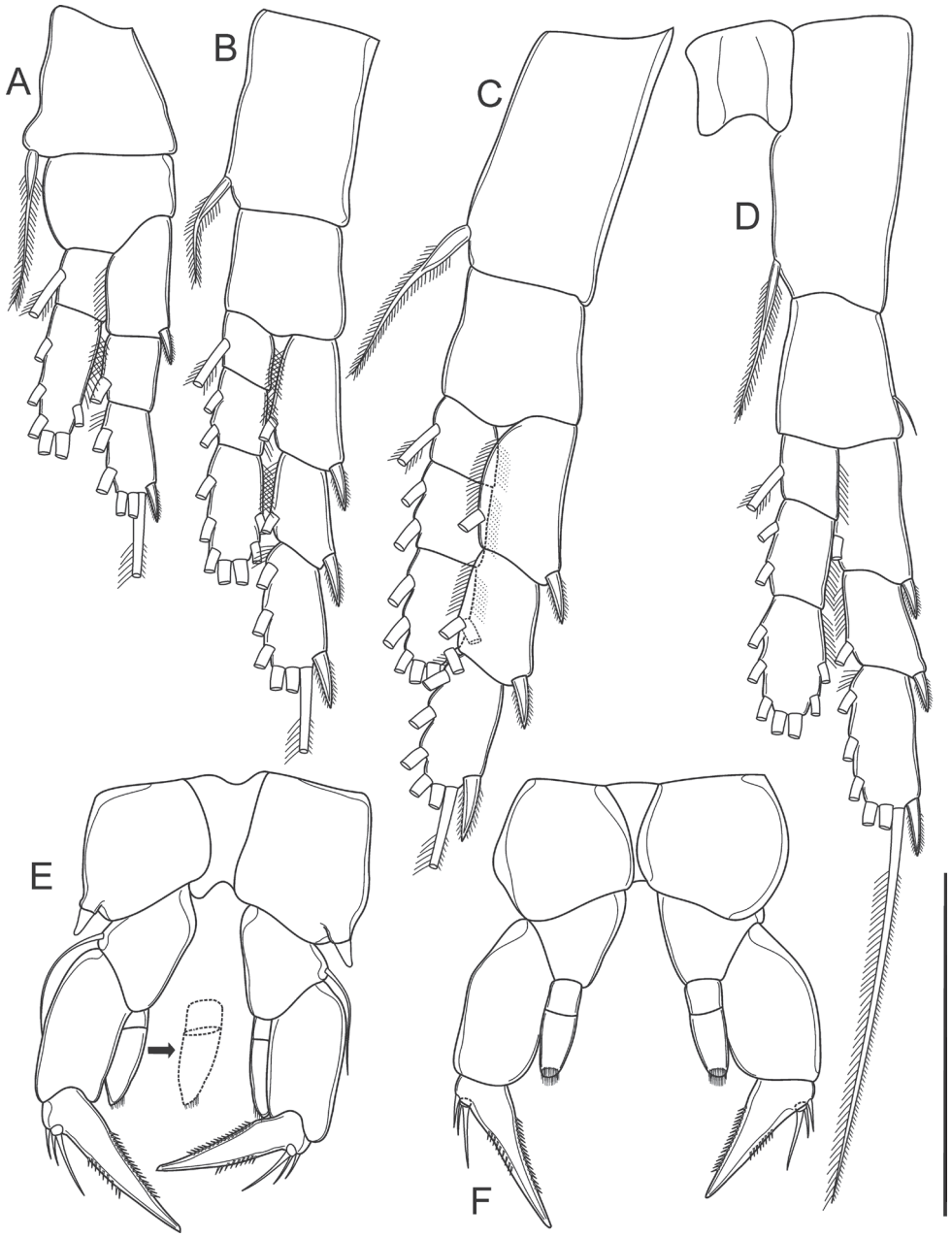

Figure 3. *Mongolodiaptomus loeiensis* sp. n. Female: **A** P1 **B** P2 **C** P3 **D** P4 **E** P5 in caudal view **F** P5 in frontal view. Scale bar 100 μm.

reaching to proximal expansion of Exp-2, with cluster of spinules at rounded tip. Left P5: coxa with thin seta inserted on posterior lobe at distal inner corner, exceeding basis, and posterolateral margin with semi-circular concave on caudal surface. Basis with long, narrow hyaline lamella at inner margin (small size than right P5); with long, thin seta at posterolateral margin on caudal surface. Exp 2-segmented: Exp-1

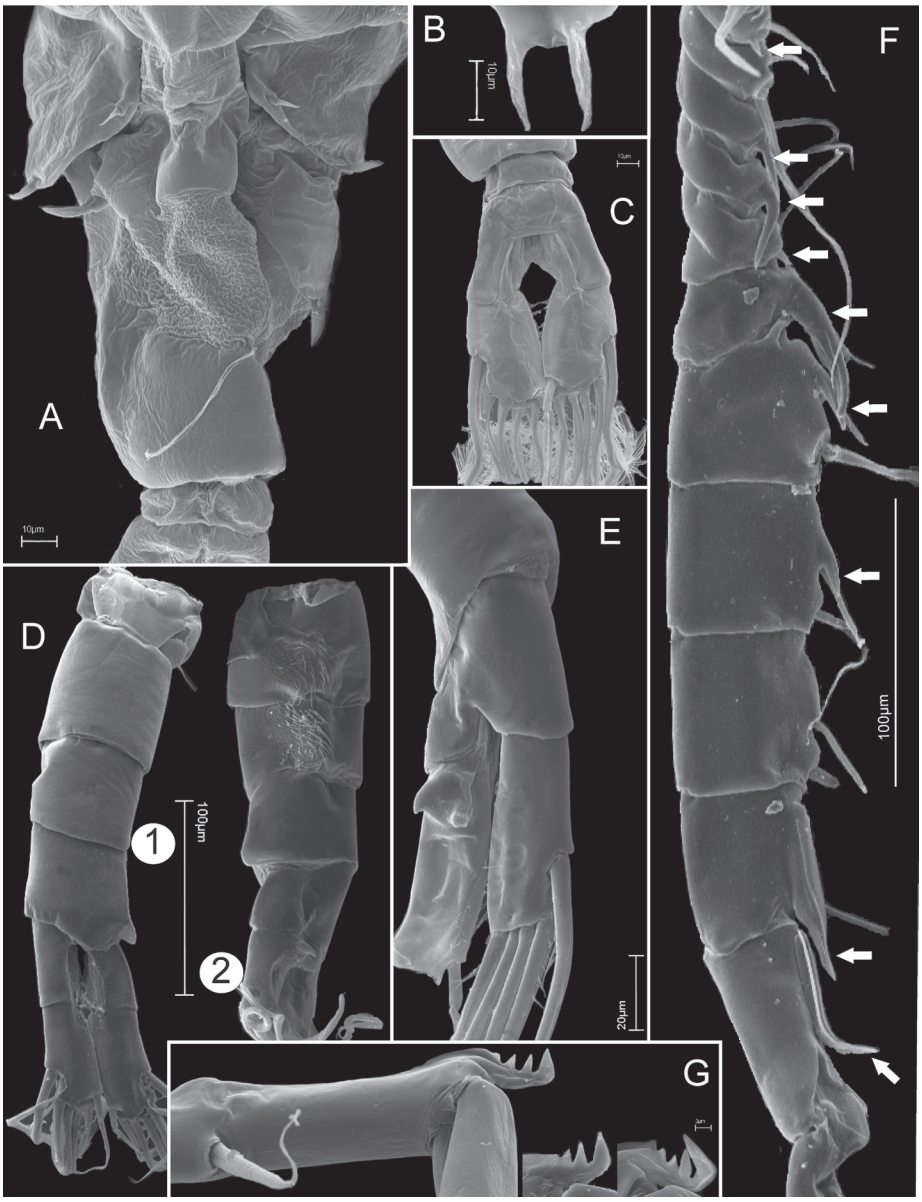

Figure 4. *Mongolodiaptomus loeiensis* sp. n., SEM photographs. Female (**A–C**): **A** pediger 5 and genital somite, dorsal view **B** rostrum, frontal view **C** urosomite 2, anal somite and caudal rami, dorsal view; Male (**D–G**): **D1** urosome in dorsal view **D2** urosome in ventro-lateral view **E** anal somite and caudal rami, ventral view **F** the right antennule segments 8–18 (white arrows point to spines) **G** spinous process on right antennule segment 20.

longer than wide, gradually tapering posteriorly, inner margin concave and outer one convex; with field of setules on inner margin at distal end. Exp-2 smaller than Exp-1, conical; with seta on inner margin at distal end on frontal surface, as long as segment;

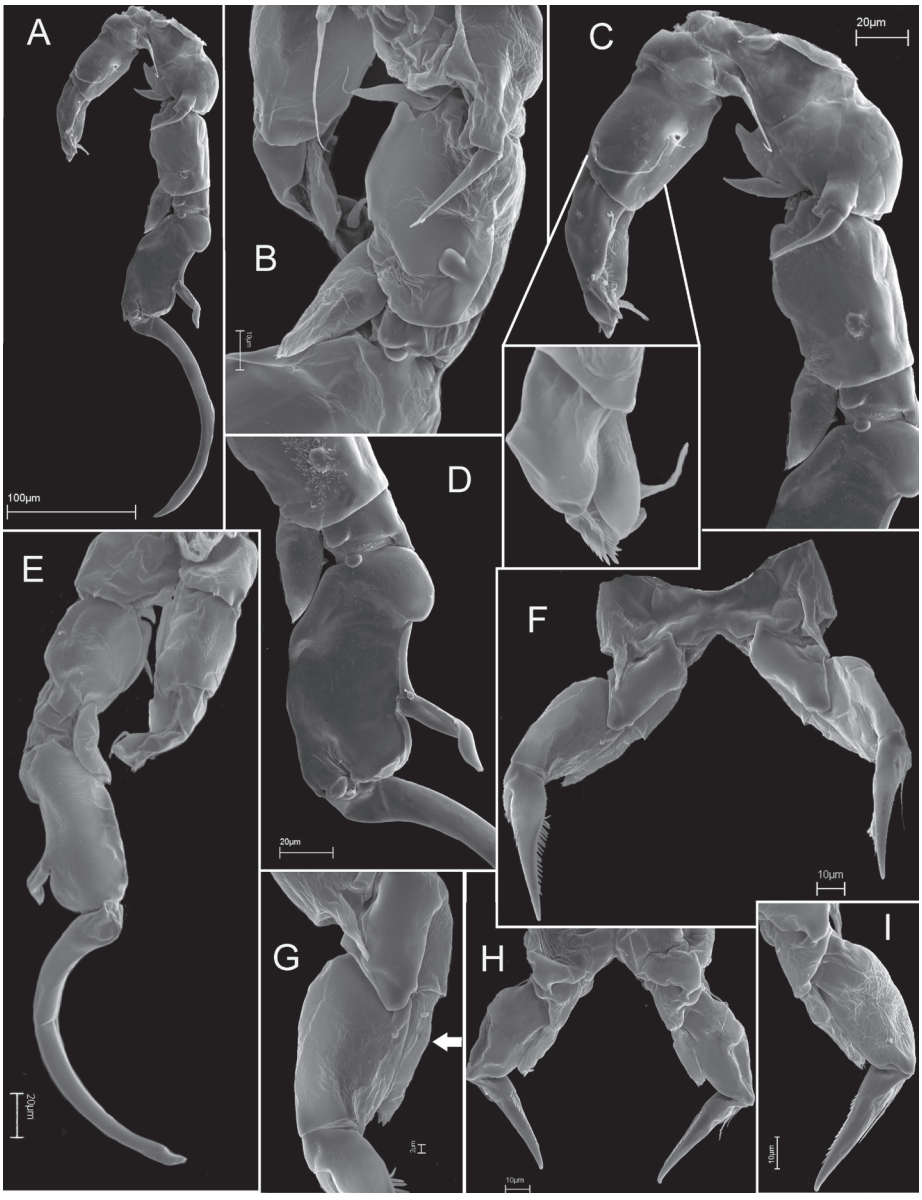

Figure 5. *Mongolodiaptomus loeiensis* sp. n., SEM photographs. Male (**A–E**): **A** P5 in caudal view **B** coxa, basis, Exp-1 of the right P5 in caudal view **C** intercoxal plate, coxa, basis, Enp of the right P5 and coxa, basis, Exp and Enp of the left P5, caudal view **D** Enp and Exp of the right P5 in caudal view **E** P5 in frontal view; Female (**F–I**): **F** P5 in caudal view **G** basis, Exp-1 and Enp in caudal view (white arrow indicated the segmented point of Enp) **H** P5 in frontal view **I** the left P5 in frontal view.

with a cluster of strong spinules along inner margin; apical process stout, bare, and short. Enp 1-segmented, longer than Exp-1, with a cluster of spinules at its tip.

Etymology. The specific name *loeiensis* refers to the place "Loei" where the new species was first recognized. The name with the Latin suffix "*-ensis*" is an adjective for place.

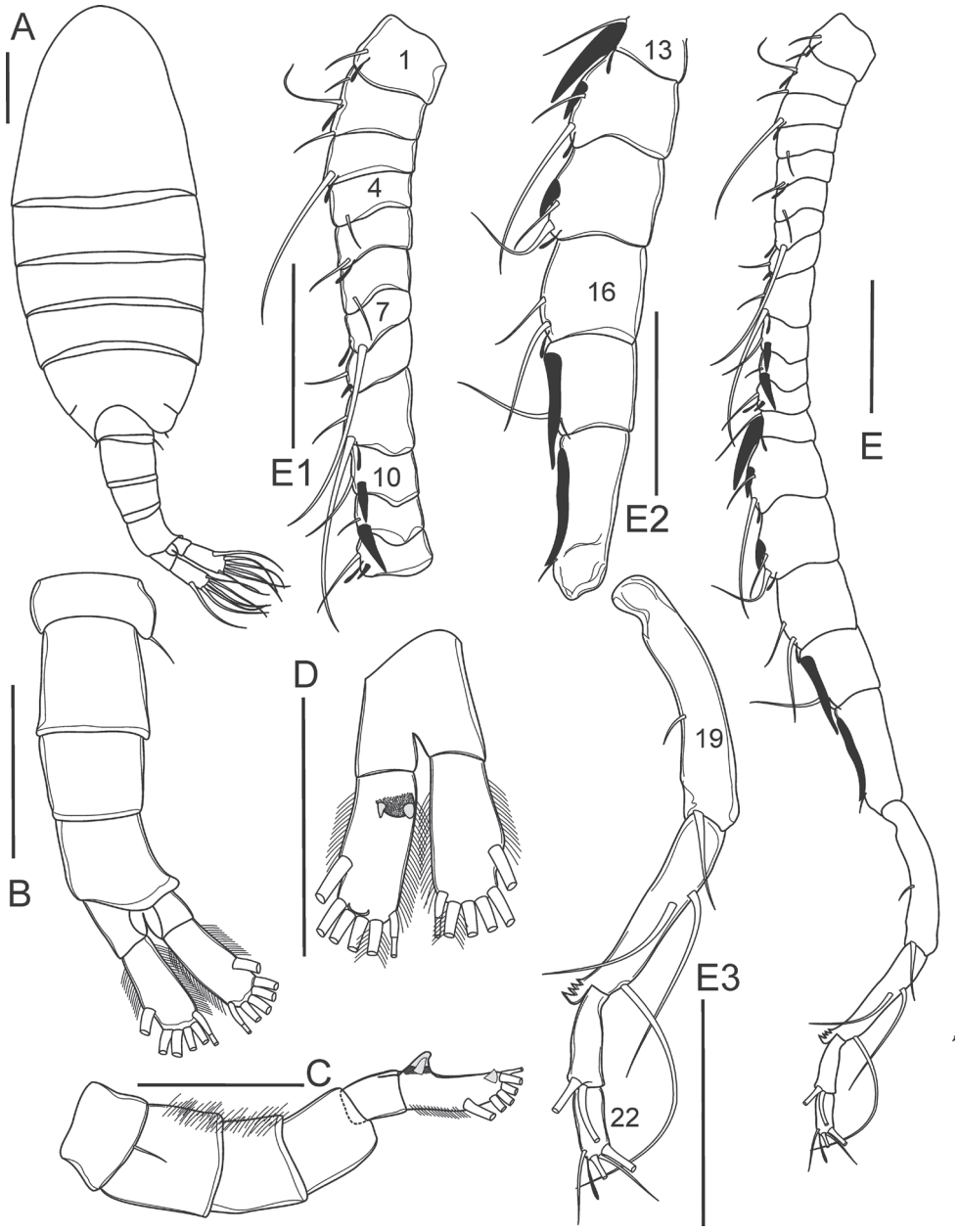

Figure 6. *Mongolodiaptomus loeiensis* sp. n. Male: **A** habitus, dorsal view **B** urosome, dorsal view **C** urosome, lateral view **D** anal somite and caudal rami, ventral view **E** antennule **E1** segments 1–12 **E2** segments 13–18 **E3** segments 19–22. Scale bar 100 μm.

Distribution and ecology of the new species and other diaptomids in the area of study. *Mongolodiaptomus loeiensis* sp. n. was found in a temporary pond with a mean water temperature of 25.5 °C, conductivity 259 μS/cm, and pH 7.6. The new species was a single calanoid copepod occurring in type locality. However,

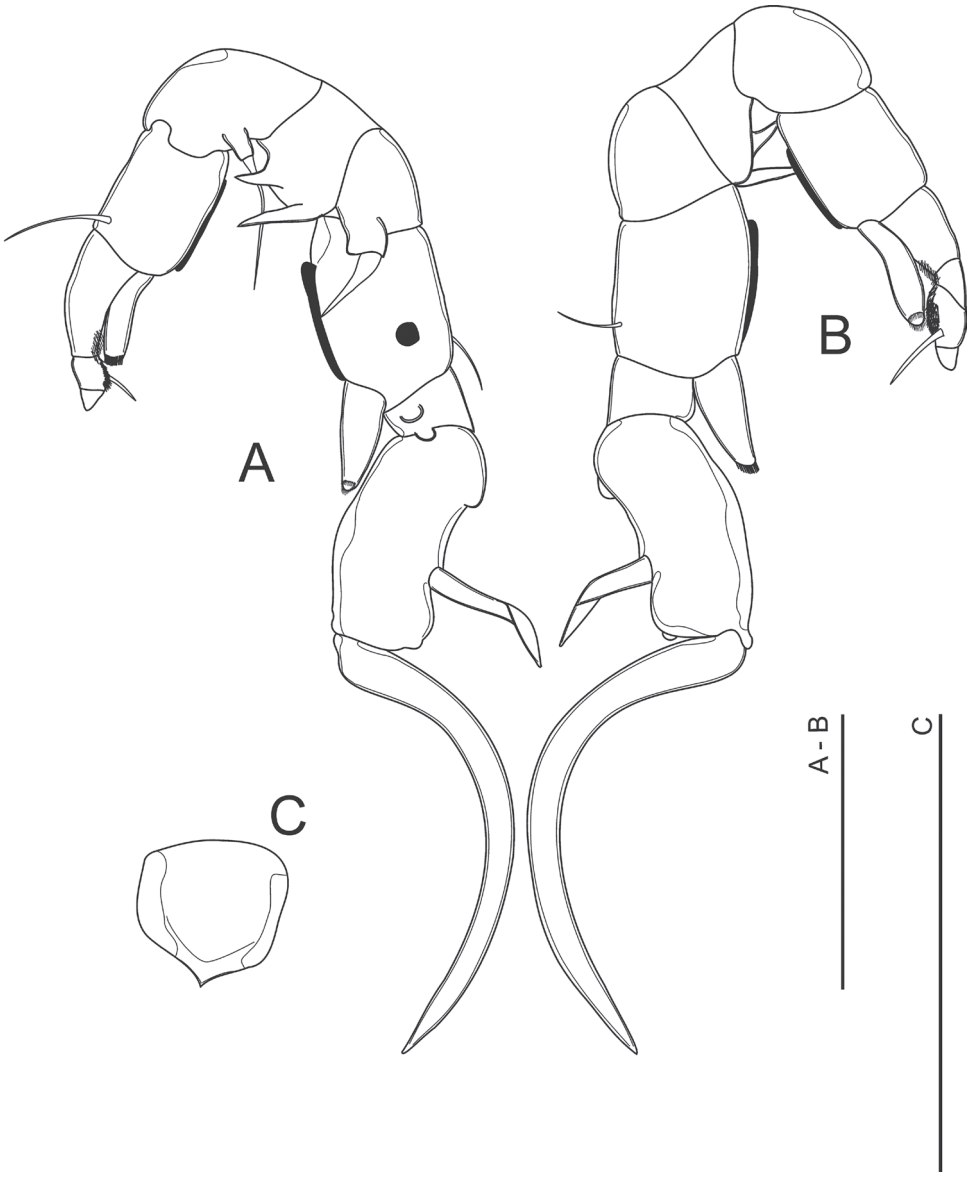

Figure 7. *Mongolodiaptomus loeiensis* sp. n. Male: **A** P5 in caudal view **B** P5 in frontal view **C** Right P5 Exp-1 in outer lateral view. Scale bar 100 μm.

it was found co-occurring with other microcrustaceans, i.e. *Diaphanosoma excisum* Sars, 1885, *Thermocyclops decipiens* (Kiefer, 1929), and *Mesocyclops thermocyclopoides* Harada, 1931. In over 3,000 samples collected from Thailand (59 samples from Loei Province provided by the first author and about 3,000 samples from other provinces by the second author and her colleagues), the new species can by considered as a rare species because it was present only in the type locality from Loei Province (Sanoamuang 2002).

The occurrence of the new species is similar to that of *Phyllodiaptomus thailandicus* Sanoamuang & Teeramaethee, 2006 and *Tropodiaptomus* cf. *ruttneri* (Brehm, 1923), which have so far been known as rare species in Thailand and here each species was found in a single location or in about 2% of collected samples. *P. thailandicus* has hitherto been found in six provinces; Prachinburi, Chanthaburi, Sa Kaeo, Suphanburi, Kanchanaburi, and Chumphon (Sanoamuang and Teeramaethee 2006, Koompoot and Sanoamuang 2012) whereas *Tropodiaptomus* cf. *ruttneri* was only known from Phayao and Nan provinces (Sanoamuang 2002). The findings of *P. thailandicus* and *Tropodiaptomus* cf. *ruttneri* in this study are a new record to northeastern Thailand and provide more understanding on its distribution range in the country. *Vietodiaptomus blachei* (Brehm, 1951) was found in a few samples or approximately 9% of collected samples whereas *P. praedictus*, *M. botulifer,* and *M. calcarus* were frequently found in about 41, 39 and 6% of collected samples, respectively.

The ranges of water variables for four other diaptomids species collected from Loei Province areas are as follows: *Tropodiaptomus* cf. *ruttneri* in water with temperature 26.9–30.1 °C, conductivity 81–100 µS/cm, and pH 7.1–7.3; *P. thailandicus* = 25.0–30.1 °C, 310–360 µS/cm, and pH 7.3–7.5; *M.calcarus* = 23.6–31.2 °C, 197–287 µS/cm, and pH 7.6–8.0; *M. botulifer* = 26.0–30.7 °C, 57–343 µS/cm, and pH 7.2–7.8; *P. praedictus* = 24.6–31.8 °C, 57–386 µS/cm, and pH 7.6–8.2; *V. blachei* = 26.0–31.4 °C, 92–527 µS/cm, and pH 7.1–8.1.

Discussion

The genus *Mongolodiaptomus* currently contains 12 species, *M. birulai*, *M. botulifer, M. calcarus*, *M. dumonti*, *M. formosanus*, *M. gladiolus*, *M. malaindosinensis*, *M. mephistopheles*, *M. pectinidactylus*, *M. rarus*, *M. uenoi*, and *M. loeiensis* sp. n. (Sanoamuang 2001, 2002 and the present study). Apart from the closest species *M. calcarus*, the male of the new species differs from its congeners by the following unique characters. The antepenultimate segment of right antennule has a comb-like spine in the new species versus it is smooth in *M. birulai*, *M. formosanus*, *M. botulifer* and *M. malaindosinensis*. The right caudal ramus has three ventral chitinous prominences in *M. loeiensis* sp. n. versus respectively 1, 1, 1, 1, none, 2 chitinous prominences (prominence is unknown for *M. gladiolus*) in *M. birulai*, *M. formosanus*, *M. mephistopheles*, *M. rarus*, *M. pectinidactylus*, and *M. dumonti*. Although right caudal ramus in *M. botulifer*, *M. malaindosinensis* and *M. uenoi* has three chitinous prominences, their shapes are different to that of the new species; *M. loeiensis* sp. n**.** has two teeth and one semi-circular ridge while *M. botulifer* and *M. malaindosinensis* have one tooth and two knobs, and *M. uenoi* has one tooth and two semi-circular ridges.

The male P5 of *M. loeiensis* sp. n. can be distinguished from its congeners by the following characters: (1) two spine-like lobes on distal margin of the intercoxal plate in the new species versus a triangular lobe in *M. birulai, M. botulifer, M. formosanus, M. pectinidactylus,* and *M. malaindosinensis* and one spine-like lobe in *M. uenoi* and no outgrowth in *M. dumonti*, *M. gladiolus, M. mephistopheles*, and *M. rarus*; on the right P5, (2) the coxal spine of the new species stronger and more robust compared to those in

other species (except *M. uenoi*), (3) basis of the new species with a hyaline membrane on inner margin, which is absent in *M. gladiolus* and *M. dumonti*, (4) chitinous prominence present on caudal surface on the basis of the new species while absent in *M. birulai*, *M. formosanus*, *M. gladiolus*, *M. mephistopheles*, *M. malaindosinensis,* and *M. uenoi* (*M. botulifer* has chitinous ridge), (5) Exp-1 of the new species with produced process at distal outer corner versus absent in *M. birulai*, *M. dumonti*, *M. gladiolus*, *M. pectinidactylus* and *M. rarus*, (6) Exp-2 of the new species with a bent principal lateral spine versus straight in *M. birulai*, *M. gladiolus*, *M. dumonti*, *M. pectinidactylus* and *M. uenoi*, (7) on left P5 basis of the new species presence of a hyaline membrane on inner margin versus absent in *M. gladiolus* and *M. formosanus*. In the female, the genital somite of *M. loeiensis* sp. n. has a large posterolaterally directed outgrowth on the right side which is absent in the others (except *M. botulifer*, *M. gladiolus*, *M. malaindosinensis* and *M. rarus*).

Key to worldwide species of *Mongolodiaptomus* Kiefer, 1938

Males:

1	Spinous process on antepenultimate segment smooth	**2**
–	Spinous process on antepenultimate segment serrate	**5**
2	P5 Enp 1-segmented	**3**
–	P5 Enp 2-segmented	**4**
3	The basis of left P5 without hyaline membrane on inner margin	***M. formosanus***
–	The basis of left P5 with hyaline membrane on inner margin	***M. birulai***
4	The basis of right P5 with triangular hyaline membrane on inner margin	***M. malaindosinensis***
–	The basis of right P5 with spherical hyaline membrane on inner margin	***M. botulifer***
5	Intercoxal plate of P5 with outgrowth on distal margin	**6**
–	Intercoxal plate of P5 without outgrowth on distal margin	**8**
6	The principal lateral spine on Exp-2 of right P5 straight	**7**
–	The principal lateral spine on Exp-2 of right P5 bent	***M. loeiensis* sp. n.**
7	Intercoxal plate of P5 with rounded lobe on distal margin	***M. pectinidactylus***
–	Intercoxal plate of P5 with spine-like lobe on distal margin	***M. uenoi***
8	The basis of right P5 with hyaline membrane on inner margin	***M. mephistopheles***
–	The basis of right P5 without hyaline membrane on inner margin	**9**
9	The basis of left P5 with hyaline membrane on inner margin	**10**
–	The basis of left P5 without hyaline membrane on inner margin	**11**
10	The principal lateral spine on Exp-2 of right P5 straight	***M. dumonti***
–	The principal lateral spine on Exp-2 of right P5 bent	***M. calcarus***
11	The basis of right P5 with chitinous spur on caudal surface	***M. rarus***
–	The basis of right P5 without any process on caudal surface	***M. gladiolus***

Females:

1 P5 Enp 1-segmented **2**
– P5 Enp 2-segmented **8**
2 Genital somite with postero-laterally directed outgrowth on right side **3**
– Genital somite without postero-laterally directed outgrowth on right side **6**
3 The left spine inserted on lobe-process of genital somite..... ***M. gladiolus***
– The left spine inserted directly on genital somite **4**
4 Genital somite with posterolateral bulging **5**
– Genital somite without posterolateral bulging..... ***M. uenoi***
5 P5 with long Enp, reaching beyond distal end of Exp-1 ..... ***M. malaindosinensis***
– P5 with short Enp, not reaching distal end of Exp-1 (2/3 of Exp length) ..... ***M. botulifer***
6 P5 Exp-3 absent..... ***M. birulai***
– P5 Exp-3 present **7**
7 Genital somite with larger spine on left side compared to right side ..... ***M. mephistopheles***
– Genital somite with similar sized spine on left and right side ***M. formosanus***
8 Genital somite with postero-laterally directed outgrowth on right side..... **9**
– Genital somite without postero-laterally directed outgrowth on right side **10**
9 Genital somite with hyaline membrane at mid-laterally on right side ..... ***M. rarus***
– Genital somite without hyaline membrane at mid-laterally on right side..... ***M. loeiensis* sp. n.**
10 The right spine inserted on small lobe of genital somite ..... ***M. pectinidactylus***
– The right spine inserted directly on genital somite **11**
11 Genital somite with larger spine on left side compared to right side ..... ***M. dumonti***
– Genital somite with larger spine on right side compared to left side ..... ***M. calcarus***

Acknowledgements

We would like to thank the Higher Education Research Promotion and National Research University project of Thailand, the Office of the Higher Education Commission (Grant No. 2559A13462002) and the Thailand Research Fund (Grant No. MRG5980183) for financial support. We are grateful to Prof. Dr. Y. Ranga Reddy for providing some literature on diaptomids and critically reviewing the manuscript. We also thank Dr. D. Defaye for her careful editing of the manuscript.

References

Baird W (1850) The natural history of the British Entomostraca: I–VII. The Ray Society, London, 364 pp.

Brehm V (1933) Mitteilungen von der Wallacea-Expedition Woltereck. Mitteilung IV. Einigeneue Diaptomiden. Zoologischer Anzeiger 103: 295–304.

Huys R, Boxshall GA (1991) Copepod evolution. The Ray Society, London, 468 pp.

Kiefer F (1937) Süsswassercopoden aus Ostasien. II. Neue Diaptomiden und Cyclopiden von der Insel Formosa. Zoologischer Anzeiger 119: 58–64.

Kiefer F (1938) Freilebende Ruderfusskrebse (Crustacea, Copepoda) von Formosa. Bulletin of the Biogeographical Society of Japan 8: 35–73.

Kiefer F (1939) Freilebende Ruderfusskrebse (Crustacea, Copepoda) ausnordwest und südindien (Pandschab, Kaschmir, Ladak, Nilgirigebirge). Memorial Indian Museum 13: 83–203.

Kiefer F (1974) Eineneue Diaptomidenart aus Malaysia (Crustacea, Copepoda, Calanoida). Zoologischer Anzeiger 192: 420–424.

Kikuchi K (1936) A new species of *Diaptomus* from Formosa. The Proceedings of the Imperial Academy (Tokyo) 12: 198–200.

Koompoot K, Sanoamuang L (2012) Calanoid copepods from Suphanburi, Kanchanaburi, Ratchaburi and Phetchaburi provinces. KKU Science Journal 40: 273–280.

Luong TD, Thanh DN, Hai HT (2016) An annotated checklist of the family Diaptomidae Sars, 1903 (Copepoda, Calanoida) in Vietnam. Tap Chi Sinh Hoc 38: 384–399. https://doi.org/10.15625/0866-7160/v38n3.8515

Reddy YR, Sanoamuang L, Dumont HJ (1998) A note on the Diaptomidae of Thailand, including redescription of three species and description of a new species (Copepoda, Calanoida). Hydrobiologia 361: 201–223. https://doi.org/10.1023/A:1003135200559

Reddy YR, Sanoamuang L, Dumont HJ (2000) Amended delimitation of *Mongolodiaptomus* against *Neodiaptomus* and *Allodiaptomus* and redescription of the little known *Mongolodiaptomus uenoi* (Kikuchi, 1936) from Thailand (Copepoda: Calanoida: Diaptomidae). Hydrobiologia 418: 99–109. https://doi.org/10.1023/A:1003859908612

Sars GO (1903) An account of the Crustacea of Norway with short descriptions and figures of all the species: IV. Copepoda Calanoida. Bergen Museum, Bergen, 177 pp.

Sanoamuang L (1999) Species composition and distribution of freshwater Calanoida and Cyclopoida (Copepoda) of north-east Thailand. In: Schram FR, Klein JVC (Eds) Crustaceans and Biodiversity Crisis, Brill Academic Publishers, Leiden, 217–230.

Sanoamuang L (2001) *Mongolodiaptomus dumonti* n. sp., a new freshwater copepod (Calanoida, Diaptomidae) from Thailand. Hydrobiologia 448: 41–52. https://doi.org/10.1023/A:1017526018189

Sanoamuang L (2002) Freshwater Zooplankton: Calanoid Copepods in Thailand. Klangnanatham Publishers (Khon Kaen), Thailand, 159 pp.

Sanoamuang L, Teeramaethee J (2006) *Phyllodiaptomus thailandicus*, a new freshwater copepod (Copepoda, Calanoida, Diaptomidae) from Thailand. Crustaceana 79: 475–487.

Shen CJ, Lee FS (1963) The estuarine Copepoda of Chiekong and Zaikong Rivers, Kwangtung Province, China. Acta Zootaxonomica Sinica 15: 571–596.

Shen CJ, Tai AY (1964) Descriptions of eight new species of freshwater Copepoda (Calanoida) from delta of the Pearl River, South China. Acta Zootaxonomica Sinica 16: 225–246. https://doi.org/10.1163/156854006777554802

Shen CJ, Tai AY (1965) Descriptions of six new species of freshwater copepods chiefly from the Pearl River delta, South China. Acta Zootaxonomica Sinica 2: 126–140.

Watiroyram S, Brancelj A, Sanoamuang L (2015) A new cave-dwelling copepod from north-eastern Thailand (Cyclopoida: Cyclopidae). Raffles Bulletin of Zoology 63: 426–437.

Watiroyram S, Sanoamuang L, Brancelj A (2017) Two new species of *Elaphoidella* (Copepoda, Harpacticoida) from caves in southern Thailand and a key to the species of Southeast Asia. Zootaxa 4282(3): 501–525. https://doi.org/10.11646/zootaxa.4282.3.5

ZooKeys 710: 33–42 (2017)
doi: 10.3897/zookeys.710.14902
http://zookeys.pensoft.net

RESEARCH ARTICLE

A peer-reviewed open-access journal
ZooKeys
Launched to accelerate biodiversity research

Ancient diversity of Afrotropical *Microborus*: three endemic species – not one widespread

Bjarte H. Jordal[1]

1 *Natural History Museum, The University Museum, University of Bergen, NO-5007 Bergen, Norway*

Corresponding author: *Bjarte H. Jordal* (bjarte.jordal@uib.no)

Academic editor: *M. Alonso-Zarazaga* | Received 6 July 2017 | Accepted 1 October 2017 | Published 19 October 2017

http://zoobank.org/480537F7-3919-4A33-B164-AC0F688C4E61

Citation: Jordal BH (2017) Ancient diversity of Afrotropical *Microborus*: three endemic species – not one widespread. ZooKeys 710: 33–42. https://doi.org/10.3897/zookeys.710.14902

Abstract

The primarily Neotropical genus *Microborus* Blandford is represented with three species in Africa and Madagascar. The previously recorded species from this region, *M. boops* Blandford, is a Neotropical species restricted to Central America and is likely not found in the Afrotropics. The previously recognised species in western parts of Africa is *M. camerunus* (Eggers) and is resurrected from synonymy under *M. boops*. Molecular and morphological data revealed a second species of this complex in Madagascar, *M. brevisetosus* Jordal. Another new species, *M. angustus* Jordal, co-occurs with *M. camerunus* in Cameroon. Substantial genetic divergence indicate that *Microborus* was established in the Afrotropical region long before human transport across oceans. A key to Afrotropical species is provided.

Keywords

Curculionidae, Scolytinae, Hexacolini, *Microborus*, molecular phylogeny, Africa, Madagascar

Introduction

Microborus Blandford, 1897 is a largely Neotropical genus consisting of eight known species, with one of these also recorded from the Afrotropical region. Species are generally small in size, but are often taken from very thick bark of large tree trunks (Wood 2007).

Figures 1–2. Typical host plant condition for species of *Microborus*. **1** Standing *Stereospermum* tree with thick bark, with attacks of ambrosia beetles, cossonine weevils and *Microborus* in the lower bole (Ankarafantsika NP, Madagascar). **2** Inner side of bark with tunnels made by *M. brevisetosus* Jordal, starting from the entrance hole of *Euplatypus madagascariensis* (Schedl).

Their breeding biology is unusual in that nests are initiated via the entrance opening of a much larger bark or ambrosia beetle species and mines away from their host gallery just inside the entrance (Figs 1–2).

Previous classifications have placed *Microborus* in the scolytine tribe Hexacolini (previously Ctenophorini, see Alonso-Zarazaga and Lyal 2009). Recent molecular phylogenies have nevertheless questioned the relationship to *Scolytodes* Ferrari and other hexacoline genera, and instead pointing towards a relatively isolated position in Scolytinae. This is a very old genus that apparently diverged from all other extant lineages more than 100 Ma (Jordal and Cognato 2012) and which experienced very little morphological change since its time of origin (Cognato and Grimaldi 2009).

The supposedly broad distribution of *Microborus boops* Blandford in the Neotropical and Afrotropical regions has been inferred as a recent introduction to Africa and Madagascar (Wood 1982). Using integrated morphological and molecular data, the Afrotropical fauna is revised, including discovery of two new species, and rejection of a globally widespread distribution in *M. boops*.

Materials and methods

Specimens included were collected during the author's field expeditions to Cameroon (2007) and Madagascar (2015). Deposition of typematerial are indicated by the following acronyms: BMNH, Natural History Museum London; CAS, California Academy of Science; NHMW, Naturhistorisches Museum Wien; ZMBN, University Museum of Bergen (formerly Zoological Museum, Bergen).

DNA was extracted from whole specimens, of which the macerated body remains were mounted on slides or glued on a pinned card. Six gene fragments were amplified: COI, EF-1α, 28S, CAD, ArgK and PABP1 (Jordal et al. 2011; Pistone et al. 2016). Sequences were concatenated for combined phylogenetic analyses using maximum likelihood and maximum parsimony in PAUP* (Swofford 2002).

Morphological examination of internal or hidden characters such as flight wings, proventriculus and male genitalia was only made for one species that had sufficient specimens available.

Taxonomy

Microborus Blandford, 1897

Type species. *Microborus boops* Blandford, 1897

Diagnosis. Small slender species with pronotum laterally costate, anteriorly unarmed; procoxae separated by broad prosternal process; eyes large, approximate below; antennal club globular without sutures, funicle 6-segmented; elytral interstriae 7 sharply raised on declivity and curved towards elytral interstriae 9 to form a postero-lateral costa on declivity.

Microborus angustus Jordal, sp. n.

http://zoobank.org/B02BF8A3-3D75-4518-BDA0-617A3D748DFC
Figs 3–4, 9–11, 18–20

Type material examined. Holotype: Cameroon, Mt. Cameroon south slope, 1600m alt., *Ficus* branch, B. Jordal 28xi-8 [28. Nov. 2007]. ZMBN/ENT_Scol4932. Paratypes (8): same data as HT (ZMBN/ENT_Scol4933-4940). (GIS: 4.12, 9.16). All types deposited in ZMBN.

Diagnosis. A very elongated, almost black species, with impressed elytral striae and a distinct costate rim along the postero-lateral margin of elytral declivity.

Description (male and female). *Length* 1.3–1.5 mm, 2.7–2.8 × longer than wide. *Colour* dark brown, almost, black, legs and antennae light brown.

Head. Eyes separated above by 1.4 × their width. Frons reticulate and deeply punctured, smooth and shiny at level of antennal insertion, vestiture consisting of a few scant fine setae.

Pronotum smooth, shiny, with densely placed punctures.

Elytra with all striae impressed, punctures deep, subconfluent; interstriae as wide as striae, with very fine irregularly spaced punctures; postero-lateral rim sharply elevated with 3–6 sharp granules. Vestiture consisting of few long, fine, erect golden setae.

Legs. Protibiae with three lateral teeth (embedded denticles), and one additional tooth just above the inner mucro; posterior face smooth.

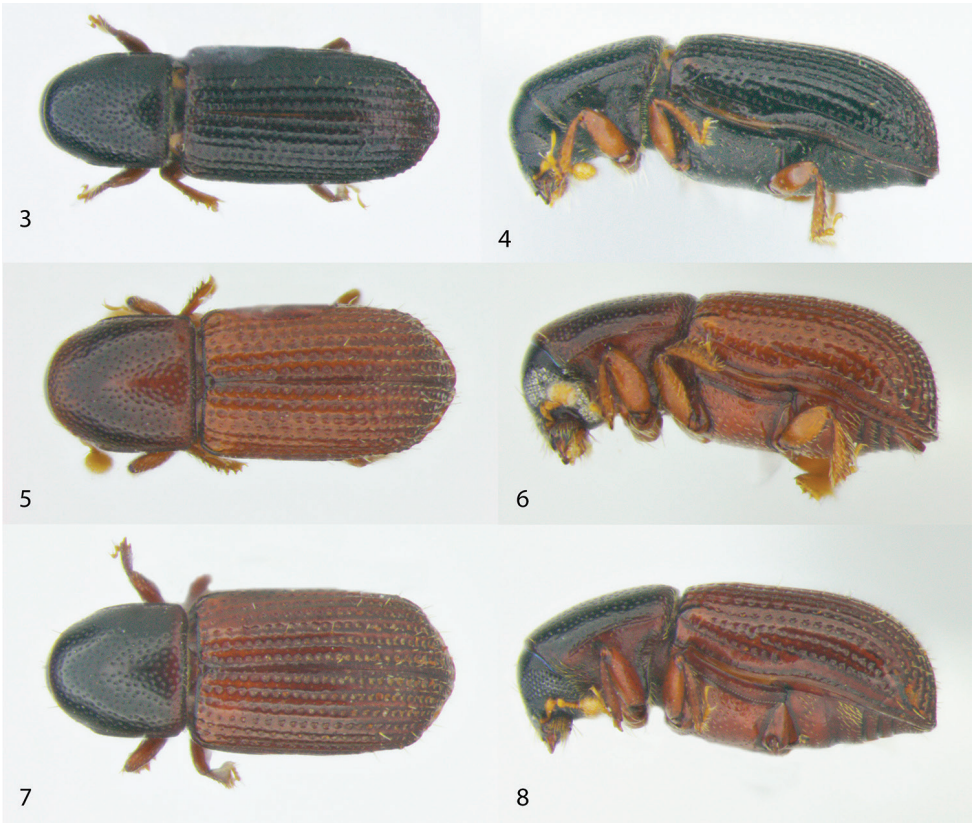

Figures 3–8. Dorsal and lateral view of the Afrotropical species of *Microborus*. **3–4** *M. angustatus* **5–6** *M. brevisetosus* **7–8** *M. camerunus.*

Ventral vestiture simple, on ventrites very fine, short setae.

Wings typical for weevils, costa with two setae close to each other near base, and one seta two-thirds the distance towards the stigmal patch; anal field missing, posterior margin with long fine setae; stigmal patch with two short, sharp setae, each on a small tubercle.

Proventriculus with apical plate well developed, median suture wide open, sutural teeth long and sharp, apical teeth and marginal bristles missing, closing teeth long and prominent, >10 large femoral teeth.

Male genitalia very simple, spiculum gastrale not present, no distinction between apophyses and aedeagal body, internal sac with granulated surface, tegmen open dorsally, gradually broader ventrally with a short manubrium.

Etymology. Latin adjective *angustus*, meaning narrow. This is the most elongated species in the genus in the Afrotropical region.

Distribution and biology. Only known from the type locality. It was taken together with *M. camerunus* (Eggers, 1919) under thick bark of a fallen *Ficus* tree. Both species used entrance holes made by *Xyleborus principalis* Eichhoff, 1878.

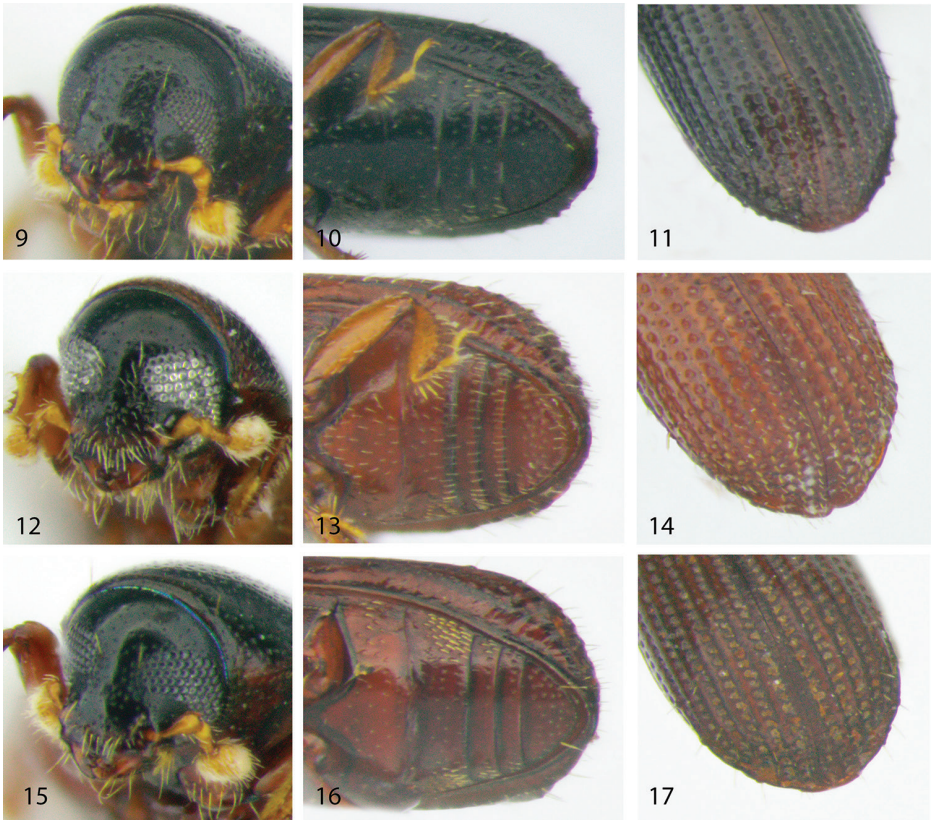

Figures 9–17. Head, venter and declivity of the Afrotropical species of *Microborus*. **9–11** *M. angustatus* **12–14** *M. brevisetosus* **15–17** *M. camerunus*.

***Microborus brevisetosus* Jordal, sp. n.**
http://zoobank.org/17AC91AF-2FA6-46B3-8D16-CB8FC53E9FA4
Figs 5–6, 12–14

Type material examined. Holotype: Madagascar, Boeny province, Ankarafantsika NP, 200 m alt. GIS [-16.264, 46.828], ex *Stereospermum* standing tree, 8.May.2015, B. Jordal leg. (ZMBN/ENT_Scol4929). Paratypes (2): same data as HT (ZMBN/ENT_Scol4930). Madagascar, Forêt de Tsimembo, 11.0 km 346° NNW Soatana, GIS [-18.995, 44.444], 21.Nov.2001, B. Fischer, BLF4508, (1). HT and one PT in ZMBN, 1 PT in CAS.

Diagnosis. Distinguished from *M. camerunus* (Eggers) by the much more abundant short setae in the lower frons, nearly moustache-like on epistoma, ventrites 2–4 with regular transverse rows of fine recumbent setae, and posterior face of protibiae with 3–5 sharp granules. It is distinguished from *M. boops* by the short and bristle-like setae on elytral interstriae on declivity.

Description (male and female). *Length* 1.4 mm, 2.6 × longer than wide. *Colour* reddish brown, pronotum darker.

Head. Eyes separated above by 0.6 × their width. Frons reticulated and lightly punctured, protruding slightly below eyes, vestiture consisting of >50 short setae, longer between eyes and some on epistoma.

Pronotum smooth, shiny, with densely placed puntures.

Elytra with striae impressed, punctures deep, spaced by distance equal to their diameter; interstriae about half as broad as striae, with very fine irregularly spaced punctures; postero-lateral interstrial rim slightly elevated with 2–3 blunt granules. Vestiture consisting of a few longer, erect, golden setae on discal interstriae, with densely placed, short, stiff setae on declivity.

Legs. Protibiae with three lateral teeth (embedded denticles), and one additional tooth just above the inner mucro; posterior face rough.

Ventral vestiture simple, on ventrites 1–4 consisting of fine, long recumbent setae forming transverse rows.

Etymology. Latin adjectives *brevis*, meaning short, and *setosus*, meaning bristly, referring to the very short stiff interstrial setae on the elytral declivity.

Distribution and biology. Madagascar: Boeny, Melaky, Diana and Analanjirofo provinces. Specimens were examined only from the western part of the island. It is presumed that Schedl's reported specimens from the east and north of the island are conspecific. The collection from Ankarafantsika (Fig. 1) was taken from brood galleries under thick bark of a standing *Stereospermum* tree, iniated via the entrance holes of *Euplatypus madagascariensis* (Chapuis, 1865).

Microborus camerunus (Eggers, 1919), stat. n.

Figs 7–8, 15–17

Pseudocrypturgus camerunus Eggers, 1919: 236, original description.
Microborus camerunus (Eggers, 1919): synonymized with *M. boops* Blandford, 1897, by Wood (1982), here resurrected.

Type material examined. Holotype of *Pseudocrypturgus camerunus* Eggers (NHMW). Holotype of *Microborus boops* Blandford (BMNH).

Diagnosis. Distinguished from *M. brevisetosus* and *M. boops* by the smooth and glabrous frons, the glabrous central area of the ventrites, the smooth posterior face of the protibiae, subconfluent strial punctures, and the slightly stouter body shape.

Description (male and female). *Length* 1.5 mm, 2.4 × longer than wide. *Colour* reddish brown, pronotum darker.

Head. Eyes separated above by 0.7 × their width. Frons smooth, shiny and lightly punctured, vestiture consisting of <10 short setae on epistoma and 2 longer setae between eyes.

Pronotum smooth, shiny, with densely placed puntures.

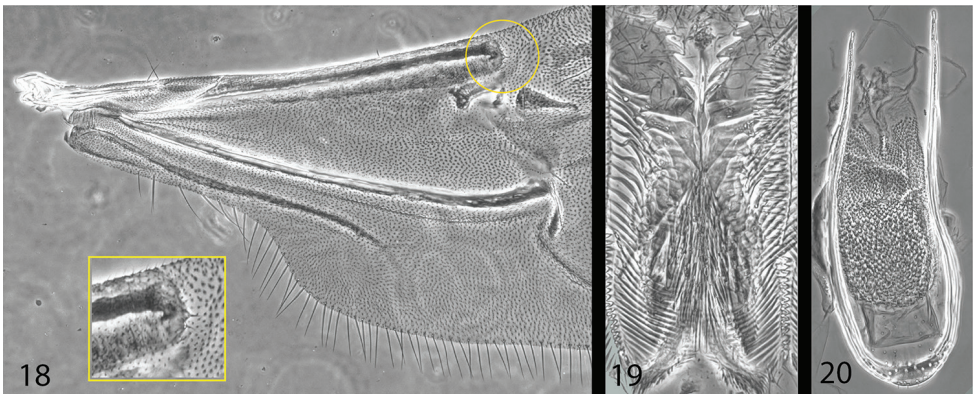

Figures 18–20. Internal features of *Microborus angustus*. **18** wing base **19** proventriculus **20** aedeagus.

Elytra with striae impressed, punctures deep, subconfluent; interstriae about as broad as striae, with very fine irregularly spaced punctures; postero-lateral (interstrial) rim slightly elevated with 2–3 blunt granules. Vestiture consisting of scattered erect, golden setae on discal interstriae, somewhat shorter on declivity.

Legs. Protibiae with three lateral teeth (embedded denticles), and one additional tooth just above the inner mucro; posterior face smooth.

Ventral vestiture simple, on ventrites consisting of a few irregularly placed short setae close to the lateral margins.

Distribution and biology. Known from Ghana, Cameroon and Congo. New record: Cameroon, Mt. Cameroon south slope, 1600 m, GIS: [4.12, 9.16], *Ficus* branch, B. Jordal 28xi-8 [28. Nov. 2007] (ZMBN/ENT_Scol4931, 4941). It was taken together with *M. angustus* under thick bark of large fallen *Ficus* tree (see above).

Key to the Afrotropical species of *Microborus*

1 Nearly black, 2.8 × longer than wide; elytral interstria 7 on declivity sharply raised and almost serrated, with 4–5 sharp tubercles. Cameroon ..... ***M. angustus* Jordal**

– Reddish brown, 2.4–2.6 × longer than wide, elytral interstria 7 on declivity raised, tubercles obscure **2**

2 Strial punctures on elytra separated on average by 0.7–1 × their diameter; ventrites 1–4 with recumbent short setae in transverse row along the posterior edge; frons with >50 small setae, rather dense and moustache-like on epistoma; posterior face of protibiae with 2–5 sharp granules. Madagascar... ..... ***M. brevisetosus* Jordal**

– Strial punctures on elytra confluent or nearly so; ventrites with few short setae scattered along their lateral sides; frons with <10 scattered setae; posterior face of protibiae smooth. Ghana-Congo ..... ***M. camerunus* (Eggers)**

Table 1. Samples included for DNA analyses.

Species	Voucher	Locality	COI	EF-1α	28S	CAD	ArgK	PABP1
Larinus sp.	ClLar01	Russia: Vladivostok	HQ883622	HQ883707	HQ883541	HQ883773	HQ883854	KX160752
Porthetes hispidus	MoPor01	South Africa: Kokstad	HQ883666	HQ883737	HQ883577	HQ883805	HQ883895	KX160765
Microborus aberrans	CtMic07	Brasil: Manaus	MF803724	MF803728	MF803715	MF803720	MF803717	MF803732
Microborus angustus	CtMic03	Cameroon: Mt. Cameroon	HQ883645	–	HQ883560	HQ883788	HQ883874	KU041929
Microborus angustus	CtMic04	Cameroon: Mt. Cameroon	MF803721	MF803725	MF803713	MF803718	MF803716	MF803729
Microborus brevisetosus	CtMic01	Madagascar: Forêt de Tsimembo	HQ883645	HQ883724	HQ883559	HQ883787	–	–
Microborus brevisetosus	CtMic06	Madagascar: Ankarafantsika NP	MF803723	MF803727	–	MF803719	–	MF803731
Microborus camerunus	CtMic05	Cameroon: Mt. Cameroon	MF803722	MF803726	MF803714	–	–	MF803730

Molecular data on Afrotropical species

Gene sequences obtained via PCR are listed by their genbank accession numbers in Table 1. Maximum likelihood and maximum parsimony provided consistent results across analyses, with all nodes maximally supported (Fig. 21). The three Afrotropical species formed a group separate from the single Neotropical species included, *M. aberrans*. *Microborus angustus* was furthermore clearly distinct from the sympatric *M. camerunus* that grouped closely with *M. brevisetosus*, suggesting a role for allopatric divergence prior to the co-existence of *M. angustatus* and *M. camerunus*. Given the limited global scope in this study, it cannot be ruled out that the Afrotropical (or the Neotropical) fauna experienced two origins for this genus.

Despite high morphological similarity, *M. brevisetosus* and *M. camerunus* differed by 15.3–16.1 % at COI. An average divergence of 2.4–3.3% at five nuclear loci leave no doubt about each species validity. The largest nuclear variation was found in 28S (3.9%), a substantial difference for morphologically similar taxa (see e.g. Jordal and Kambestad 2014). Guided by the molecular data, a search for consistent morphological differences was found in the frons, elytral declivity and the venter of these beetles. Hence, the overall similarity that has led previous researchers to synonymise *M. camerunus* with *M. boops* (Wood 1982), emphasizes the need for careful consideration of possible semi-cryptic character differences. The low rate of change in morphological characters for the genus as a whole, as documented by the close similarity to the mid-Cretaceous fossil *M. inertus* Cognato & Grimaldi, 2009 (see Cognato and Grimaldi 2009), makes it advisable to base new synonymies on genetic data and rigorous morphological examination.

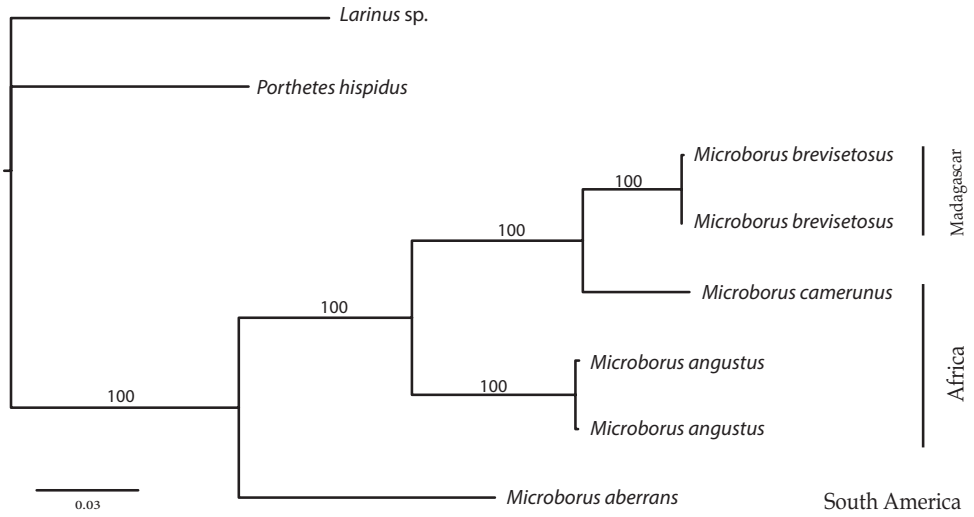

Figure 21. Maximum likelihood phylogeny based on six gene fragments and a GTR model of gene evolution. Tree topology and bootstrap values were identical in the maximum parsimony analysis (L = 1657, CI = 0.85, RI = 072).

Acknowledgements

I would like to thank T.H.Atkinson for providing pictures of two specimens of central American *Microborus boops*.

References

Alonso-Zarazaga MA, Lyal CHC (2009) A catalogue of family and genus group names in Scolytinae and Platypodinae with nomenclatural remarks (Coleoptera: Curculionidae). Zootaxa 2258: 1–134.

Blandford WFH (1897) Family Scolytidae. Biologia Centrali-Americana, Coleoptera 4: 145–184.

Cognato AI, Grimaldi D (2009) 100 million years of morphological conservation in bark beetles (Coleoptera: Curculionidae: Scolytinae). Systematic Entomology 34: 93–100. https://doi.org/10.1111/j.1365-3113.2008.00441.x

Eggers H (1919) 60 neue Borkenkäfer (Ipidae) aus Afrika, nebst zehn neuen Gattungen, zwei Abarten. Entomologische Blätter 15: 229–243.

Jordal BH, Cognato AI (2012) Molecular phylogeny of bark and ambrosia beetles reveals multiple origins of fungus farming during periods of global warming. BMC Evolutionary Biology 12: 133. https://doi.org/10.1186/1471-2148-12-133

Jordal BH, Kambestad M (2014) DNA barcoding of bark and ambrosia beetles reveals excessive NUMTs and consistent east-west divergence across Palearctic forests. Molecular Ecology Resources 14: 7–17. https://doi.org/10.1111/1755-0998.12150

Jordal BH, Sequeira AS, Cognato AI (2011) The age and phylogeny of wood boring weevils and the origin of subsociality. Molecular Phylogenetics and Evolution 59: 708–724. https://doi.org/10.1016/j.ympev.2011.03.016

Pistone D, Mugu S, Jordal BH (2016) Genomic Mining of Phylogenetically Informative Nuclear Markers in Bark and Ambrosia Beetles. PLoS ONE 11: e0163529. https://doi.org/10.1371/journal.pone.0163529

Swofford D (2002) PAUP*. Phylogenetic Analysis Using Parsimony (*and other methods) version 4. Sinauer Associates, Sunderland, Massachusetts.

Wood SL (1982) The bark and ambrosia beetles of North and Central America (Coleoptera: Scolytidae), a taxonomic monograph. Great Basin Naturalist Memoirs 6: 1–1359.

ZooKeys 710: 43–63 (2017)
doi: 10.3897/zookeys.710.14714
http://zookeys.pensoft.net

RESEARCH ARTICLE

A peer-reviewed open-access journal
ZooKeys
Launched to accelerate biodiversity research

An Early Miocene bumble bee from northern Bohemia (Hymenoptera, Apidae)

Jakub Prokop[1], Manuel Dehon[2], Denis Michez[2], Michael S. Engel[3,4]

1 *Department of Zoology, Charles University, Viničná 7, CZ-128 44 Praha 2, Czech Republic* **2** *Laboratory of Zoology, Research Institute of Biosciences, University of Mons, Place du Parc 20, 7000 Mons, Hainaut, Belgium* **3** *Division of Entomology, Natural History Museum, and Department of Ecology & Evolutionary Biology, 1501 Crestline Drive – Suite 140, University of Kansas, Lawrence, Kansas 66045, USA* **4** *Division of Invertebrate Zoology, American Museum of Natural History, Central Park West at 79th Street, New York, New York 10024-5192, USA*

Corresponding authors: *Manuel Dehon* (manuel.dehon@umons.ac.be); *Michael S. Engel* (msengel@ku.edu)

Academic editor: *M. Ohl* | Received 26 June 2017 | Accepted 5 October 2017 | Published 19 October 2017

http://zoobank.org/6A55D61B-A280-48D1-B957-ABC57DE569A0

Citation: Prokop J, Dehon M, Michez D, Engel MS (2017) An Early Miocene bumble bee from northern Bohemia (Hymenoptera, Apidae). ZooKeys 710: 43–63. https://doi.org/10.3897/zookeys.710.14714

Abstract

A new species of fossil bumble bee (Apinae: Bombini) is described and figured from Early Miocene (Burdigalian) deposits of the Most Basin at the Bílina Mine, Czech Republic. *Bombus trophonius* **sp. n.**, is placed within the subgenus *Cullumanobombus* Vogt and distinguished from the several species groups therein. The species is apparently most similar to the Nearctic *B.* (*Cullumanobombus*) *rufocinctus* Cresson, the earliest-diverging species within the clade and the two may be related only by symplesiomorphies. The age of the fossil is in rough accordance with divergence estimations for *Cullumanobombus*.

Keywords

Anthophila, Apoidea, *Bombus*, Burdigalian, geometric morphometrics, Neogene

Introduction

Bumble bees (Bombini: *Bombus* Latreille) are among the most recognized and studied of all bees, second only to the honey bees (Apini: *Apis* Linnaeus) and perhaps tied with the stingless bees (Meliponini). These robust, densely setose, and variably colored species are mainly found in colder temperate regions (Rasmont et al. 2015), and are distributed throughout the Americas, across the Palearctic and Oriental Regions, but are characteristically absent from Africa and Australia (Michener 2007). Together with the orchid bees (Euglossini) and the aforementioned Apini and Meliponini, bumble bees represent one of the four surviving tribal lineages of the corbiculate Apinae (Engel 2001a, Michener 2007). Varied extinct lineages representing stem groups or breaking the otherwise long branches between our modern corbiculates have been discovered from the Paleogene (Cockerell 1908, Engel 1998a, 2001a, Wappler and Engel 2003, Patiny et al. 2007, Engel et al. 2013, 2014), and some of these reveal that the bombine habitus is overall generalized and plesiomorphic for the Corbiculata (*e.g.*, Engel 2001a). These extinct clades are also the fossils for which the most information has been accumulated regarding their pollen-collecting behaviors (Wappler et al. 2015, Grímsson et al. 2017). While controversy remains regarding their relationship to either Meliponini or Meliponini + Apini (*e.g.*, Michener 1990, Schultz et al. 1999, 2001, Engel 2000a, 2001b, Noll 2002, Cardinal and Packer 2007, Kawakita et al. 2008, Kwang et al. 2017), the 263 extant species of Bombini are likely a comparatively young, monophyletic crown group at the apex of an otherwise older lineage diverging from a common ancestor with meliponines and apines sometime in the latest Cretaceous (Engel 2000, 2001a), leaving a ghost record of stem groups between this divergence and perhaps the Early to mid-Eocene. It is possible that the origin of the crown group for bumble bees could have been associated with a global cooling event that occurred during the mid-Eocene (Hansen et al. 2013, Pound and Salzmann 2017). In fact, this same pattern seems to be true also for euglossines (crown group perhaps of Eocene-Oligocene age) and perhaps apines (latest Eocene or earliest Oligocene age), while crown-group meliponines extend back to the Maastrichtian (Michener and Grimaldi 1988, Engel 2000b). In general, the geological history of the corbiculate bees encompasses one of the more extensive records of fossils among the Apoidea (Michez et al. 2012), with diverse representatives spanning the Cenozoic for the highly eusocial Apini (Engel 1998b, 1999a, 2006, unpubl. data, Engel et al. 2009, Kotthoff et al. 2011, 2013) and Meliponini (Michener 1982, Camargo et al. 2000, Engel 2001a, unpubl. data, Greco et al. 2011, Engel and Michener 2013a, 2013b). Fossils of the communal or solitary Euglossini (Engel 1999b, 2014, Hinojosa-Díaz and Engel 2007) and the primitively eusocial Bombini (Michez et al. 2012, Wappler et al. 2012) are less common, and for this reason are of greater interest when new material becomes available. It is in this context that we provide here a descriptive account for a fossil *Bombus* from the Early Miocene of northern Bohemia (Fig. 1), representing an early record of the subgenus *Cullumanobombus* Vogt. We provide this description here so that the species' name might be available for use in a forthcoming work on the general review of fossil record of Bombini (Dehon et al. in prep.).

Material and methods

Geological setting. The Early Miocene coal seam overlaying deposits of the Most Basin at Bílina Mine represents one of the classic paleontological localities in northern Bohemia, studied intensively since the 19th century. The depositional environment and stratigraphy of the upper coal seam deposits at Bílina Mine have been summarized by Kvaček et al. (2004) and updated by Pešek et al. (2014), while the age of the primary insect-bearing layers within the Holešice Member corresponds to the early Burdigalian, from 18–20 Ma (Shrbený et al. 1994, Rajchl et al. 2009). The locality at the time was characterized by a subtropical/warm temperate and temperate climate (Kvaček et al. 2004). The insect fauna at Bílina Mine includes more than 350 specimens of terrestrial and aquatic groups assigned to 31 families in 11 orders (*e.g.*, Prokop and Nel 2000, Prokop 2003, Fikáček et al. 2008), with specimens of Hymenoptera, particularly ants, being most prevalent (Prokop and Nel 2003, Wappler et al. 2014). In addition, the overlaying deposits at Bílina Mine have been studied intensively for their remarkably well-preserved record of plant-arthropod interactions (*e.g.*, Prokop et al. 2010, Knor et al. 2012, 2013). The bumble bee described here is preserved in a fine clay overlaying the coal seam, and has become carbonized, thus the chitinous integument is modified by the process of fossilization (Figs 1–3).

Specimen repository and descriptive terminology. The fossil reported herein was retrieved from the collection of Zdeněk Dvořák, deposited in the museum holdings of the Bílina Mine Enterprises in Bílina, Czech Republic. The specimen was examined dry using a Nikon SMZ 645 stereomicroscope. Photographs were taken using a Canon EOS 550D digital camera coupled to a MP-E 65 mm macro lens. The description is provided here in the aim of improving diagnostic and species-level accounts of living and fossil bees (*e.g.*, Engel 2011, Gonzalez et al. 2013). Morphological terminology follows that of Engel (2001a) and Michener (2007), with the format for the descriptions augmented from those of Wappler et al. (2012) and Dehon et al. (2014).

Geometric morphometric analyses of forewing shape. Prior to description using traditional venational traits, the present fossil was analyzed for its placement among other *Bombus* based on a geometric morphometric analysis of wing shape using vein landmarks. This method has proved useful in placing otherwise difficult to treat fossil species (*e.g.*, Kotthoff et al. 2011, 2013, Dewulf et al. 2014, Dehon et al. 2017), including fossil bombines (Wappler et al. 2012, Dehon et al. in prep.). Geometric morphometric analysis (Pavlinov 2001) of insect wings is a valuable tool given that it is easily implemented, comparatively inexpensive, and the wings themselves are comparatively rigid, two-dimensional structures, species specific, and frequently well preserved in fossil specimens, albeit at times taphonomically distorted. Furthermore, forewing veins and their intersections are homologous among bees with three submarginal cells, like bumble bees (Ross 1936, Michener 2007). The method is rather robust at diagnosing and discriminating taxa at different levels (*e.g.*, Pretorius 2005, Petit et al. 2006, Sadeghi et al. 2009, Francoy et al. 2012, Perrard et al. 2014), and has been employed successfully in palaeontological studies for evaluating the taxonomic affini-

ties of otherwise difficult to determine fossils (*e.g.*, Kennedy et al. 2009, Michez et al. 2009, Dehon et al. 2014, 2017, Dewulf et al. 2014, Perrard et al. 2016). Moreover, several studies have demonstrated the application of forewing shape analyses for discriminating subgenera, species, and populations of bumble bees (*e.g.*, Aytekin et al. 2007, Wappler et al. 2012, Barkan and Aytekin 2013).

Morphometric analyses followed the procedures as outlined by Wappler et al. (2012) and Dehon et al. (2017, in prep.). As in Dehon et al. (2017), we employed three datasets to assess the taxonomic affinities of the fossil at different taxonomic levels by sampling broadly across extant and extinct tribes with the same number of submarginal cells as bumble bees. The first dataset consisted of a comprehensive sampling of bee tribes in order to maximize the shape diversity of our analyses, and this dataset was previously tested by Dehon et al. (2017). The dataset includes 20 specimens and four species per tribe, and whenever possible five specimens per species, and ultimately represented 979 female specimens from seven families, 18 subfamilies, 50 tribes, 135 genera, and 226 species. This first dataset was used to estimate the similarity of the fossil relative to the tribe Bombini (Suppl. material 1), and to determine a group of five tribes (i.e., Ancylaini, Tarsaliini, Emphorini, Euglossini, and Tetrapediini) exhibiting an overall similar wing shape to bumble bees. A second dataset sampled species more extensively across the tribe Bombini and the aforementioned four tribes with similar wing shapes. This was done in order to extend the shape diversity inside the target group. This dataset sampled 15 subgenera and 210 species of bumble bees, accounting for a total of 841 specimens, each species represented by a maximum of five specimens (Suppl. material 2). The dataset represented 100% of the subgeneric diversity and more than 80% of the world's species. In addition, this second dataset included additional Ancylaini and Tarsaliini (two genera, nine species, and 25 specimens), Emphorini (four genera, 12 species, and 28 specimens), Euglossini (five genera, 11 species, and 55 specimens), and Tetrapediini (two genera, seven species, and 26 specimens) in the second dataset. Lastly, after confirmation of the affinities of the fossil with contemporary Bombini based on the second dataset, we considered a third dataset restricted entirely to bumble bee specimens so as to better assess the affinities of the fossil among modern subgenera of *Bombus* (*i.e.*, the dataset from Suppl. material 2 with all groups except Bombini excluded).

For the reference datasets, left forewings were photographed using an Olympus SZH10 microscope combined with a Nikon D200 camera. Photographs were input in the software tps-UTIL 1.69 (Rohlf 2013a). The forewing shape was then captured by digitizing two-dimensional Cartesian coordinates of 18 landmarks on the wing venation and cells (refer to diagram of landmarks presented in Dehon et al., 2017: their figure 1), with the software tps-DIG version 2.27 (Rohlf 2013b). The configurations of the landmarks were superimposed using the GLS Procrustes superimposition in R version 3.0.2 (Rohlf and Slice 1990, Bookstein 1991, Adams and Otárola-Castillo 2013, R Development Core Team 2013). The closeness of the tangent space to the curved shape space was assessed using the software tps-SMALL v1.25 (Rohlf 2013c) by calculating the least-squares regression slope and the correlation coefficient between the Euclidean distances in the tangent space with the Procrustes distances in the shape

space (Rohlf 1999). Prior to assignment of the Bílina fossil, discrimination of the wing shapes of the various taxa was assessed by Linear Discriminant Analyses (LDA) of the projected aligned landmark configurations. We did a LDA with the second dataset (*i.e.*, bumblebees + five similar tribes), with tribe level as *a priori* groupings (Suppl. material 3) (a similar test was already performed for the first dataset by Dehon et al. (2017)). Lastly, we performed a LDA on the third dataset considering the subgenera as *a priori* groupings (Suppl. material 4).

Discriminant analyses were performed by using the software R (R Development Core Team 2013). LDA effectiveness was assessed by the percentages of individuals correctly classified to their original taxon (*i.e.*, hit-ratio) in a leave-one-out (LOO) cross-validation procedure based on the posterior probabilities (pp) of assignment. Given the observed scores of an "unknown", the posterior probability equals the probability of the unit to belong to one group compared to all others. The unit is consequently assigned to the group for which the posterior probability is the highest (Huberty and Olejnik 2006). Taxonomic affinities of the Bílina fossil were assessed based on the score in the predictive discriminant space of shapes. Aligned coordinates of the specimens from the three datasets (including the fossil) were used to calculate the same five LDA as discussed above (*vide supra*). We included *a posteriori* the fossil in the five computed LDA space as an "unknown" specimen and calculated its score. Assignment of the fossil was estimated by calculating the Mahalanobis Distance (MD) between "unknown" and the group mean for each taxon (Suppl. materials 5–7). Principal Component Analyses (PCA) were also computed to visualize shape affinities between the fossil and the extant groups in the last dataset (Fig. 7).

Results

Shape variation within the datasets. Analyses based on the first dataset with family, subfamily, and tribe *a priori* groupings are detailed in Dehon et al. (2017), with contemporary families, subfamilies, and tribes well discriminated. Contemporary tribes are also well discriminated in the second dataset (*i.e.*, *Bombus* s.l. and most similar tribes), with a global hit-ratio of 99.6% (Suppl. material 3). Only the extinct tribes Electrapini and Melikertini are not well discriminated, with hit-ratios of 50.0% and 66.7%, respectively. Contemporary subgenera of *Bombus* s.l. are well discriminated in the bumble bee dataset, with a global hit-ratio of 87.4% and 106 misclassified specimens out of 841. Three subgenera show a hit-ratio of 100%: *Alpinobombus* Skorikov, *Kallobombus* Dalla Torre, and *Mendacibombus* Skorikov. Two subgenera have a hit-ratio between 90.0% and 99.0% – *Cullumanobombus* and *Psithyrus* Lepeletier – while two are poorly discriminated in the LDA – *Melanobombus* Dalla Torre and *Orientalibombus* Richards (72.1% and 70.0%, respectively) (Suppl. material 4). Overall, the results show a great reliability for classifying specimens based on the similarity of their forewing shape relative to our reference dataset of forewings. The cross-validation therefore allows us to be confident in the discrimination.

***A posteriori* assignment of the fossil.** The present fossil was assigned to Apidae, to "Non-parasitic Apidae", and to Bombini by using the first dataset (Suppl. materials 5–7). When using the second dataset the fossil was assigned within *Bombus* s.l. (Suppl. material 8), and to subgenus *Cullumanobombus* by the third dataset (Suppl. material 9) (Fig. 7), although it could not discriminate the species as being part of the stem versus crown group. Accordingly, placement of the fossil from the Bílina Mine within *Cullumanobombus* is strongly supported by forewing shape. Continued work including all known fossil Bombini with living relatives will hopefully further refine this placement (Dehon et al. in prep.), particularly in combination with a heuristic phylogenetic exploration of forewing shape (analogous to that of Dehon et al. 2017).

Systematic paleontology

Genus *Bombus* Latreille, 1802
Subgenus *Cullumanobombus* Vogt, 1911

***Bombus* (*Cullumanobombus*) *trophonius* sp. n.**
http://zoobank.org/9FBA6F95-5C97-4F9E-ABC0-EAA8F73403B7
Figs 1–6

Bombus sp. indet.; Prokop and Nel 2003: 166, Dvořák et al. 2010: 36, 78.

Diagnosis. The new species has a wing shape that is consistent with species of the subgenus *Cullumanobombus* (Dehon et al. in prep.). Within this group, the fossil has a wing pattern most similar to *Bombus* (*Cullumanobombus*) *rufocinctus* Cresson, a species distributed widely across the Nearctic (Milliron 1973, Williams et al. 2014), with both species having a similar combination of 3Rs about as long as r-rs but shorter than 4Rs, the basal vein basad 1cu-a, 2Rs arched posteriorly but not as greatly prolonged proximally as in several other species of *Cullumanobombus* (*e.g.*, Milliron 1971), 1m-cu entering second submarginal cell near midpoint (refer to Discussion). The convex pterostigmal border within the marginal cell, less apically narrowed marginal cell, and less arched 2rs-m minimally serve to distinguish the fossil species from *B. rufocinctus*.

Description. ♀: Wings and integument black as preserved (taphonomically altered; coloration and membrane pigmentation as in life unknown) (Figs 1–3); forewing total length 14.6 mm; maximum width 5.10 mm (Figs 2, 4, 5); basal vein (1M) weakly arched at base, comparatively straight along length, basad 1cu-a by about vein width, in line with 1Rs; Rs+M originating anteriorad, 1Rs slightly shorter than r-rs; pterostigma short, slightly longer than wide, border inside marginal cell convex, prestigma nearly as long as pterostigma; marginal cell length 5.1 mm, width 1.1 mm, tapering slightly across its length, free portion of cell slightly shorter than portion bordering submarginal cells, apex rounded and offset from anterior wing margin by

Figure 1. Photograph of holotype of *Bombus* (*Cullumanobombus*) *trophonius*, sp. n., from the Early Miocene of Bílina Mine in northern Bohemia, Czech Republic.

much more than vein width, not appendiculate; 2Rs strongly arched basally and then gently arched outward, giving second submarginal cell distinct proximal extension; r-rs about as long as 3Rs; 4Rs only slightly longer than 3Rs; three submarginal cells of comparatively similar sizes, albeit third slightly larger than first or second; first submarginal cell length 0.9 mm, width 1.0 mm; second submarginal cell length 1.3 mm, width 0.9 mm; third submarginal cell length 1.6 mm, width 1.2 mm; 1rs-m straight, comparatively orthogonal with Rs; 2rs-m arched distally in posterior half; 1m-cu distinctly angulate anteriorly near M, entering second submarginal cell near cell's midlength; 2m-cu weakly and gently arched apically, meeting third submarginal cell at cell's apical

Figures 2–3. Photographs of wings of holotype of *Bombus* (*Cullumanobombus*) *trophonius*, sp. n. **2** Left forewing and right forewing and hind wing **3** Right hind wing.

fifth of length. Hind wing length 9.4 mm, width 2.6 mm (Figs 3, 6). Preserved portion of thorax and legs difficult to discern and interpret, although portion of metatibial corbicula preserved (basal quarter to third), and most sclerites with numerous, long setae.

♂: *Latet*.

Holotype. ♀ (caste uncertain, likely a worker), ZD0003, Early Miocene, Most Formation, Clayey Superseam Horizon, Holešice Member (No. 30), Bílina Mine near Bílina, Czech Republic; deposited in the museum collection of the Bílina Mine Enterprises, Bílina, Czech Republic.

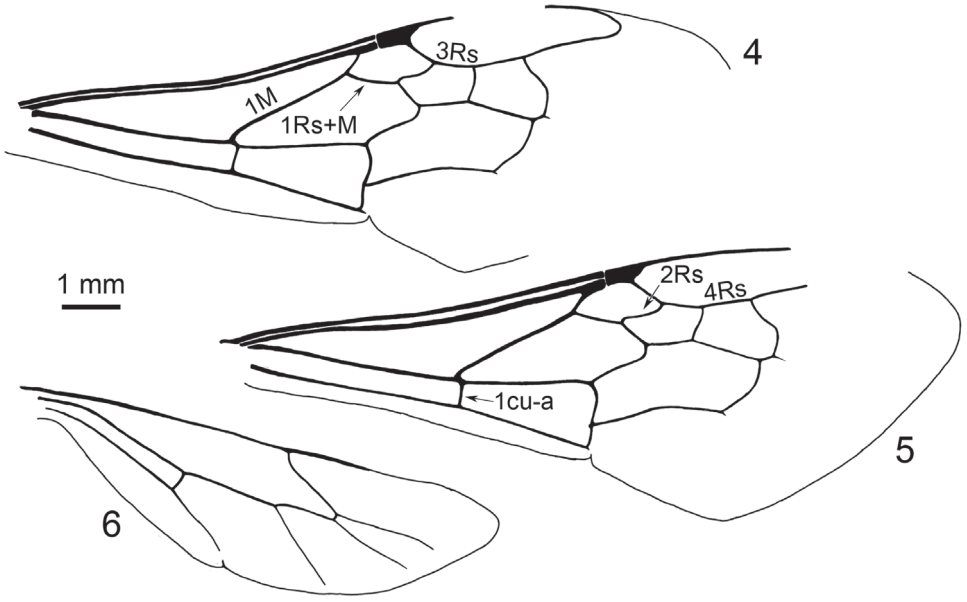

Figures 4–6. Line drawings of wing venation of holotype of *Bombus* (*Cullumanobombus*) *trophonius*, sp. n., as preserved. **4** Left forewing **5** Right forewing **6** Right hind wing.

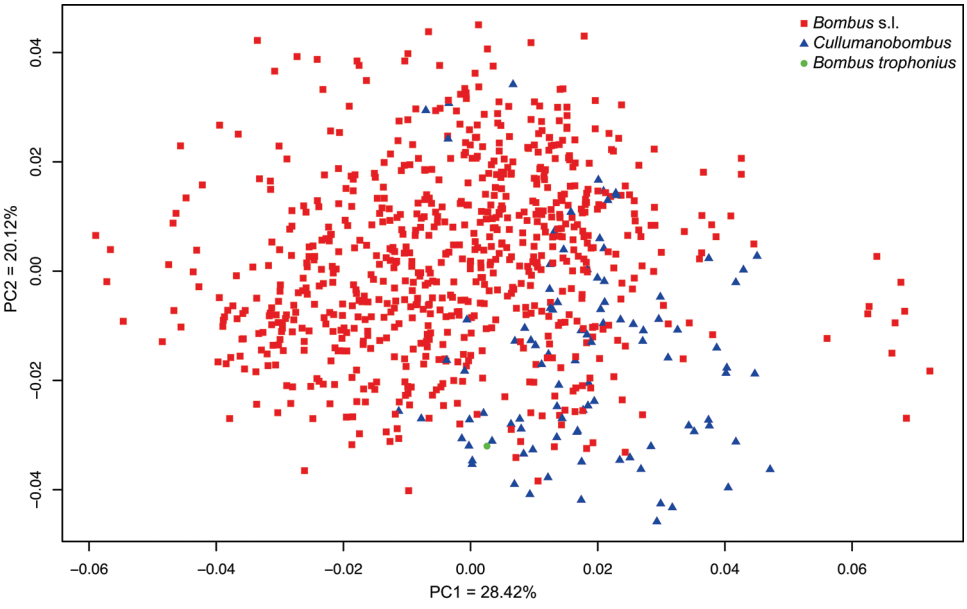

Figure 7. Ordination of the fossil along the two axes of the PCA (PC1 = 28.42% and PC2 = 20.12%) in the *Bombus* s.l. dataset, with extant specimens of *Cullumanobombus* highlighted in blue.

Etymology. The specific epithet is taken from the Greek mythological hero, Trophonius, one of the two brothers who absconded with the treasure of King Hyrieus and who fled into caverns at Lebadaea (today's Livadeia in Boeotia). Trophonius is generally associated with bees and the underworld since, according to legend, it was a swarm of bees that led a boy to rediscover his cave, bringing his spirit honor and peace.

Discussion

Naturally, it is challenging in the absence of clear characters from the head, mandibles, genitalia, or patterns of coloration to make a globally satisfactory assessment of the present fossil. Nonetheless, a morphometric shape analysis of the fossil among other living and fossil bombines confidently placed *B. trophonius* within the subgenus *Cullumanobombus*, in the broad sense as advocated by Williams et al. (2008). Most species of *Cullumanobombus* have New World distributions, except for *B. cullumanus* (Kirby), *B. semenoviellus* Skorikov, *B. unicus* Morawitz, and *B. vogti* Friese which are found in the Old World (Milliron 1973, Williams 1985). The overall combination of wing traits tends to exclude *B. trophonius* from all groups within *Cullumanobombus* with the exception of one. For example, in most species of the *robustus*, *fraternus*, *griseocollis*, *cullumanus*, *rubicundus*, and *brachycephalus* species groups 3Rs is longer than r-rs (rather than about as long as r-rs in *B. trophonius*), and in some, such as the latter two groups, it is also longer than 4Rs (rather than 4Rs longer than 3Rs as is the case in *B. trophonius*). In addition, in several groups 1m-cu enters the second submarginal cell basal its midpoint (*e.g.*, *brachycephalus* and *fraternus* groups), rather than near the midpoint in *B. trophonius*. The second submarginal cell is frequently more pronouncedly elongate proximally, owing to a more dramatically arched 2Rs, in many species of the *rubicundus* and *robustus* groups, while 2rs-m is less arched in the *brachycephalus*, *robustus*, *fraternus*, and *griseocollis* groups and the basal vein and 1cu-a are usually confluent in *B.* (*C.*) *brachycephalus* Handlirsch. The only species within the clade that has the same combination of features as are present in the fossil is *B.* (*C.*) *rufocinctus*. The latter species is common from North Amercia to Mexico. Interestingly, *B. rufocinctus* is considered basal within *Cullumanobombus* (Cameron et al. 2007, Hines 2008), and the overall shared pattern between their wings may be symplesiomorphies (based on the plesiomorphic placement of *B. rufocinctus* and its wing venation relative to more derived species of *Cullumanobombus*), which would be intuitively pleasing if *B. trophonius* were representative of a stem group to the subgenus. In *B. rufocinctus* the marginal cell is often more narrowed apically than in *B. trophonius*, and the former has worker forewing lengths shorter than in the fossil (approximately 11 mm in *B. rufocinctus*, versus over 14 mm in *B. trophonius*). However, queens of *B. rufocinctus* can easily exceed 14 mm in forewing length, and if the holotype of *B. trophonius* was a queen, then the two would be of approximately similar proportions. The age of *B. trophonius* is in general accordance with what one might except of a stem-group *Cullumanobombus* based on the divergence time estimations of Hines (2008). The palaeoclimate of the Bílina

locality was subtropical/warm temperate and temperate (Kvaček et al. 2004), while extant species of *Cullumanobombus* exploit a wide variety of climatic niches, mainly dry and warm, but not boreal. While there remains a plethora of questions regarding the complete characterization of *B. trophonius*, the species apparently represents an important record for *Cullumanobombus* and the discovery of more complete material in the future will undoubtedly continue to bring revelations regarding bumble bee evolution and biogeography during the Neogene.

Acknowledgements

We thank Zdeněk Dvořák (Bílina Mine Enterprises) for access to the collection and loan of the bumble bee described in the present work. The senior author acknowledges financial support from the Grant Agency of the Czech Republic (No. 14-23108S). This is a contribution of the Division of Entomology, University of Kansas Natural History Museum.

References

Adams DC, Otárola-Castillo E (2013) Geomorph: an R package for the collection and analysis of geometric morphometric shape data. Methods in Ecology and Evolution 4(4): 393–399. https://doi.org/10.1111/2041-210X.12035

Aytekin AM, Terzo M, Rasmont P, Çağatay N (2007) Landmark based geometric morphometric analysis of wing shape in *Sibiricobombus* Vogt (Hymenoptera: Apidae: *Bombus* Latreille). Annales de la Sociéte Entomologique de France 43(1): 95–102. https://doi.org/10.1080/00379271.2007.10697499

Barkan NP, Aytekin AM (2013) Systematical studies on the species of the subgenus *Bombus* (*Thoracobombus*) (Hymenoptera: Apidae, *Bombus* Latreille) in Turkey. Zootaxa 3737(2): 167–183. https://doi.org/10.11646/zootaxa.3737.2.5

Bookstein FL (1991) Morphometric tools for landmark data: geometry and biology. Cambridge University Press, Cambridge, 435 pp.

Camargo JMF, Grimaldi DA, Pedro SRM (2000) The extinct fauna of stingless bees (Hymenoptera: Apidae: Meliponini) in Dominican amber: Two new species and redescription of the male of *Proplebeia dominicana* (Wille and Chandler). American Museum Novitates 3293: 1–24. https://doi.org/10.1206/0003-0082(2000)293<0001:TEFOSB>2.0.CO;2

Cameron SA, Hines HM, Williams PH (2007) A comprehensive phylogeny of the bumble bees (*Bombus*). Biological Journal of the Linnean Society 91(1): 161–188.

Cardinal S, Packer L (2007) Phylogenetic analysis of the corbiculate Apinae based on morphology of the sting apparatus (Hymenoptera: Apidae). Cladistics 23(2): 99–118. https://doi.org/10.1111/j.1095-8312.2007.00784.x

Cockerell TDA (1908) Descriptions and records of bees–XX. Annals and Magazine of Natural History, Eighth Series 2(10): 323–334.

Dehon M, Michez D, Nel A, Engel MS, De Meulemeester T (2014) Wing shape of four new bee fossils (Hymenoptera: Anthophila) provides insights to bee evolution. PLOS ONE 9(10): e108865. https://doi.org/10.1371/journal.pone.0108865

Dehon M, Perrard A, Engel MS, Nel A, Michez D (2017) Antiquity of cleptoparasitism among bees revealed by morphometric and phylogenetic analysis of a Paleocene fossil nomadine (Hymenoptera: Apidae). Systematic Entomology 42(3): 543–554. https://doi.org/10.1111/syen.12230

Dewulf A, De Meulemeester T, Dehon M, Engel MS, Michez D (2014) A new interpretation of the bee fossil *Melitta willardi* Cockerell (Hymenoptera, Melittidae) based on geometric morphometrics of the wing. ZooKeys 389: 35–48. https://doi.org/10.3897/zookeys.389.7076

Dvořák Z, Mach K, Prokop J, Knor S (2010) Třetihorní Fauna Severočeské Hnědouhelné Pánve. Nakladatelství Granit, Prague, 175 pp.

Engel MS (1998a) A new species of the Baltic amber bee genus *Electrapis* (Hymenoptera: Apidae). Journal of Hymenoptera Research 7(1): 94–101.

Engel MS (1998b) Fossil honey bees and evolution in the genus *Apis* (Hymenoptera: Apidae). Apidologie 29(3): 265–281. https://doi.org/10.1051/apido:19980306

Engel MS (1999a) The taxonomy of Recent and fossil honey bees (Hymenoptera: Apidae; *Apis*). Journal of Hymenoptera Research 8(2): 165–196.

Engel MS (1999b) The first fossil *Euglossa* and phylogeny of the orchid bees (Hymenoptera: Apidae; Euglossini). American Museum Novitates 3272: 1–14.

Engel MS (2000a) Fossils and phylogeny: A paleontological perspective on social bee evolution. In: Bitondi MMG, Hartfelder K (Eds) Anais do IV Encontro sobre Abelhas. Universidade de São Paulo, Ribeirão Preto, 217–224.

Engel MS (2000b) A new interpretation of the oldest fossil bee (Hymenoptera: Apidae). American Museum Novitates 3296: 1–11. https://doi.org/10.1206/0003-0082(2000)3296<0001:ANIOTO>2.0.CO;2

Engel MS (2001a) A monograph of the Baltic amber bees and evolution of the Apoidea (Hymenoptera). Bulletin of the American Museum of Natural History 259: 1–192. https://doi.org/10.1206/0003-0090(2001)259<0001:AMOTBA>2.0.CO;2

Engel MS (2001b) Monophyly and extensive extinction of advanced eusocial bees: Insights from an unexpected Eocene diversity. Proceedings of the National Academy of Sciences, USA 98(4): 1661–1664. https://doi.org/10.1073/pnas.98.4.1661

Engel MS (2006) A giant honey bee from the middle Miocene of Japan (Hymenoptera: Apidae). American Museum Novitates 3504: 1–12. https://doi.org/10.1206/0003-0082(2006)504[0001:AGHBFT]2.0.CO;2

Engel MS (2011) Systematic melittology: where to from here? Systematic Entomology 36(1): 2–15. https://doi.org/10.1111/j.1365-3113.2010.00544.x

Engel MS (2014) An orchid bee of the genus *Eulaema* in Early Miocene Mexican amber (Hymenoptera: Apidae). Novitates Paleoentomologicae 7: 1–15. https://doi.org/10.17161/np.v0i7.4726

Engel MS, Michener CD (2013a) A minute stingless bee in Eocene Fushan [sic] amber from northeastern China (Hymenoptera: Apidae). Journal of Melittology 14: 1–10.

Engel MS, Michener CD (2013b) Geological history of the stingless bees (Apidae: Meliponini). In: Vit P, Roubik DW (Eds) Stingless Bees Process Honey and Pollen in Cerumen Pots. Facultad de Farmacia y Bioanálisis, Universidad de Los Andes, Mérida, 1–7.

Engel MS, Hinojosa-Díaz IA, Rasnitsyn AP (2009) A honey bee from the Miocene of Nevada and the biogeography of *Apis* (Hymenoptera: Apidae: Apini). Proceedings of the California Academy of Sciences, Series 4 60(3): 23–38.

Engel MS, Ortega-Blanco J, Nascimbene PC, Singh H (2013) The bees of Early Eocene Cambay amber (Hymenoptera: Apidae). Journal of Melittology 25: 1–12. https://doi.org/10.17161/jom.v0i25.4659

Engel MS, Breitkreuz LCV, Ohl M (2014) The first male of the extinct bee tribe Melikertini (Hymenoptera: Apidae). Journal of Melittology 30: 1–18. https://doi.org/10.17161/jom.v0i30.4698

Fikáček M, Hájek J, Prokop J (2008) New records of the water beetles (Coleoptera: Dytiscidae, Hydrophilidae) from the central European Oligocene-Miocene deposits, with a confirmation of the generic attribution of *Hydrobiomorpha enspelense* Wedmann 2000. Annales de la Société Entomologique de France 44(2): 187–199. https://doi.org/10.1080/00379271.2008.10697555

Francoy TM, de Faria Franco F, Roubik DW (2012) Integrated landmark and outline-based morphometric methods efficiently distinguish species of *Euglossa* (Hymenoptera, Apidae, Euglossini). Apidologie 43(6): 609–617. https://doi.org/10.1007/s13592-012-0132-2

Gonzalez VH, Griswold T, Engel MS (2013) Obtaining a better taxonomic understanding of native bees: where do we start? Systematic Entomology 38(4): 645–653. https://doi.org/10.1111/syen.12029

Greco MK, Welz PM, Siegrist M, Ferguson SJ, Gallmann P, Roubik DW, Engel MS (2011) Description of an ancient social bee trapped in amber using diagnostic radioentomology. Insectes Sociaux 58(4): 487–494. https://doi.org/10.1007/s00040-011-0168-8

Grímsson F, Zetter R, Labandeira CC, Engel MS, Wappler T (2017) Taxonomic description of *in situ* bee pollen from the middle Eocene of Germany. Grana 56(1): 37–70. https://doi.org/10.1080/00173134.2015.1108997

Hansen J, Sato M, Russell G, Kharecha P (2013) Climate sensitivity, sea level and atmospheric carbon dioxide. Philosophical Transactions of the Royal Society A 371(2001): 20120294. https://doi.org/10.1098/rsta.2012.0294

Hines HM (2008) Historical biogeography, divergence times, and diversification patterns of bumble bees (Hymenoptera: Apidae: *Bombus*). Systematic Biology 57(1): 58–75. https://doi.org/10.1080/10635150801898912

Hinojosa-Díaz IA, Engel MS (2007) A new fossil orchid bee in Colombian copal (Hymenoptera: Apidae). American Museum Novitates 3589: 1–7. https://doi.org/10.1206/0003-0082(2007)3589[1:ANFOBI]2.0.CO;2

Huberty CJ, Olejnik S (2006) Applied MANOVA and Discriminant Analysis [2nd Edition]. Wiley, New Jersey, 488 pp. https://doi.org/10.1002/047178947X

Kawakita A, Ascher JS, Sota T, Kato M, Roubik DW (2008) Phylogenetic analysis of the corbiculate bee tribes based on 12 nuclear protein-coding genes (Hymenoptera: Apoidea: Apidae). Apidologie 39(1): 163–175. https://doi.org/10.1051/apido:2007046

Kennedy WJ, Reyment RA, MacLeod N, Krieger J (2009) Species discrimination in the Lower Cretaceous (Albian) ammonite genus *Knemiceras* von Buch, 1848. Palaeontographica, Abteilung A: Paläozoologie–Stratigraphie 290(1–3): 1–63. https://doi.org/10.1127/pala/290/2009/1

Knor S, Prokop J, Kvaček Z, Janovský Z, Wappler T (2012) Plant-arthropod associations from the Early Miocene of the Most Basin in North Bohemia – palaeoecological and palaeoclimatological implications. Palaeogeography, Palaeoclimatology, Palaeoecology 321–322: 102–112. https://doi.org/10.1016/j.palaeo.2012.01.023

Knor S, Skuhravá M, Wappler T, Prokop J (2013) Galls and gall makers on plant leaves from the Lower Miocene (Burdigalian) of the Czech Republic: systematic and palaeoecological implications. Review of Palaeobotany and Palynology 188: 38–51. https://doi.org/10.1016/j.revpalbo.2012.10.001

Kotthoff U, Wappler T, Engel MS (2011) Miocene honey bees from the Randeck Maar, southwestern Germany (Hymenoptera, Apidae). ZooKeys 96: 11–37. https://doi.org/10.3897/zookeys.96.752

Kotthoff U, Wappler T, Engel MS (2013) Greater past disparity and diversity hints at ancient migrations of European honey bee lineages into Africa and Asia. Journal of Biogeography 40(10): 1832–1838. https://doi.org/10.1111/jbi.12151

Kvaček Z, Böhme M, Dvořák Z, Konzalová M, Mach K, Prokop J, Rajchl M (2004) Early Miocene freshwater and swamp ecosystems of the Most Basin (northern Bohemia) with particular reference to the Bílina Mine section. Journal of the Czech Geological Society 49(1–2): 1–40.

Kwong WK, Medina LA, Koch H, Sing K-W, Soh EJY, Ascher JS, Jaffé R, Moran NA (2017) Dynamic microbiome evolution in social bees. Science Advances 3(3): e1600513. https://doi.org/10.1126/sciadv.1600513

Latreille PA (1802) Histoire naturelle des fourmis, et recueil de memoires et d'observations sur les abeilles, les araignées, les faucheurs, et autres insectes. Crapelet, Paris, 445 pp.

Michener CD (1982) A new interpretation of fossil social bees from the Dominican Republic. Sociobiology 7(1): 37–45.

Michener CD (1990) Classification of the Apidae (Hymenoptera). University of Kansas Science Bulletin 54(4): 75–163.

Michener CD (2007) The Bees of the World [2nd Edition]. Johns Hopkins University Press, Baltimore, 953 pp. [20 pls.]

Michener CD, Grimaldi DA (1988) A *Trigona* from Late Cretaceous amber of New Jersey (Hymenoptera: Apidae: Meliponinae). American Museum Novitates 2917: 1–10.

Michez D, De Meulemeester T, Nel A, Rasmont P, Patiny S (2009) New fossil evidence of the early diversification of bees: *Paleohabropoda oudardi* from the French Paleocene (Hymenoptera, Apidae, Anthophorini). Zoologica Scripta 38(2): 171–181 https://doi.org/10.1111/j.1463-6409.2008.00362.x

Michez D, Vanderplanck M, Engel MS (2012) Fossil bees and their plant associates. In: Patiny S (Ed.) Evolution of Plant-Pollinator Relationships. Cambridge University Press, Cambridge, 103–164.

Milliron HE (1971) A monograph of the Western Hemisphere bumblebees (Hymenoptera: Apidae; Bombinae). I. The genera *Bombus* and *Megabombus* subgenus *Bombias*. Memoirs of the Entomological Society of Canada 82: 1–80. https://doi.org/10.4039/entm10382fv

Milliron HE (1973) A monograph of the Western Hemisphere bumblebees (Hymenoptera: Apidae; Bombinae). III. The genus *Pyrobombus* subgenus *Cullumanobombus*. Memoirs of the Entomological Society of Canada 91: 239–333.

Noll FB (2002) Behavioral phylogeny of corbiculate Apidae (Hymenoptera; Apinae), with special reference to social behavior. Cladistics 18(2): 137–153. https://doi.org/10.1111/j.1096-0031.2002.tb00146.x

Patiny S, Engel MS, Vanmarsenille P, Michez D (2007) A new record of *Thaumastobombus andreniformis* Engel 2001 in Eocene amber (Hymenoptera: Apidae). Annales de la Société Entomologique de France 43(4): 505–508. https://doi.org/10.1080/00379271.2007.10697540

Pavlinov IY (2001) Geometric morphometrics, a new analytical approach to comparison of digitized images. Information Technology in Biodiversity Research, Abstracts of the 2nd International Symposium, Saint Petersburg, 41–90.

Perrard A, Baylac M, Carpenter JM, Villemant C (2014) Evolution of wing shape in hornets: why is the wing venation efficient for species identification? Journal of Evolutionary Biology 27(12): 2665–2675. https://doi.org/10.1111/jeb.12523

Perrard A, Lopez-Osorio F, Carpenter JM (2016) Phylogeny, landmark analysis and the use of wing venation to study the evolution of social wasps (Hymenoptera: Vespidae: Vespinae). Cladistics 32(4): 406–425. https://doi.org/10.1111/cla.12138

Pešek J, Brož B, Brzobohatý R, Dašková J, Doláková N, Elznic A, Fejfar O, Franců J, Hladilová Š, Holcová K, Honěk J, Hoňková K, Kvaček J, Kvaček Z, Macůrek V, Mikuláš R, Opluštil S, Rojík P, Spudil J, Svobodová M, Sýkorová I, Švábenická L, Teodoridis V, Tomanová-Petrová P (2014) Tertiary Basins and Lignite Deposits of the Czech Republic. Czech Geological Survey, Prague, 284 pp.

Petit D, Picaud F, Elghadraoui L (2006) Géométrie morphologique des ailes des Acrididae (Orthoptera: Caelifera): sexe, stridulation, caractère. Annales de la Société Entomologique de France 42(1): 63–73. https://doi.org/10.1080/00379271.2006.10697450

Pound MJ, Salzmann U (2017) Heterogeneity in global vegetation and terrestrial climate change during the Late Eocene to Early Oligocene transition. Scientific Reports 7: 43386. https://doi.org/10.1038/srep43386

Pretorius E (2005) Using geometric morphometrics to investigate wing dimorphism in males and females of Hymenoptera – a case study based on the genus *Tachysphex* Kohl (Hymenoptera: Sphecidae: Larrinae). Australian Journal of Entomology 44(2): 113–121. https://doi.org/10.1111/j.1440-6055.2005.00464.x

Prokop J (2003) Remarks on palaeoenvironmental changes based on reviewed Tertiary insect associations from the Krušné hory piedmont basins and the České Středohoří Mts in northwestern Bohemia (Czech Republic). Acta Zoologica Cracoviensia 46(Supplement-Fossil Insects): 329–344.

Prokop J, Nel A (2000) *Merlax bohemicus* gen. n., sp. n., a new fossil dragonfly from the Lower Miocene of northern Bohemia (Odonata: Aeshnidae). European Journal of Entomology 97(3): 427–431. https://doi.org/10.14411/eje.2000.065

Prokop J, Nel A (2003) New fossil Aculeata from the Oligocene of the České Středohoří Mts and the Lower Miocene of the Most Basin in northern Czech Republic (Hymenoptera: Apidae, Vespidae). Acta Musei Nationalis Pragae, Series B, Natural History 59(3–4): 163–171 [1 pl.]

Prokop J, Wappler T, Knor S, Kvaček Z (2010) Plant-arthropod associations from the Lower Miocene of the Most Basin in northern Bohemia (Czech Republic): a preliminary report. Acta Geologica Sinica 84(4): 903–914. https://doi.org/10.1111/j.1755-6724.2010.00262.x

R Development Core Team (2013) A language and environment for statistical computing, version 3.0.2, ISBN 3-900051-07-0, R Foundation for Statistical Computing, Vienna.

Rajchl M, Uličný D, Grygar R, Mach K (2009) Evolution of basin architecture in an incipient continental rift: The Cenozoic Most Basin, Eger Graben (central Europe). Basin Research 21(3): 269–294. https://doi.org/10.1111/j.1365-2117.2008.00393.x

Rasmont P, Franzén M, Lecocq T, Harpke A, Roberts SPM, Biesmeijer JC, Castro L, Cederberg B, Dvořák L, Fitzpatrick Ú, Gonseth Y, Haubruge E, Mahé G, Manino A, Michez D, Neumayer J, Ødegaard F, Paukkunen J, Pawlikowski T, Potts SG, Reemer M, Settele J, Straka J, Schweiger O (2015) Climatic risk and distribution atlas of European bumblebees. BioRisk 10: 1–236. https://doi.org/10.3897/biorisk.10.4749

Rohlf FJ (1999) Shape statistics: Procrustes superimpositions and tangent spaces. Journal of Classification 16(2): 197–223. https://doi.org/10.1007/s003579900054

Rohlf FJ (2013a) tpsUTIL Version 1.56. Department of Ecology and Evolution, State University of New York at Stony Brook, New York.

Rohlf FJ (2013b) tpsDIG Version 2.17. Department of Ecology and Evolution, State University of New York at Stony Brook, New York.

Rohlf FJ (2013c) tpsSMALL Version 1.25. Department of Ecology and Evolution, State University of New York at Stony Brook, New York.

Rohlf FJ, Slice D (1990) Extensions of the Procrustes method for the optimal superimposition of landmarks. Systematic Zoology 39(1): 40–59. https://doi.org/10.2307/2992207

Ross HH (1936) The ancestry and wing venation of the Hymenoptera. Annals of the Entomological Society of America 29(1): 99–111. https://doi.org/10.1093/aesa/29.1.99

Sadeghi S, Adriaens D, Dumont HJ (2009) Geometric morphometric analysis of wing shape variation in ten European populations of *Calopteryx splendens* (Harris, 1782) (Zygoptera: Calopterygidae). Odonatologica 38(4): 341–357.

Schultz TR, Engel MS, Prentice M (1999) Resolving conflict between morphological and molecular evidence for the origin of eusociality in the corbiculate bees (Hymenoptera: Apidae): a hypothesis-testing approach. University of Kansas Natural History Museum Special Publication 24: 125–138.

Schultz TR, Engel MS, Ascher JS (2001) Evidence for the origin of eusociality in the corbiculate bees (Hymenoptera: Apidae). Journal of the Kansas Entomological Society 74(1): 10–16.

Shrbený O, Bůžek Č, Čtyroký P, Fejfar O, Konzalová M, Kvaček Z, Malecha A, Šantrůček P, Václ J (1994) Terciér Českého masívu [Tertiary of the Bohemian Massif]. In: Klomínský J (Ed.) Geologický Atlas České Republiky. Stratigrafie [Geological Atlas of the Czech Republic]. Český Geologický Ústav, Prague, map 3. [In Czech and English]

Vogt O (1911) Studien über das Artproblem. 2 Mitteilung. Über das Variieren der Hummeln. 2 Teil. Sitzungsberichte der Gesellschaft Natuforschender Freunde zu Berlin 1911: 31–74.

Wappler T, Engel MS (2003) The middle Eocene bee faunas of Eckfeld and Messel, Germany (Hymenoptera, Apoidea). Journal of Paleontology 77(5): 908–921. https://doi.org/10.1017/S0022336000044760

Wappler T, De Meulemeester T, Aytekin AM, Michez D, Engel MS (2012) Geometric morphometric analysis of a new Miocene bumble bee from the Randeck Maar of southwestern Germany (Hymenoptera: Apidae). Systematic Entomology 37(4): 784–792. https://doi.org/10.1111/j.1365-3113.2012.00642.x

Wappler T, Dlussky GM, Engel MS, Prokop J, Knor S (2014) A new trap-jaw ant species of the genus *Odontomachus* (Hymenoptera: Formicidae: Ponerinae) from the Early Miocene (Burdigalian) of the Czech Republic. Paläontologische Zeitschrift 88(4): 495–502. https://doi.org/10.1007/s12542-013-0212-2

Wappler T, Labandeira CC, Engel MS, Zetter R, Grímsson F (2015) Specialized and generalized pollen-collection strategies in an ancient bee lineage. Current Biology 25(23): 3092–3098. https://doi.org/10.1016/j.cub.2015.09.021

Williams PH (1985) A preliminary cladistic investigation of relationships among the bumble bees (Hymenoptera, Apidae). Systematic Entomology 10(2): 239–255. https://doi.org/10.1111/j.1365-3113.1985.tb00529.x

Williams PH, Cameron SA, Hines HM, Cederberg B, Rasmont P (2008) A simplified subgeneric classification of the bumblebees (genus *Bombus*). Apidologie 39(1): 46–74. https://doi.org/10.1051/apido:2007052

Williams PH, Thorp R, Richardson L, Colla S (2014) Bumble Bees of North America: An Identification Guide. Princeton University Press, Princeton, 208 pp.

Supplementary material 1

Table S1

Authors: Jakub Prokop, Manuel Dehon, Denis Michez, Michael S. Engel

Data type: Microsoft Word Document (.docx)

Explanation note: First dataset for geometric morphometric analyses encompassing 988 specimens from 234 species, 141 genera, 53 tribes, 18 subfamilies, and seven families of Anthophila (Apoidea). All included groups have three submarginal cells. N1= number of species; N2 = number of specimens.

Link: https://doi.org/10.3897/zookeys.710.14714.suppl1

Supplementary material 2

Table S2

Authors: Jakub Prokop, Manuel Dehon, Denis Michez, Michael S. Engel

Data type: Microsoft Excel Worksheet (.xlsx)

Explanation note: Second dataset for the geometric morphometric analyses. This sample includes 872 specimens from 247 species, 14 genera, and six tribes of Apidae. N = number of specimens.

Link: https://doi.org/10.3897/zookeys.710.14714.suppl2

Supplementary material 3

Table S3

Authors: Jakub Prokop, Manuel Dehon, Denis Michez, Michael S. Engel

Data type: Microsoft Excel Worksheet (.xlsx)

Explanation note: Specimen assignment in tribes using the cross-validation procedure in the LDA of forewing shape in the "*Bombus* s.l. + comparison groups" dataset. Original groups are along the rows, predicted groups are along the columns. The hit ratio (HR%) is given for each tribe.

Link: https://doi.org/10.3897/zookeys.710.14714.suppl3

Supplementary material 4

Table S4

Authors: Jakub Prokop, Manuel Dehon, Denis Michez, Michael S. Engel

Data type: Microsoft Excel Worksheet (.xlsx)

Explanation note: Specimen assignment in subgenera using the cross-validation procedure in the LDA of forewing shape in the dataset of *Bombus* s.l. Original groups are along the rows, predicted groups are along the columns. The hit ratio (HR%) is given for each subgenus.

Link: https://doi.org/10.3897/zookeys.710.14714.suppl4

Supplementary material 5

Table S5

Authors: Jakub Prokop, Manuel Dehon, Denis Michez, Michael S. Engel

Data type: Microsoft Excel Worksheet (.xlsx)

Explanation note: Mahalanobis distances (MD) between familial centroids and the 979 specimens, and the fossils and familial centroids in the tribal dataset.

Link: https://doi.org/10.3897/zookeys.710.14714.suppl5

Supplementary material 6

Table S6

Authors: Jakub Prokop, Manuel Dehon, Denis Michez, Michael S. Engel

Data type: Microsoft Excel Worksheet (.xlsx)

Explanation note: Mahalanobis distances (MD) between subfamilial centroids and the 979 specimens, and the fossils and subfamilial centroids in the tribal dataset.

Link: https://doi.org/10.3897/zookeys.710.14714.suppl6

Supplementary material 7

Table S7

Authors: Jakub Prokop, Manuel Dehon, Denis Michez, Michael S. Engel

Data type: Microsoft Excel Worksheet (.xlsx)

Explanation note: Mahalanobis distances (MD) between tribal centroids and the 979 specimens, and the fossils and tribal centroids in the tribal dataset.

Link: https://doi.org/10.3897/zookeys.710.14714.suppl7

Supplementary material 8

Table S8

Authors: Jakub Prokop, Manuel Dehon, Denis Michez, Michael S. Engel

Data type: Microsoft Excel Worksheet (.xlsx)

Explanation note: Mahalanobis distances (MD) between tribal centroids and the 975 specimens, and the fossils and tribal centroids in the "*Bombus* s.l. + comparison groups" dataset.

Link: https://doi.org/10.3897/zookeys.710.14714.suppl8

Supplementary material 9

Table S9

Authors: Jakub Prokop, Manuel Dehon, Denis Michez, Michael S. Engel

Data type: Microsoft Excel Worksheet (.xlsx)

Explanation note: Mahalanobis distances (MD) between subgeneric centroids and the 841 specimens, and the fossils and subgeneric centroids in the *Bombus* s.l. dataset.

Link: https://doi.org/10.3897/zookeys.710.14714.suppl9

ZooKeys 710: 65–76 (2017)
doi: 10.3897/zookeys.710.15047
http://zookeys.pensoft.net

RESEARCH ARTICLE

A peer-reviewed open-access journal
ZooKeys
Launched to accelerate biodiversity research

Scolytinae in hazelnut orchards of Turkey: clarification of species and identification key (Coleoptera, Curculionidae)

Celal Tuncer[1], Milos Knizek[2], Jiri Hulcr[3]

1 *Ondokuz Mayis University, Faculty of Agriculture – Department of Plant Protection, Samsun, Turkey* **2** *Forestry and Game Management Research Institute, Jiloviste – Strnady, Praha 5 – Zbraslav, CZ – 156 00, Czech Republic* **3** *School of Forest Resources and Conservation, University of Florida, Gainesville, FL 32611, USA*

Corresponding author: *Celal Tuncer* (celalt@omu.edu.tr)

Academic editor: *M. Alonso-Zarazaga* | Received 13 July 2017 | Accepted 24 September 2017 | Published 19 October 2017

http://zoobank.org/9BA7A937-1165-408D-BD27-F912D1ED2CA7

Citation: Tuncer C, Knížek M, Hulcr J (2017) Scolytinae in hazelnut orchards of Turkey: clarification of species and identification key (Coleoptera, Curculionidae). ZooKeys 710: 65–76. https://doi.org/10.3897/zookeys.710.15047

Abstract

Hazelnut, a very important cash crop in Turkey, is frequently colonized by bark and ambrosia beetle species (*Scolytinae*). Some scolytine species may cause economic damage while other species do not; therefore, proper identification is important in orchard management. Extensive sampling demonstrated that the most common pest species in Turkey's hazelnut orchards are *Anisandrus dispar*, *Xylosandrus germanus*, and *Xyleborinus saxesenii. Hypothenemus eruditus* can also be common, but only colonizes branches that are already dead. *Lymantor coryli*, *Hypoborus ficus*, *Taphrorychus ramicola,* and *Taphrorychus hirtellus* are rare and do not causes damage to live plants. *Xyleborinus saxesenii* appears to have been frequently misidentified and misreported as either *L. coryli* or *Xyleborus xylographus*. The former is rare, and the latter probably does not occur in Turkey. To avoid future misidentifications, a dichotomous identification key is provided for bark and ambrosia beetles of hazelnut orchards in Turkey.

Keywords

ambrosia beetles, bark beetles, pests

Introduction

Turkey is the world's largest hazelnut producer, supplying nearly 80% of the total global production. The plantations in Turkey occupy nearly 690,000 ha (Anonymous 2013), produce 430,000 – 800,000 tons/year (TUIK 2011), and generate approximately 2 billion USD (Anonymous 2016). It is one of the primary cash crops for many farmers, especially in the Black Sea region. Hazelnut crops are also beneficial in that they protect the land against erosion.

Although Turkey is the world's primary hazelnut producer, its productivity per area is lower than that of hazelnut-growing Western countries. Besides agronomic reasons, insect and mite pests appear to be a major impediment to efficient production. Hundreds of insect and mite species have been found to be pests in Turkish hazelnut orchards (Tuncer and Ecevit 1997), ten of which have been classified as significant pests in hazelnut production, including bark and ambrosia beetles.

Bark and ambrosia beetles (Coleoptera: Curculionidae: Scolytinae) are a well-known and diverse group of insects often capable of causing serious damage estimated in millions of US dollars (Knížek and Beaver 2007). They are also one of the major pest groups in Turkish hazelnut orchards (Tuncer and Ecevit 1997). Weakened hazelnut trees are frequently heavily infested and eventually killed by these insects, especially in orchards along the Black Sea coast where drainage problems occur (Tuncer and Ecevit 1997). Other factors that exacerbate bark and ambrosia beetle attacks include placement of hazelnut orchards close to forested areas, and placement on steep slopes; neither situation is typically managed well. Until today, six bark and ambrosia beetle species were reported from Turkish hazelnut orchards: *Anisandrus dispar* (Fabricius, 1792), *Hypothenemus eruditus* (Westwood, 1834), *Lymantor coryli* (Perris, 1855), *Xylosandrus germanus* (Blandford, 1894), *Xyleborinus saxesenii* (Ratzeburg, 1937) and *Xyleborus xylographus* (Say, 1826) (Işık et al. 1987; Ak et al. 2005a, b). Some of these species have also been found in hazelnut orchards in Italy, USA, and elsewhere (Anonymous 1935; Speranza et al. 2009). Because simple chemical control is not feasible due to the phenology and the cryptic nature of these insects (Ak et al. 2005a), it is important to develop a more sophisticated, integrated approach to the prevention of damage. A key step in the development of any integrated pest management program is accurate identification of the involved organisms.

Bark and ambrosia beetles are a diverse group of small insects with uniform morphology making them notoriously difficult to identify (Wood 1982). It appears that earlier reports on the identities of bark and ambrosia beetles in Turkish hazelnut orchards may have been erroneous. Early studies in Turkish hazelnut orchards claimed that there were four bark and ambrosia beetle species, *A. dispar*, *H. eruditus*, *L. coryli,* and *X. xylographus*, but lacked sufficient evidence to support such claims (Işık et al. 1987). Ak et al. (2005a, b) reported the same four species. Neither of these studies reported *X. saxesenii*, yet photographs of alleged *L. coryli* damage actually resemble damage inflicted by *X. saxesenii.* Ak et al. (2010) also recorded *L. coryli* as a new fruit pest of Kiwi using a photograph to support the claim. However, the photograph was actually of *X. saxesenii* and not *L.coryli*. *Xyleborinus saxesenii* was not identified correctly in studies carried out

in Turkish hazelnut orchards until 2013 (Saruhan and Akyol 2013). Additionally, the identification of *X. xylographus* warrants scepticism because this species is distributed in the Nearctic region (Wood and Bright 1992; Knížek 2011); it is not possible to confirm studies (Işık et al. 1987; Ak et al. 2005) reporting occurrence of *X. xylographus* in Turkey, but it is highly probable that the specimens were misidentified *X. saxesenii* (Wood 1982) and the species does not occur in Turkey at all. Though Wood and Bright (1992) claim that *X. saxesenii* is a native species in Turkey, the lack of evidence concerning the species' presence in previous studies involving hazelnut orchards strengthens the assertion that it was a misidentification. Ak et al. (2011) found two species, *A. dispar* and *X. germanus,* in kiwi orchards by ethanol trapping, establishing likely the first record of *X. germanus* in Turkey (Knížek 2011). Recently, more extensive study carried out by Tuncer et al. (unpublished 2012-2016) on bark and ambrosia beetles in hazelnut orchards revealed that *A. dispar, H. eruditus, Hypoborus ficus* Erichson,1836, *L. coryli, Taphrorychus hirtellus* Eichhoff,1878, *X. germanus* and *X. saxesenii* are present.

Without experience in identification, *X. saxesenii* tended to be mistaken for *L. coryli*, and *A. dispar* (male) for *X. germanus.* Frequent misidentification occurred whether the specimen was viewed under a microscope or with the naked eye and are especially troublesome during field studies. Therefore, to prevent future misidentifications of these species and to increase the efficiency of hazelnut pest management, a simple and easy identification key for bark and ambrosia beetles in hazelnut orchards is needed.

Materials and methods

Examined material consisted of samples belonging to five species which were obtained from hazelnut orchards in the mid-Black Sea region. Specimens were collected with ethanol-baited traps as well as extracted from infested hazelnut trunks. Two species (*H. ficus* and *T. hirtellus*) were only obtained by excision directly from hazelnut wood. Though *T. ramicola* and *X. xylographus* were not sampled in this work, they were included in the key due to their presence in early records. *X. xylographus* was provided by the Museum of Entomology (FSCA) at the Division of Plant Industry (DPI) of the Florida Department of Agriculture and Consumer Services, Gainesville, FL, USA. Pictures used in this paper were taken using an Olympus SZX 16 stereomicroscope and Olympus DP72 camera, with STREAM BASIC 1.9 software. HELICON FOCUS 6.2.2 and HELICON FILTER 5.4 were used to stack photos for better depth of field. Studies were carried out in the Forest Entomology laboratory at the School of Forest Resources and Conservation, University of Florida (Gainesville, FL, USA), Department of Plant Protection in Ondokuz Mayis University (Samsun, Turkey), and Department of Forest Protection Service in Forestry and Game Management Research Institute (Jíloviště, Czechia). The nomenclature used by Wood and Bright (1992) as well as later taxonomic and systematic adjustments (Hulcr et al. 2007, Knížek 2011) are followed in this work. The measurement parameters of the species were taken from Pfeffer (1995) and Wood (1982).

Results

A list of the bark and ambrosia beetles present in hazelnut orchards of Turkey is provided in Table 1 (in alphabetical order).

Table 1. Scolytinae species in hazelnut orchards of Turkey and their distribution in Turkey and in the World.

Species	Distribution in Turkey	World distribution
Anisandrus dispar (Fabricius, 1792)	Adana, Ankara, Artvin, Bartın, Bolu, Bursa, Çorum, Denizli, Duzce, Giresun, Gümüşhane, Hatay, İstanbul, Karabük, Kastamonu, Muğla, Niğde, Ordu, Rize, Sakarya, Samsun, Trabzon, Zonguldak, Western Mediterranien	Asia, Europe, Nearctic, Oriental
Hypoborus ficus Erichson, 1836	Adana, İstanbul, İzmir, Mersin, Sakarya	Asia, Europe, North Africa
Hypothenemus eruditus (Westwood, 1834)	Aydın, Mersin, Samsun	Afrotropical, Asia, Australia, Europe, Nearctic, Neotropical, North Africa, Oriental
Lymantor coryli (Perris, 1855)	Düzce, Samsun	Asia, Europe
Taphrorychus hirtellus Eichhoff, 1878	Hatay, İstanbul, Sakarya, Sinop	Asia, Europe, North Africa
Taphrorychus ramicola Reitter, 1895	Bartın, Hatay, Sakarya, Trabzon, Western Mediterranien,	Asia, Europe
Xyleborinus saxesenii (Ratzeburg, 1937)	Amasya, Antalya, Artvin, Bolu, Düzce, Giresun, Hatay, Isparta, İstanbul, Kocaeli, Konya, Mersin, Muğla, Ordu, Rize, Sakarya, Samsun, Sinop, Trabzon, Zonguldak	Afrotropical, Asia, Australia, Europe, Nearctic, Neotropical, North Africa, Oriental
Xylosandrus germanus (Blandford, 1894)	Duzce, Ordu, Samsun	Asia, Europe, Nearctic, Oriental

Key to bark and ambrosia beetles from hazelnut orchards of Turkey

1 Body shortly oval, stout, length-to-width ratio of pronotum 0.6, basal margin of elytra procurved, elevated and armed by marginal crenulations. 1.0–1.3 mm..... tribe ***Hypoborini*, *Hypoborus ficus*** (Figs 1–2)

– Body elongated, cylindrical, length-to-width ratio of pronotum 0.9–1.1, basal margin of elytra straight, transverse, unarmed..... ..... tribes ***Cryphalini, Dryocoetini*** and ***Xyleborini*...2**

2 Body covered with flattened setae or erect scales, particularly the elytral declivity; antennal club segments of approximately the same size, with a distinct partial septum (dark incision) (Fig. 5); 0.7–0.8 mm in ♂, 1.0–1.8 mm in ♀ ... .tribe ***Cryphalini*, *Hypothenemus eruditus*** (Figs 3–5)

- Body mostly shining, covered with fine setae which are not flattened, antennal club rounded, the first segment much more prominent than the second and third, septum absent, (Figs 6–7).. tribes ***Dryocoetini*** and ***Xyleborini*...3**

Figures 1–2. *Hypoborus ficus*, adult. **1** dorsal aspect **2** lateral aspect.

Figures 3–4. *Hypothenemus eruditus*, adult. **3** lateral aspect **4** dorsal aspect.

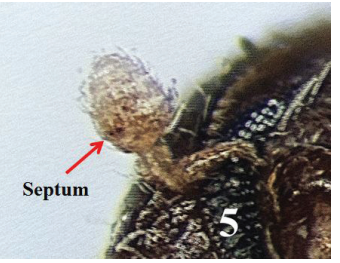

Figures 5–7. Antennal club. **5** *Hypothenemus eruditus* **6** *Lymantor coryli* **7** *Xylosandrus germanus.*

3 First suture on the antennal club procurved, convex, the first segment round (Fig. 6) ; base of pronotum (area adjacent to elytra) coarsely and densely punctured ..... tribe ***Dryocoetini***...**4**

– First suture on the antennal club recurved, concave, the first segment sickle-shaped (Fig. 7). Basal part of pronotum only finely and sparsely punctured, shining or reticulated .....tribe ***Xyleborini***...**6**

4 Pronotum oval from dorsal view, convex with no distinct summit from lateral view, approximately first third asperate, posterior two thirds punctate, smooth and shining in between the punctures, hair-like setae missing in elytral and declivital disc, restricted only along the suture and lateral parts on elytral declivity. 1.6–2.2 mm..... ***Lymantor coryli*** (Figs 8–9)

– Pronotum cylindrical from dorsal view and with an indicated summit from lateral view, first half asperate, posterior half punctate, smooth and shagreened, semi-shining in-between the punctures, elytral vestiture occurring on the whole surface of elytral disc and declivity..... ***Taphrorychus***...**5**

8

9

Figures 8–9. *Lymantor coryli*, adult. **8** dorsal aspect **9** lateral aspect.

5 Pronotum convex with no distinct summit from lateral view; elytra shining, with clearly visible slightly impressed punctured striae. 1.2–2.0 mm..... ..... ***Taphrorychus ramicola*** (Figs 10–11)

– Pronotum clearly marked by summit in the middle from lateral view; elytra matt, without punctured impressed striae. 1.6–1.8 mm..... ..... ***Taphrorychus hirtellus*** (Figs 12–13)

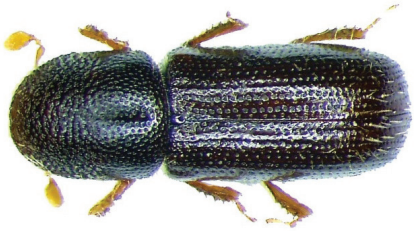

10

11

Figures 10–11. *Taphrorychus ramicola,* adult. **10** dorsal aspect **11** lateral aspect.

Figures 12–13. *Taphrorychus hirtellus*, adult. **12** dorsal aspect **13** lateral aspect.

6 Robust; black or very dark brown when mature; the anterior margin of pronotum with a row of flat teeth (serrations) 7

– Slender; orange to brown, if dark brown then elytra darker than pronotum; the anterior margin of pronotum without elevated teeth (only with asperities appressed to the surface); **8**

7 Procoxae widely separated, the gap wider than antennal scapus (the first long segment) (Fig. 14); surface of the pronotal base shining (Fig. 15). 1.0–1.8 mm in ♂, 2.0–2.3 mm in ♀ ..... ***Xylosandrus germanus*** (Figs 14–17)

– Procoxae only narrowly separated (Fig. 18); the gap not wider than scapus; surface of the pronotal base dull, reticulated, not shining (Fig. 19). 1.8–2.1 mm in ♂, 3.2–3.6 mm in ♀ ..... ***Anisandrus dispar*** (Figs 18–21)

Figures 14–17. *Xylosandrus germanus*. **14** female separation of procoxa **15** female, lateral aspect **16** female, dorsal aspect **17** male, lateral aspect.

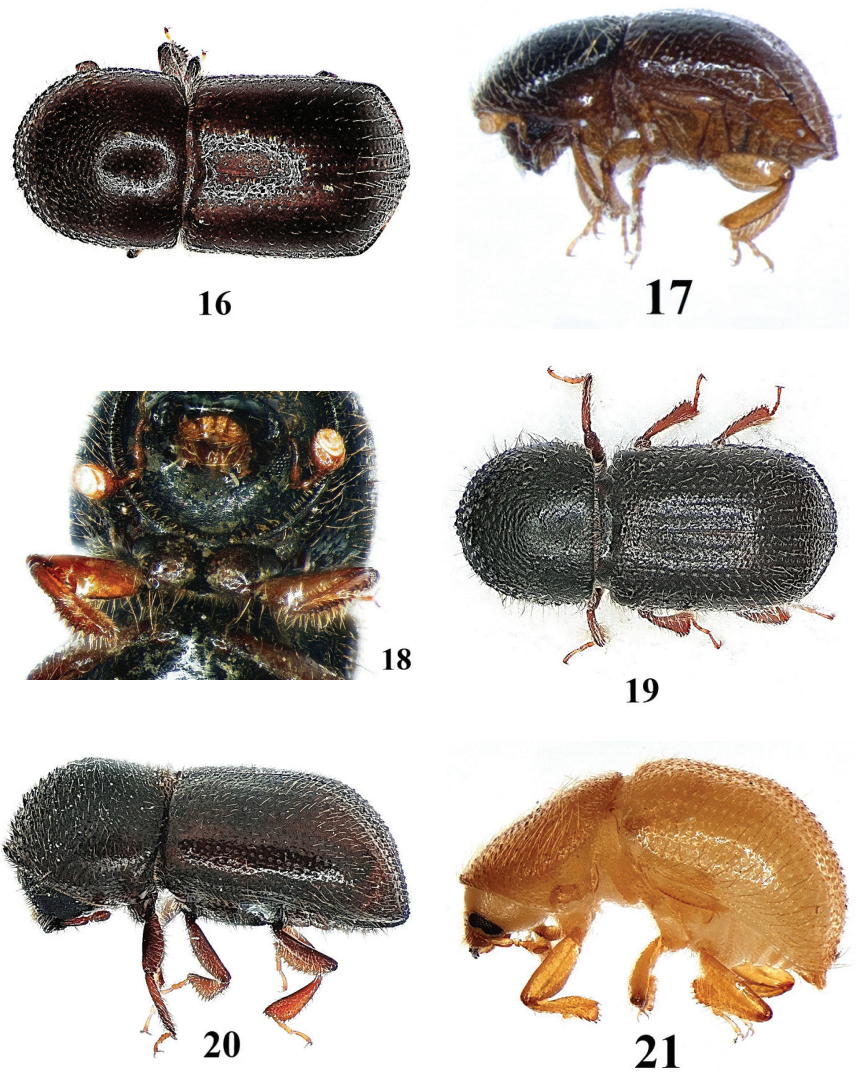

Figures 18–21. *Anisandrus dispar*. **18** female, separation of procoxae **19** female, dorsal aspect **20** female, lateral aspect **21** male, lateral aspect.

8 Scutellum small, conical ("knob-like"), nearly concealed by a tuft of setae (Fig. 22); elytral declivity surrounded by small sharp denticles, but striae 1, 2, and 3 (spaces between rows of punctures) on the declivity without any denticles. 1.6–1.8 mm in ♂, 2.0–2.4 mm in ♀..... ***Xyleborinus saxesenii*** (Figs 22–25)

– Scutellum triangular, flush with surface of elytra, easily visible; all striae on elytral declivity with uniform small dull granules in all striae, 1.9 mm in ♂, 2.3–2.7 mm in ♀..... ***Xyleborus xylographus*** (Figs 26–27)

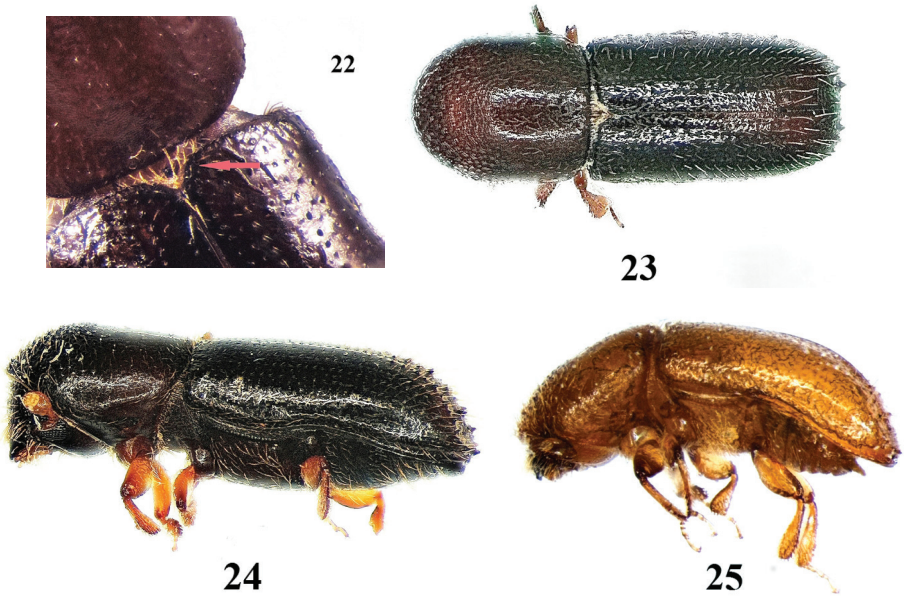

Figures 22–25. *Xyleborinus saxesenii*. **22** female, scutellum **23** female, dorsal aspect **24** female, lateral aspect **25** male, lateral aspect.

Figures 26–27. *Xyleborus xylographus*, female. **23** dorsal aspect **24** lateral aspect.

Discussion

The sampling revealed that *A. dispar*, *X. saxesenii*, *X. germanus*, and *H. eruditus* are common in hazelnut plantations. In addition, a few specimens of *L. coryli, T. hirtellus,* and *H. ficus* were collected by examining the hazelnut tree trunks. It therefore appears that *A. dispar*, *H. eruditus*, *X. germanus,* and *X. saxesenii* are regularly found in hazelnut orchards, while *T. hirtellus* and *L. coryli* are not very common. *Hypoborus ficus* is a common species on fig trees in Turkey (Selmi 1998), and thus was probably

an unusual occurrence in hazelnut. The reports of *X. xylographus* appear to be the result of repeated misidentification (Selmi 1998). We hope this identification key will help prevent future misidentifications of bark and ambrosia beetles in hazelnut and other orchards.

It is worth noting that several species treated here [*A. dispar*, *X. germanus* (Ak et al. 2011), and *X. saxesenii* (Ak et al. 2010)] were also recorded as pests in kiwi orchards, which are grown in the same region of Turkey as hazelnut. Hence, this identification key will also help with studies on kiwi insects.

Additional species are likely to be found on hazelnut in Turkey in the future. One reason is that bark beetle surveys in the country have by no means been comprehensive, and many areas remain to be explored. For example, *Scolytus carpini* (Ratzeburg, 1837) and *Dryocoetes alni* (Georg, 1856) were both reported as pests on hazelnut in western Russia and may also occur in Turkey (Mandelshtam and Nikitsky 2015, Pomerantzev 1903). *Taphrorychus villifrons* (Dufour, 1843) is common in the Black Sea coastal region and is polyphagous in broad-leaved trees (Mandelshtam and Nikisky 2015). Another reason is that several exotic species have established in the region recently and may spread to Turkey. These include *Xyleborinus attenuatus* (Blandford, 1894), a polyphagous ambrosia beetle now common throughout Europe, and *Scolytoplatypus tycon* Blandford, 1893, introduced to Caucasus (Zamotajlov and Nikitsky 2010). Neither of these species was reported from hazelnuts in Turkey yet, but identifiers and pest managers should be aware of the possibility of their presence.

Acknowledgements

We thank to Turkish MEVLANA program and TUBITAK project (TOVAG-111O788) that financially supported the travels for studies in this paper. This research was also partly supported by the project of the Ministry of Agriculture of the Czech Republic – Resolution RO0116 (reference number 10462/2016-MZE-17011), by the USDA Forest Service, USDA Farm Bill Section 10007, the National Science Foundation. The Florida State Collection of Arthropods kindly loaned several specimens. The authors wish to thank Mr. Zachary Nolen (M.Sc.) from University of Florida (USA), who assisted in improving the language of the manuscript, and Drs. Bjarte H. Jordal and Michail Yu. Mandelshtam for their helpful reviews.

References

Ak K, Güçlü Ş, Tuncer C (2010) Kivide Yeni Bir Meyve Zararlısı: *Lymantor coryli* (Perris, 1853) (Coleoptera: Scolytidae). Türkiye Entomoloji Dergisi 34(3): 391–397. http://dergipark.ulakbim.gov.tr/entoted/article/view/5000005919/5000006422

Ak K, Uysal M, Tuncer C (2005a) Giresun, Ordu ve Samsun İllerinde Fındık Bahçelerinde Zarar Yapan Yazıcıböcek (Coleoptera: Scolytidae) Türleri, Kısa Biyolojileri ve Bulunuş

Oranları. Ondokuz Mayıs Üniversitesi Ziraat Fakültesi Dergisi 20(2): 37–44. http://dergi.omu.edu.tr/omuanajas/article/view/1009002328

Ak K, Saruhan İ, Akyol H (2014) Determination of performance of different trap types against *Xyleborus dispar* (Fabricius, 1792) and *Xyleborinus saxesenii* (Ratzeburg, 1837) (Coleoptera: Curculionoidae: Scolytidae). Anadolu Journal of Agricultural Sciences 29(1): 26–35. https://doi.org/10.7161/anajas.2014.29.1.26

Ak K, Saruhan İ, Tuncer C, Akyol H, Kılıç A (2011) Ordu İli Kivi Bahçelerinde Yazıcı böcek (Coleoptera: Scolytidae) türlerinin tespiti ve zarar oranları. Türkiye Entomoloji Bülteni (4): 229–234. http://dergipark.ulakbim.gov.tr/entoteb/article/viewFile/1014000066/1014000076

Ak K, Uysal M, Tuncer C (2006) Yazıcı Böceklerin Samsun İli Fındık Bahçelerindeki Populasyon Değişimi ve Kitle Yakalama Yöntemi Üzerinde Araştırmalar. Selçuk Üniversitesi Ziraat Fakültesi Dergisi 20(39): 16–23. http://stgbd.selcuk.edu.tr/stgbd/ article/viewFile/407/319

Ak K, Uysal M, Tuncer C, Akyol H (2005b) Orta ve Doğu Karadeniz Bölgesinde Fındıklarda Zararlı Önemli Yazıcıböcek (Colepotera:Scolytidae) Türleri ve Çözüm Önerileri. Selçuk Üniversitesi Ziraat Fakültesi Dergisi 19(37): 37–40. http://stgbd.selcuk.edu.tr/stgbd/ article/download/486/391

Anonymous (1935) Walnut and Filbert Blight and Insect Pests and Their Control. Oregon State Agricultural College Extension Service Corvallis, Oregon, March 1935, Extension Bulletin, 476 pp.

Anonymous (2013) T.C. Gümrük ve Ticaret Bakanlığı Kooperatifçilik Genel Müdürlüğü. 2012. Yılı Fındık Raporu, Ankara, 26 pp.

Anonymous (2016) http://www.kib.org.tr/files/downloads/ulke2016.pdf [Accessed: 30.1.2017]

Hulcr J, Dole SA, Beaver RA, Cognato AI (2007) Cladistic review of generic taxonomic characters in Xyleborina (Coleoptera: Curculionidae: Scolytinae). Systematic Entomology 32: 568–584. https://doi: 10.1111/j.1365-3113.2007.00386.x

Işık M, Ecevit O, Kurt MA, Yücetin T (1987) Doğu Karadeniz Bölgesi fındık bahçelerinde entegre savaş olanakları üzerinde araştırmalar. Ondokuz Mayıs Üniversitesi Yayınları No. 20, 95 pp.

Knížek M (2011) Scolytinae, In: Löbl I, Smetana A (Eds) Catalogue of Palaearctic Coleoptera, Apollo Books, Stenstrup 7: 86–87, 204–251.

Knížek M, Beaver RA (2007) Taxonomy and Systematics of Bark and Ambrosia Beetles. In: Lieutier et al. (Eds) Bark and Wood Boring Insects in Living Trees in Europe, A Synthesis, 41–54.

Kurt MA (1982) Doğu Karadeniz Bölgesinde Fındık Zararlıları, Tanınmaları, Yayılış ve Zararları, Yaşayışları ve Savaş Yöntemleri. TOB Zirai Mücadele ve Zirai Karantina Genel Müdürlüğü, Mesleki kitaplar serisi No 26. Ankara, 75 pp.

Löbl I, Smetana A (2011) Catalogue of Palearctic Coleoptera. Vol. 7, Curculionidea I, Apollo Books, 373 pp.

Mandelshtam MYu, Nikitsky NB (2015) Bark beetles (Coleoptera: Curculionidae: Scolytinae) and some other xylophilous and mycetophilous beetles from Streletsky and Kazatsky areas of Tsentral-Chernozem Nature Reserve, Russia. Euroasian Entomological Journal 14(4): 334–341.

Pfeffer A (1995) Zentral- und westpaläarktische Borken- und Kernkäfer (Coleoptera: Scolytidae, Platypodidae). Pro Entomologia, Basel, 310 pp.

Pomerantzev DV (1903) Attacks of *Scolytus carpini* on Corylus [In Russian]. Horae Societatis Entomologicae Rossicae 36: 118–124.

Saruhan İ, Akyol H (2013) Monitoring population density and fluctuations of *Xyleborus dispar* and *Xyleborinus saxesenii* (Coleoptera: Scolytidae) with red winged sticky traps in hazelnut orchards. African Journal of Agricultural Research 8(19): 2189–2194. https://doi: 10.5897/AJAR11.1317

Selmi E (1998) Türkiye kabuk böcekleri ve savaşı. Emek Matbaacılık, İstanbul, 196 pp.

Speranza S, Bucini D, Paparatti B (2009) European shot-hole borer [*Xyleborus dispar* (F.)]: comparison between capture with chemio-chromotropic Rebell Rosso traps and modified Mastrap L traps. Acta Horticulture 845: 535–537. https://doi.org/10.17660/ActaHortic.2009.845.83

TUIK (2011) Tarım İstatistikleri Özeti. The Summary of Agricultural Statistics 2011. Türkiye İstatistik Kurumu (Turkish Statistical Institute), Ankara, 92 pp.

Tuncer C, Ecevit O (1997) Current status of hazelnut pest in Turkey. Acta Hort. 445: 545–552. https://doi.org/10.17660/ActaHortic.1997.445.70

Viggiani G (1984) Avversita, malttie e fitogafi del nocciolo. Regione campania servizio agricoltura, caccia e pesca. Serie manuali 7. Decembre, 1984.

Wood SL (1982) Great Basin Naturalist Memoirs the Bark and Ambrosia Beetles of North and Central America (Coleoptera: Scolytidae), a Taxonomic Monograph. Number 6. Brigham Young University, 1370 pp.

Wood SL, Bright DE (1992) A Catalog of Scolytidae and Platypodidae (Coleoptera), Part 2: Taxonomic Index. Great Basin Naturalist Memoirs (13). Brigham Young University, Provo, Utah, 1553 pp.

Zamotajlov AS, Nikitsky NB (2010) Coleopterous insects (Insecta, Coleoptera) of Republic of Adygheya (annotated catalogue of species). Fauna conspecta of Adygheya. No 1. Adyghei State University Publishers, Maykop, 404 pp.

ZooKeys 710: 77–96 (2017)
doi: 10.3897/zookeys.710.14033
http://zookeys.pensoft.net

RESEARCH ARTICLE

A peer-reviewed open-access journal
ZooKeys
Launched to accelerate biodiversity research

Morphology of the limbs in the semi-fossorial desert rodent species of *Tympanoctomys* (Octodontidae, Rodentia)

M. Julieta Pérez[1], Rubén M. Barquez[2], M. Mónica Díaz[1,2]

1 *PIDBA (Programa de Investigaciones de Biodiversidad Argentina), PCMA (Programa de Conservación de los Murciélagos de Argentina), CONICET (Consejo Nacional de Investigaciones Científicas y Técnicas), Facultad de Ciencias Naturales e IML-Universidad Nacional de Tucumán. Miguel Lillo 251, 4000. Tucumán, Argentina*
2 *Fundación Miguel Lillo. Miguel Lillo 205, 4000. Tucumán, Argentina*

Corresponding author: *M. Julieta Pérez* (mariju_perez@hotmail.com)

Academic editor: *R. López-Antoñanzas* | Received 7 June 2017 | Accepted 26 September 2017 | Published 19 October 2017

http://zoobank.org/4E701E29-1D3E-4092-B150-94BD7C52957B

Citation: Pérez MJ, Barquez RM, Díaz MM (2017) Morphology of the limbs in the semi-fossorial desert rodent species of *Tympanoctomys* (Octodontidae, Rodentia). ZooKeys 710: 77–96. https://doi.org/10.3897/zookeys.710.14033

Abstract

Here, a detailed description of the forelimbs and hindlimbs of all living species of the genus *Tympanoctomys* are presented. These rodents, highly adapted to desert environments, are semi-fossorial with capacity to move on the surface as well as to build burrows. The shape, structure, and size of the limbs are described. Contrary to what was expected for scratch digging semi-fossorial species, *Tympanoctomys* have slender humerus, radius and ulna; with narrow epicondyles of the humerus and short olecranon of the ulna with poorly developed processes. Following our descriptions, no intrageneric morphological variation regarding to the configuration of the limbs was detected, probably due to phylogenetic proximity, and not related to specific variations in response to different use of substrates or habits. The obtained results constitute a source of previously unpublished information as well as an important base for future analysis in different studies, such as morphometric, morpho-functional, or phylogenetic researches.

Keywords

Argentina, Chalchalero Vizcacha Rat, description, morphology

Introduction

Tympanoctomys is member of a clade of the family Octodontidae, restricted to Argentina (Reig 1989; Ojeda et al. 2013; Díaz et al. 2015). Octodontid rodents are highly diverse in eco-morphological aspects, including six genera with terrestrial, semi-fossorial, fossorial and subterranean forms (Ojeda et al. 2013; Verzi et al. 2015). Due to their broad ecological and geographical diversity at both sides of the Andean mountain range, these rodents represent a very interesting group in biogeographical and evolutionary aspects (Lessa et al. 2008; Ojeda 2010; Ojeda et al. 2013).

It was estimated that *Tympanoctomys* diverged about six million years ago (Gallardo and Kirsch 2001) in coincidence with the origin of deserts at Late Miocene (Gallardo et al. 2006); but other authors mentioned different times of divergence from 2.5 to 6.5 million years (see Upham and Patterson 2012; Gallardo et al. 2013; Upham and Patterson 2015; Verzi et al. 2016; Suárez-Villota et al. 2016; Álvarez et al. 2017). This genus is one of the few mammals (all rodents) most highly adapted to desert environments (Mares 1975, 1993; Bozinovic and Contreras 1990; Ojeda et al. 1996; Mares et al. 2000; Honeycutt et al. 2003). *Tympanoctomys* is a polytypic genus containing four living species: *T. aureus*, *T. barrerae*, *T. kirchnerorum*, and *T. loschalchalerosorum*, of which two species were originally described as separate genera (*Pipanacoctomys aureus* and *Salinoctomys loschalchalerosorum*) and *T. kirchnerorum* was recently described from the central Patagonia of Argentina (see Díaz et al. 2000; Barquez et al. 2002; Díaz and Verzi 2006; Gallardo et al. 2004, 2013, 2009; Teta et al. 2014; Díaz et al. 2015). Recently Suárez-Villota et al. (2016) tested the monophyly of these species through a molecular phylogenetic, and the analysis supported the notion that *Salinoctomys* and *Pipanacoctomys* are not distinct from *Tympanoctomys*. These results are in accordance with previous morphological and molecular researches where *Pipanacoctomys* is placed external to *Tympanoctomys-Salinoctomys* (Barquez et al. 2002; Upham and Patterson 2015, 2016).

Tympanoctomys is a small- sized octodontid, with body mass ranging from 67–104 g, head and body length from 130–170 mm (Mares et al. 2000; Teta et al. 2014); *T. aureus* is the largest species in the genus, with head and body length mean of 170 mm, *T. barrerae* is a middle size, with head and body length mean of 145 mm, only slightly larger than *T. loschalchalerosorum* (144–156 mm), and finally, *T. kirchnerorum* is the smallest, with head and body length mean of 129.4 mm (Verzi et al. 2015). They are endemic to arid regions of central and western Argentina, within the Monte, Chaco, and Patagonian Desert biomes, inhabiting salt basins, sand dunes, and open scrubland in Catamarca, Chubut, La Rioja, Mendoza, San Juan, La Pampa, and Neuquén provinces (see Verzi et al. 2015). Ecological aspects of the species are poorly known, *T. barrerae* being the best studied. The colonization success and expanded range of *T. barrerae* has been suggested to be the result of a set of behavioral, ecomorphological, and physiological features that allows better utilization of salt basin, open xeric habitats, and hypersaline food resources (Mares et al. 1997; Ojeda et al. 1999; Gallardo et al. 2007; Ojeda et al. 2013).

Members of the genus *Tympanoctomys* have the capability to move on the surface as well as to build complex burrows (Ojeda et al. 2013; Teta et al. 2014; Díaz et al. 2015), a feature that distinguishes the semi-fossorial forms (Eisenberg 1981). According to Lessa et al. (2008), this digging ability is not reflected in substantial changes in the locomotor system of subterranean octodontids, strongly suggesting that during the early evolution of these rodents, behavioral events have preceded and probably promoted subsequent morphological changes. In addition, among fossorial rodents two burrow strategies have been developed: with the incisors (chisel-tooth digging) or with the forelimbs (scratch-digging), while they can use both types or only one of them. The craniodental morphology of *Tympanoctomys* is not similar to that of those corresponding to chisel-tooth digging as the case of *Spalacopus*, subterranean octodontid (Vassallo and Verzi 2001; Bacigalupe et al. 2002; Verzi 2002; Olivares et al. 2004; Lessa et al. 2008; Becerra et al. 2012). Based on this idea, some authors have analyzed skeletal features in few related genera and members of the family, but including only one species of *Tympanoctomys* (*T. barrerae*), proposing novel functional inferences (Morgan and Verzi 2006; Lessa et al. 2008; Morgan 2009; Morgan and Verzi 2011; Morgan and Álvarez 2013).

However, studies of postcranial anatomy of this genus are insufficient. The objective of our research was to describe in detail the morphology of the forelimbs and hindlimbs of all species of the genus *Tympanoctomys*, mainly analyzing shape and size of some elements. Expecting to generate new data set that allow infer correlation between postcranial morphology and digging strategy.

Materials and methods

Sixty specimens of all the living species of the genus *Tympanoctomys* were examined: *Tympanoctomys aureus* (22), *Tympanoctomys barrerae* (35), *Tympanoctomys kirchnerorum* (2), and *Tympanoctomys loschalchalerosorum* (1). All with complete postcranial skeletons deposited in three argentine collections, CML (Colección Mamíferos Lillo; Universidad Nacional de Tucumán, Tucumán), CNP (Colección de Mamíferos "Elio Massoia", Centro Nacional Patagónico, Puerto Madryn, Chubut), and CMI (Colección de Mamíferos IADIZA, Mendoza). Also, four individuals of *Ctenomys opimus* were measured for comparisons with the species of *Tympanoctomys*. The specific localities and collection numbers of specimens are given in Appendix I.

The morphology of elements of the stylopodium and zeugopodium, excluding the autopodial elements, of the limbs was described considering form, size, and orientation. For a more comprehensive description, it was divided into A) forelimb: humerus, radius, and ulna; and B) hindlimb: femur, tibia, and fibula. The nomenclature for the anatomical description follows that of previous studies on different groups of mammals (Evans 1993; Argot 2001, 2002, 2003; Sargis 2001, 2002a, b; Horovitz and Sánchez-Villagra 2003; Bezuidenhout and Evans 2005; Selthofer et al. 2006; Flores and Díaz 2009; Morgan and Verzi 2011). The anterior and posterior autopodium are not included because they are not complete or conserved in most analyzed specimens.

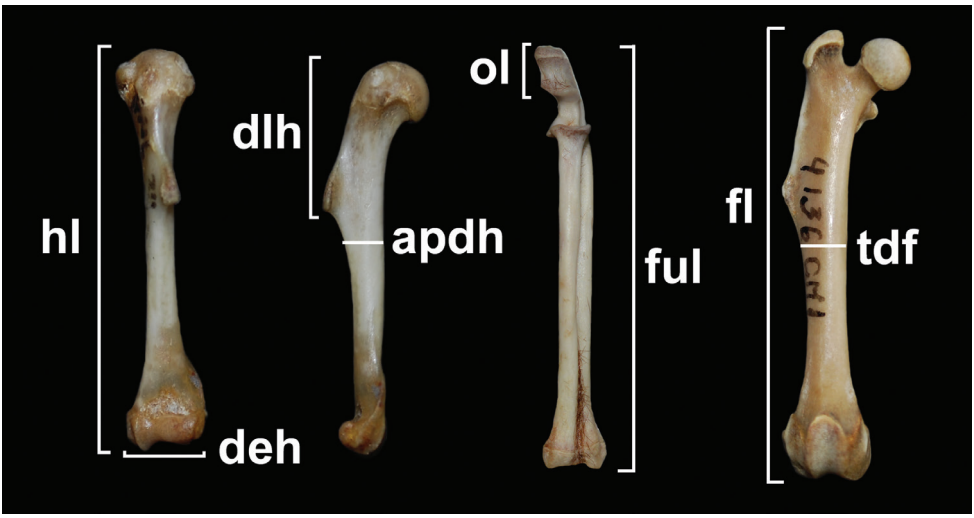

Figure 1. Measurements of the long bones. apdh, anteroposterior diameter of the humerus; deh, diameter of the epicondyles; dlh, deltoid length of the humerus; fl, functional femur length; hl, functional humerus length; ful, functional ulna length; ol, length of the olecranon process; tdf, transverse diameter of the femur.

Based on the previous researches by Biknevicius (1993), Elissamburu and Vizcaíno (2004), Morgan and Verzi (2006), and Hopkins and Samuels (2009), eight measurements of the humerus, ulna, and femur (Fig. 1) corresponding to diameters and functional lengths (length among articular surfaces) of the bones and muscular insertion sites, were taken with digital calipers to the nearest 0.01 mm. Five indexes with functional significance, calculated from linear measurements were selected, based on a qualitative assessment and previous proposals (Bicknevicius et al. 1993; Fernández et al. 2000; Elissamburu and Vizcaíno 2004; Morgan and Verzi 2006). These indexes are: 1) Shoulder moment index (SMI): dlh/hl × 100, where dlh is the deltoid length of the humerus and hl is the functional length of the humerus; this index is an indication of the mechanical advantage of the deltoid and major pectoral muscles acting across the shoulder joint; 2) Epicondyle index (EI): deh/hl × 100, where deh is the epicondylar width of the humerus; this index is considered a good indicator of fossoriality; 3) Humeral robustness index (HWL): apdh/hl × 100, where apdh is the anteroposterior diameter of the humerus; it is a good indicator of general resistance of the bone; 4) Index of fossorial ability (IFA): ol/(ful-ol) × 100, ol is the length of the olecranon process and ful is the functional ulna length; this index gives a measure of the mechanical advantage of the triceps and dorsoepitrochlearis muscles in elbow extension, it is also a good indicator of fossoriality; 5) Femur robustness index (FRI): tdf/fl × 100, where tdf is the transverse diameter of the femur; this index gives an idea of capacity for supporting body mass and to withstand the vertical forces associated with speed increase.

Results

Description

Humerus. The diaphysis is robust with a cross-section angled in *T. loschalchalerosorum* and more cylindrical in the other species (Fig. 2). In all species of *Tympanoctomys*, the head is oval, elongated in the sagittal plane, and becomes narrower distally with a posterior extension forming a "peak" (Fig. 2). In *T. loschalchalerosorum* and *T. barrerae*, the greater and lesser tubercles are separated by a deep and narrow bicipital groove, which is shallower and broader in *T. aureus* and *T. kirchnerorum*. The greater tubercle is oval, has an irregular surface, posteriorly extended, and can be observed in caudal view, with a marked humeral lateral tuberosity. The lesser tubercle is oval and more extended toward the proximo-medial portion in *T. loschalchalerosorum*; furthermore, it is more developed in *T. kirchnerorum* than in the other species, and medially projected. In all analyzed species, the tubercles do not surpass the height of the humeral head (Fig. 2). In *T. loschalchalerosorum* and *T. barrerae,* a small foramen is located between the two tubercles.

The deltoid crest is located, in all species, in the proximal half portion of the diaphysis, it is well developed and greatly expanded laterally in *T. loschalchalerosorum* and *T. barrerae*, and ends as a pointed tip; whereas in *T. aureus* the distal tip is rounded and slightly extends laterally, it is more cranially oriented, similar to *T. kirchnerorum*. In the distal epiphysis, the capitulum is flattened, expanded, and separated from the trochlea by a well-marked groove. The trochlea is broader than the capitulum, is pulley-shaped, and its orientation with respect to the longitudinal axis of the humerus is straight in *T. barrerae* and oblique in the other species. The lateral epicondylar crest is well developed in *T. loschalchalerosorum* (Fig. 2C) in comparison to the other species, whereas the medial epicondyle is equal in size in all species. The supratrochlear foramen is observed in all specimens of all species analyzed (the greatest development was observed in *T. aureus*), except in specimens of *T. barrerae* in which it can be present or absent; when the foramen was completely ossified it was considered as absent. In *T. loschalchalerosorum* and *T. kirchnerorum*, the radial and olecranon fossa are shallow, whereas in *T. aureus* the radial fossa, and in *T. barrerae* the olecranon fossa, are the deepest. In all species analyzed, the entepicondylar foramen is absent and a notch on the articular surface with the radius is observed.

Radius and ulna. In *T. loschalchalerosorum*, *T. barrerae*, and *T. kirchnerorum* the diaphysis of the radius is somewhat cylindrical, with a flat side on the contact surface with the ulna, whereas in *T. aureus* it is more compressed (Figs 3, 4). In the proximal epiphysis, the central fossa of the radius is oval and concave in all species. The anterior edge of the proximal epiphysis (opposed surface to the articulation with the ulna) has a notch (Fig. 3) clearly evident in *T. loschalchalerosorum* and *T. kirchnerorum*, less evident in *T. aureus*, and almost imperceptible in *T. barrerae*. The articular fovea is well-marked and oval in all species, with a less concave surface in *T. aureus* and *T. barrerae*. The neck is well marked, more evident in *T. kirchnerorum*. The radial tuberosity is well developed

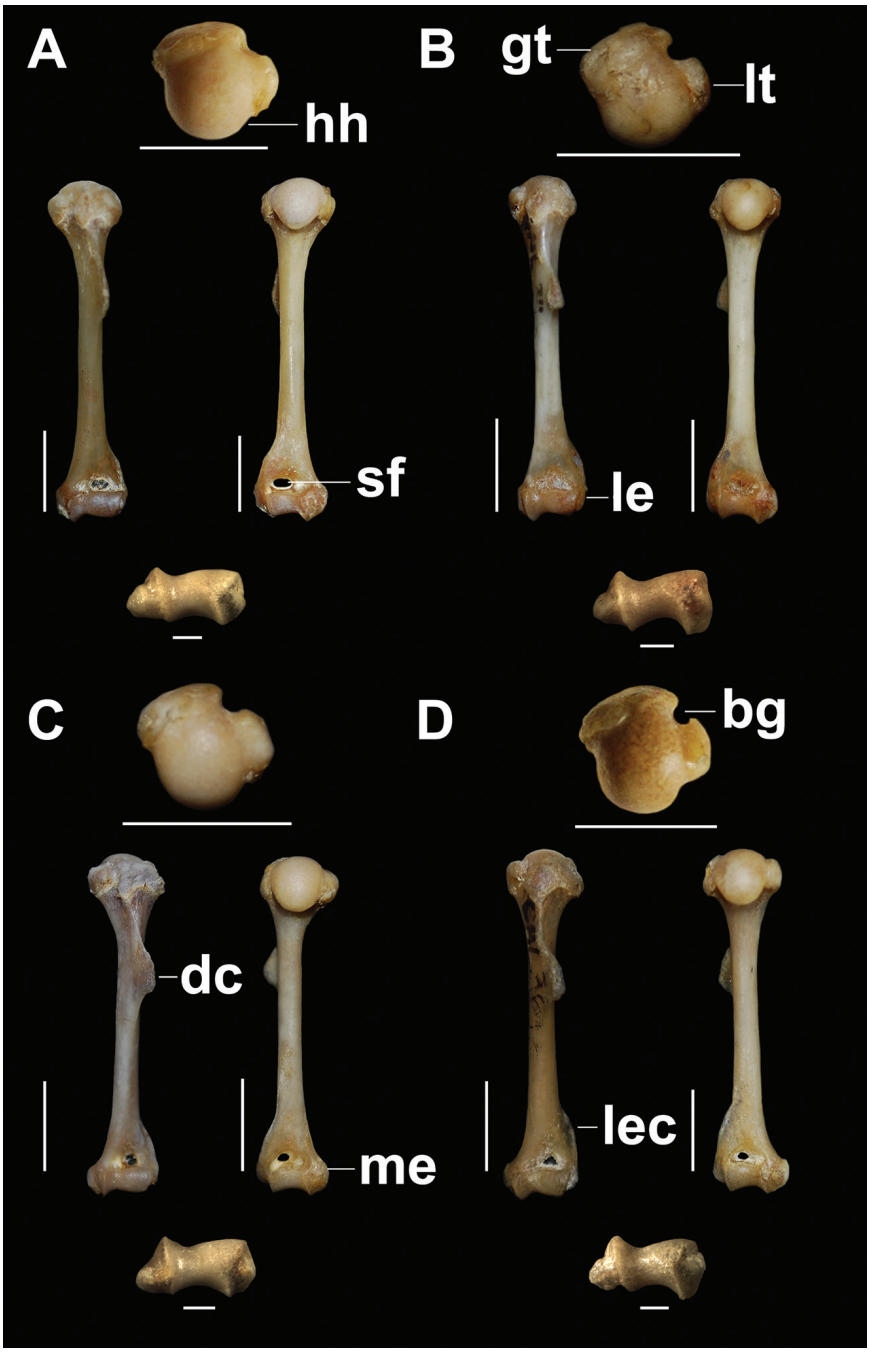

Figure 2. Left humerus, proximal, anterior, posterior, and distal views. **A** *Tympanoctomys aureus* **B** *Tympanoctomys barrerae* **C** *Tympanoctomys kirchnerorum* **D** *Tympanoctomys loschalchalerosorum*. bg, bicipital groove; dc, deltoid crest; gt, greater tuberosity; hh, humeral head; le, lateral epicondyle; lec, lateral epicondylar crest; lt, lesser tuberosity; me, medial epicondyle; sf, supratrochlear foramen. Scale bars 5 mm for all views except distal view where the scale bars are 1 mm.

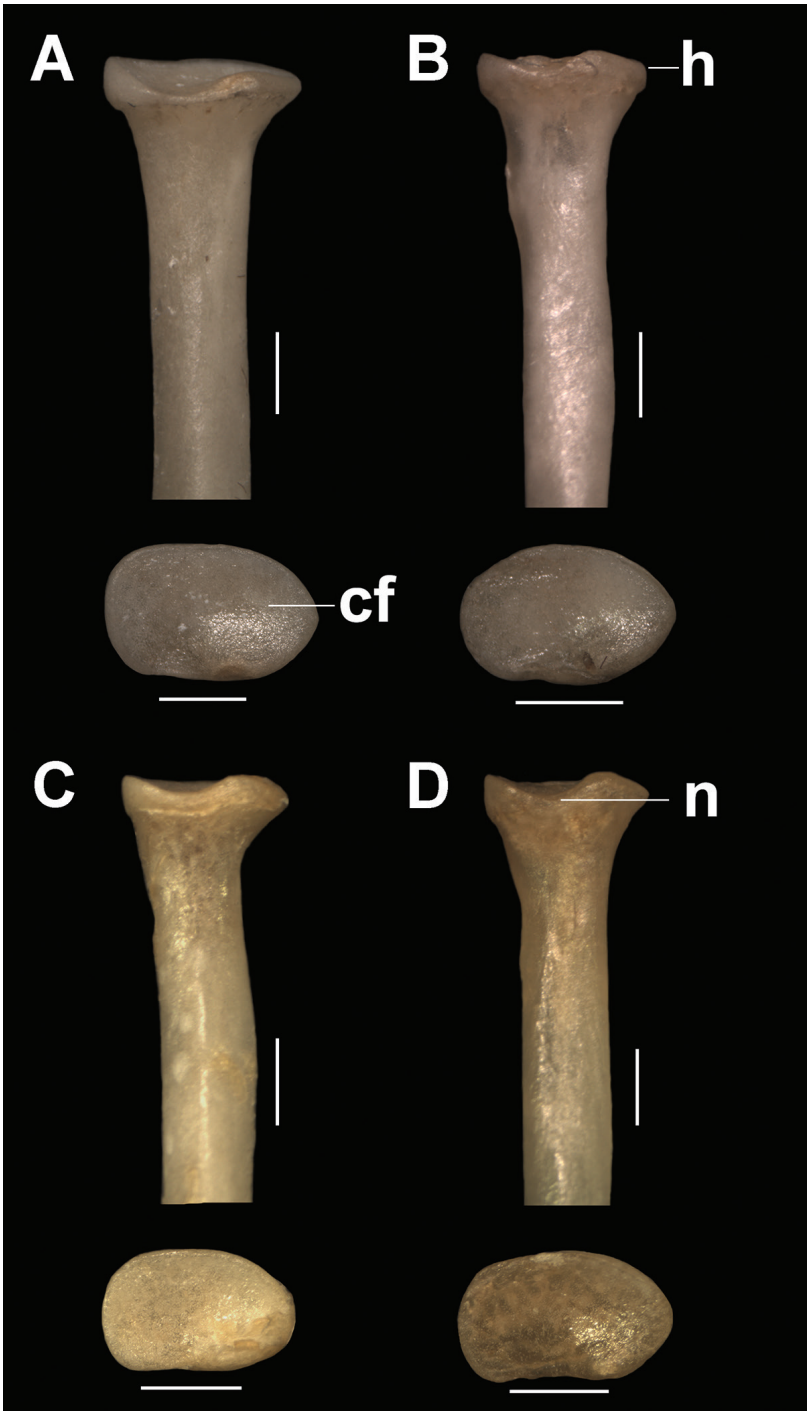

Figure 3. Cranial and proximal views of the proximal portion of the right radio. **A** *Tympanoctomys aureus* **B** *Tympanoctomys barrerae* **C** *Tympanoctomys kirchnerorum* **D** *Tympanoctomys loschalchalerosorum*. cf, central fossa; h, head; n, notch. Scale bars 1mm.

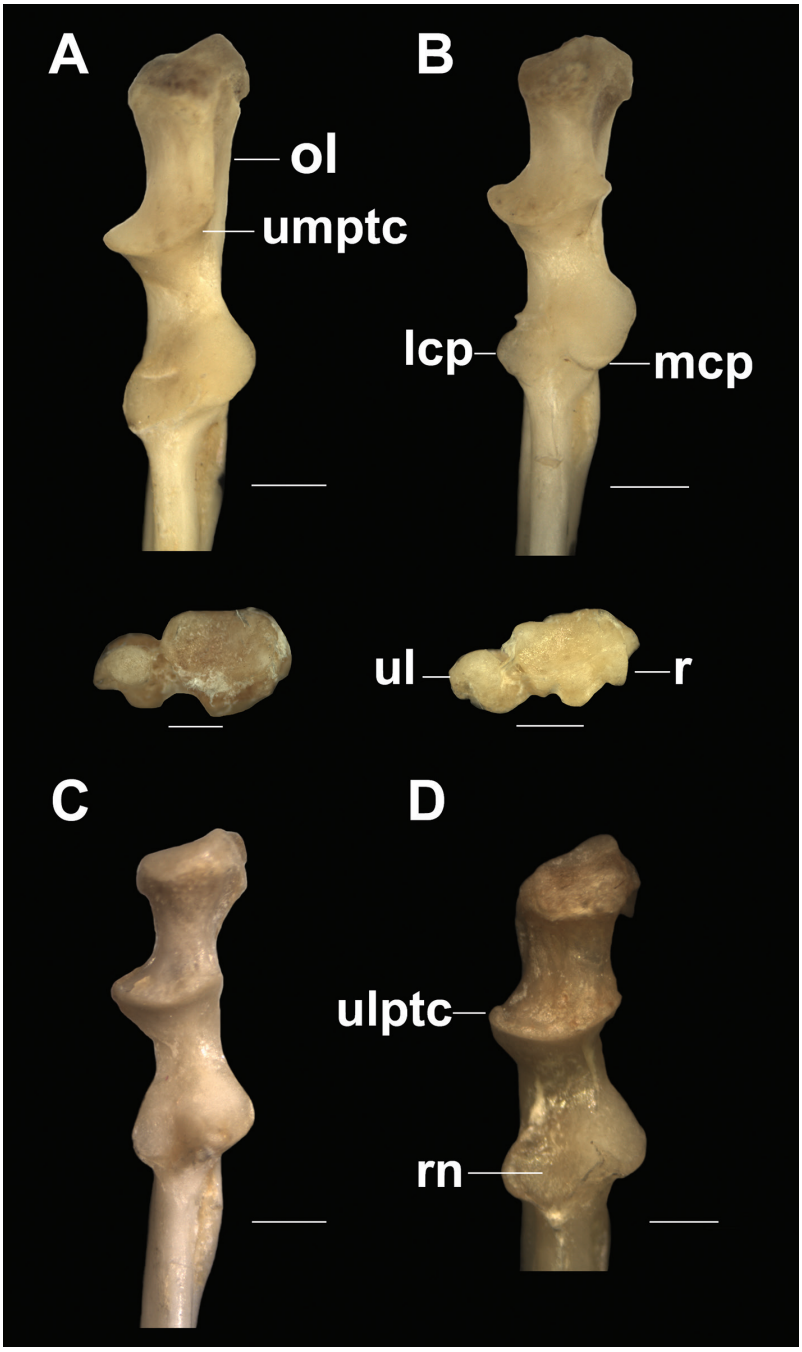

Figure 4. Right ulna, proximal portion in cranial and distal views of radio and ulna. **A** *Tympanoctomys aureus* **B** *Tympanoctomys barrerae* **C** *Tympanoctomys kirchnerorum* **D** *Tympanoctomys loschalchalerosorum*. lcp, lateral coronoid process; mcp, medial coronoid process; ol, olecranon; r, radio distal surface; rn, radial notch; ul, ulnar distal surface; ulptc, ulnar lateral proximal trochlear crest; umptc, ulnar medial proximal trochlear crest. Scale bars 1 mm.

in all species except in *T. barrerae*. The proximal portion of the diaphysis is slightly curved cranially, and the posterior proximal border is straight.

In the ulna (Fig. 4), the olecranon is short, more robust in *T. loschalchalerosorum* (Fig. 4D) and thinner in *T. kirchnerorum* (Fig. 4C) than in the other species. The anconeal process is poorly developed and defined by two small crests: the ulnar lateral proximal trochlear crest (ulptc) and the ulnar medial proximal trochlear crest (umptc). The umptc varies among specimens of *T. aureus*; in the holotype (CML 6137) is similar to the other three species where the angle is not greater than 30°, while in the paratype (CML 4137) and other examined specimens from the CMI, this crest is markedly oblique at an angle of 45° with respect the body axis of the ulna. The trochlear notch is relatively open. The lateral coronoid process is well developed in *T. barrerae* and the holotype of *T. aureus*, less developed in *T. loschalchalerosorum* and *T. kirchnerorum*, and tiny in the paratypes and other specimens examined of *T. aureus*. The medial coronoid process protrudes anteriorly and is less developed in some specimens of *T. aureus*. The radial notch is wide and concave in all species; in *T. loschalchalerosorum* and *T. barrerae* is rounded and oblique, in *T. aureus* it is less oblique and in *T. kirchnerorum* it is almost horizontal (Fig. 4). The lateral fossa is deep in all species.

The distal epiphysis of the radius and ulna are here described for only two species (*T. aureus* and *T. barrerae*), because in other species these structures were broken and missing in the specimens examined. The medial styloid process of the radius is poorly developed in both species; the carpal surface is more concave and triangular in *T. barrerae*, whereas it is crescent-shaped in *T. aureus*. The medial styloid process of the ulna is well developed in both species, being proportionally longer in *T. barrerae*, and rounder in *T. aureus* (Fig. 4)

Femur. The femur is robust with a straight and cylindrical diaphysis. In the proximal epiphysis, the femoral head is spherical and dorso-medially oriented with a short neck (Fig. 5). The greater and lesser trochanters are well developed; the greater trochanter slightly extends dorsally above the head. The lesser trochanter is postero-medially oriented. The third trochanter is poorly developed in *T. loschalchalerosorum*, *T. barrerae*, and *T. kirchnerorum*, and more developed in *T. aureus*. In *T. loschalchalerosorum* the third trochanter lies in the middle of the diaphysis, whereas in *T. barrerae, T. aureus,* and *T. kirchnerorum* it is more proximally located. The trochanteric fossa is well developed in all species, but is deeper in *T. aureus*.

In the distal epiphysis, the lateral condyle is slightly wider than the medial condyle, which is more distally projected. The intercondylar fossa is narrow and deep, being shallower in *T. aureus* and *T. barrerae* than the other two species. The patellar groove is narrow and bordered by two parallel ridges.

Tibia and fibula. In the analyzed specimens of *T. loschalchalerosorum* and *T. kirchnerorum*, the tibias were broken and distal epiphyses were missing, so that many of the characters could not be described (Figs 6, 7). In *T. aureus* and *T. barrerae*, the tibia is approximately 25% longer than the femur. The lateral and medial condyles are oval; in *T. loschalchalerosorum*, they are sub-equal in size (Fig. 7D), whereas in the other species the lateral condyle is slightly larger than the medial condyle. In *T. loschalchalerosorum*,

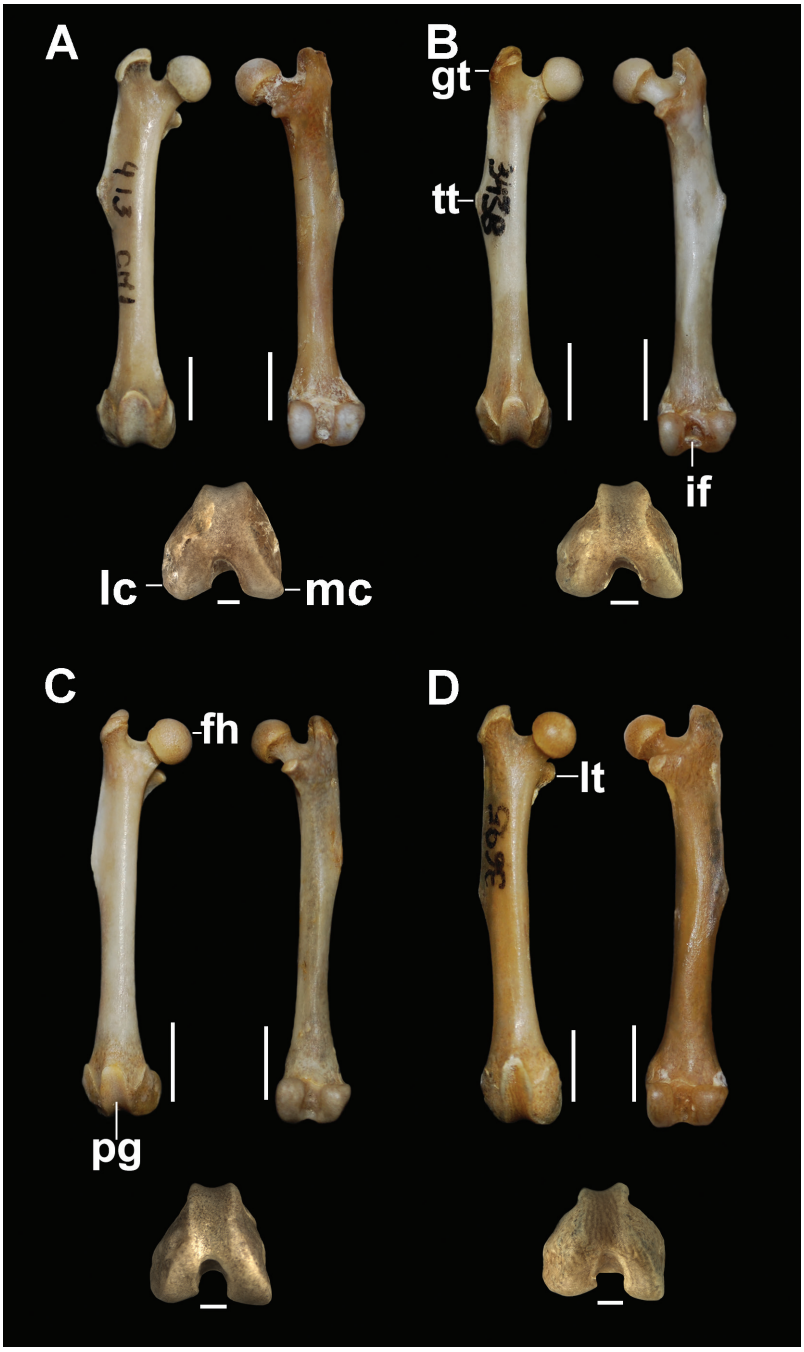

Figure 5. Right femur, anterior, posterior, and distal views. **A** *Tympanoctomys aureus* **B** *Tympanoctomys barrerae* **C** *Tympanoctomys kirchnerorum* **D** *Tympanoctomys loschalchalerosorum*. fh, femoral head; gt, greater trochanter; if, intercondylar fossa; lc, lateral condyle; lt, lesser trochanter; mc, medial condyle; pg, patellar groove; tt, third trochanter. Scale bars 5 mm for all views except distal view where the scale bars are 1 mm.

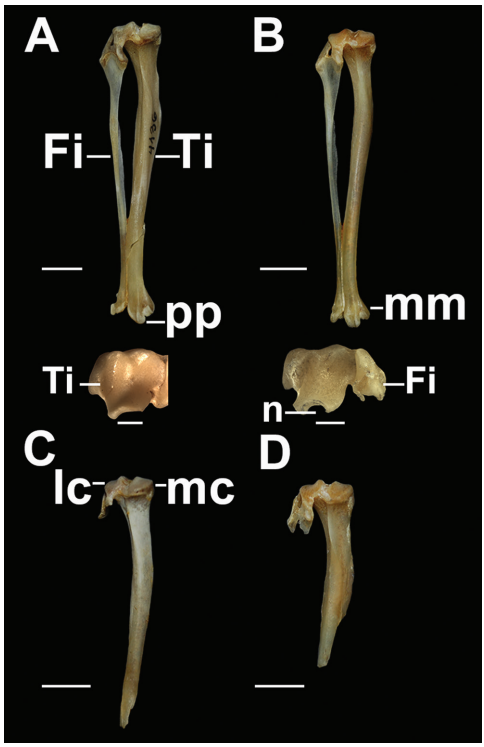

Figure 6. Caudal and distal views of the right tibia and fibula. **A** *Tympanoctomys aureus* **B** *Tympanoctomys barrerae* **C** *Tympanoctomys kirchnerorum* **D** *Tympanoctomys loschalchalerosorum*. Fi, fibula; lc, lateral condyle; mc, medial condyle; mm, medial malleolus; n, notch; pp, posterior process; Ti, tibia. Scale bars 5 mm for all views except distal view where the scale bars are 1 mm.

the two condyles are slightly concave, and tend to be flattened; in *T. barrerae* and *T. kirchnerorum* the lateral condyle is slightly more concave than the medial, and in *T. aureus* the medial condyle is flatter than the lateral (Fig. 7). The lateral condyle is somewhat higher than the medial and has a caudal projection. In *T. loschalchalerosorum* and *T. barrerae*, the intercondylar area is narrow and concave with an evident groove; this intercondylar area is caudally wider in *T. aureus*, and wider and deeper in *T. kirchnerorum*. The popliteal notch is narrow with a well-marked fossa in *T. loschalchalerosorum* and *T. barrerae*, broad and shallower in *T. aureus*, and narrow and deeper in *T. kirchnerorum*. The tibial tuberosity is developed and anteriorly projected below the condyles. In *T. loschalchalerosorum*, the tibial crest is more strongly developed and antero-medially extended, than in the other species, and in *T. barrerae* the crest is located slightly closer to the proximal tip. A caudal crest, observed between the condyles and the popliteal notch, is well developed in *T. loschalchalerosorum*, less developed in *T. barrerae* and *T. kirchnerorum*, and absent in *T. aureus*.

In *T. aureus*, the two foveae on the distal epiphysis are oval, and the medial fovea is narrower and more concave than the lateral one (Fig. 6A). In *T. barrerae* (Fig. 6B),

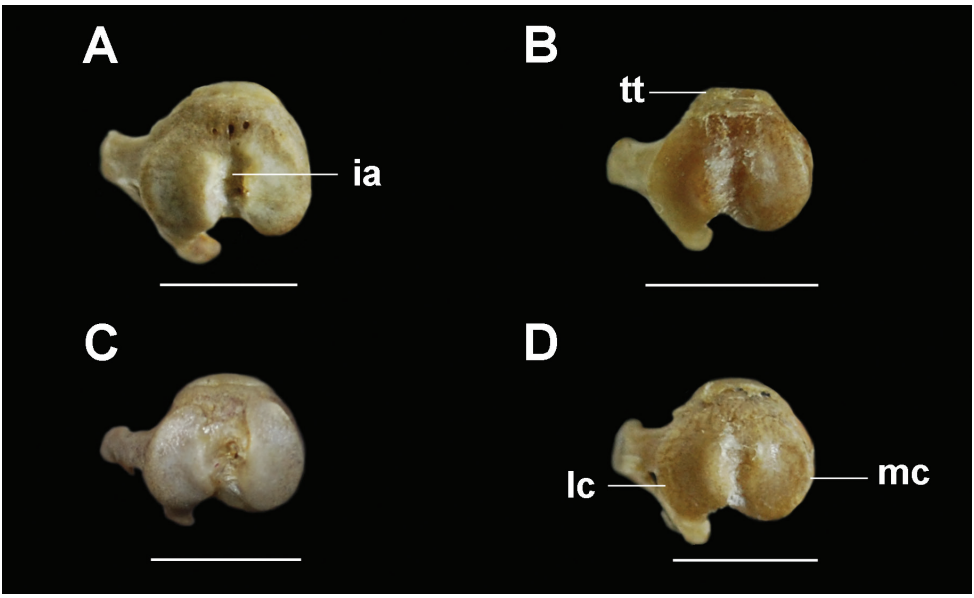

Figure 7. Proximal view of the tibia. **A** *Tympanoctomys aureus* **B** *Tympanoctomys barrerae* **C** *Tympanoctomys kirchnerorum* **D** *Tympanoctomys loschalchalerosorum*. a, intercondylar area; lc, lateral condyle; mc, medial condyle; tt, tibial tuberosity. Scale bars 5mm.

these foveae are more rounded and the medial is also deeper than the lateral, but not as much as in *T. aureus*. The ridge that divides the two foveae is well developed in *T. aureus* and less developed in *T. barrerae*. The medial malleolus is sub-quadrangular, short, and transversally wide in *T. barrerae* and slightly longer and sub-triangular in *T. aureus*. Distal edge of medial malleolus is more pointed in *T. barrerae* than *T. aureus*. In both species, the posterior process and the groove for tendon of *flexor digitorum tibialis* are evident; the posterior edge of the process is concave, but in *T. barrerae* a marked notch is observed (Fig. 6A, B).

The fibula (Fig. 6) shows the distal portion cylindrical and the proximal portion compressed. The head is fan-shaped. In the proximal union with the tibia, a well-developed foramen is observed. The lateral fibular malleolus is more rounded in *T. barrerae* than in the other species, whereas it is slightly elongated with an irregular surface in *T. aureus*.

Indexes. For each species, the results are indicated in Table 1. In the humerus, the averages for the genus are: SMI=42.65, EI=21.6, and HWL=8.76. *Tympanoctomys aureus* shows the highest values of SMI, HWL, and EI. *Tympanoctomys kirchnerorum* has the lowest SMI while *T. loschalchalerosorum* has the lowest HWL. For the ulna, IFA average is 11.56, values are the highest in *T. aureus*, followed by *T. barrerae*, *T. kirchnerorum* and *T. loschalchalerosorum* with the lowest. Finally, in the femur, for FRI the average is 10.03, with the lowest value in *T. kirchnerorum* and the highest in *T. loschalchalerosorum*. Additionally, these indexes were also calculated for *C. opimus* for

Table 1. Mean, standard deviation, and number of specimens in brackets are indicated for each index and species.

	T. aureus	*T. barrerae*	*T. kirchnerorum*	*T. loschalchalerosorum*	*Ct. opimus*
SMI	44.43 1.76 (21)	42.96 2.05 (30)	41.44 1.52 (2)	41.77 - (1)	51.45 2.55 (4)
HWL	9.46 0.73 (21)	9.04 0.57 (30)	8.71 0.12 (2)	7.86 - (1)	11.1 0.62 (4)
EI	22.54 0.9 (21)	21 1.3 (30)	21.55 0.58 (2)	21.28 - (1)	30 0.8 (4)
IFA	15.71 3.2 (2)	13.02 1 (4)	9.02 0.02 (2)	8.51 - (1)	20 0.5 (3)
FRI	9.66 0.55 (7)	9.65 0.53 (28)	9.18 0.66 (2)	11.41 - (1)	10.27 0.8 (4)

comparisons with the semifossorial *Tympanoctomys*, and although it has the highest values in most of the indexes, it is worth noting the value of the epicondylar development (EI) of the humerus as well as the fossorial ability (IFA). This analysis is preliminary and aims to help in the description and comparison among species.

Discussion

Generally, most studies have been limited to one species of *Tympanoctomys* (*T. barrerae)* therefore there is almost no information about morphological change within species. This study provides a detailed description of the postcranial elements of the limbs of all species of the genus *Tympanoctomys* including the holotype of *T. loschalchalerosorum*, one of the only two known specimens of this species in the world, and the recently described *T. kirchnerorum*. As taxonomists know, using descriptions based on a single specimen is not the best protocol; nevertheless, it is useful in phylogenetic reconstructions. Because this unique material is not available in systematic collections and the animals are very rare in natural environments, the descriptions presented here represent the first qualitative approach for the species of the genus *Tympanoctomys* and for the genus as such. The information here would be useful for future comparisons with the rest of the octodontids.

The morphological differences among the species of the genus are still under revision. Therefore, here is the importance of including new evidence, such as postcranial characters in phylogenetic analysis. Mares et al. (2000), based on external and cranial morphology, suggested a greater affinity between *T. loschalchalerosorum* and *T. aureus*. However, when a fourth species (*T. kirchnerorum*) was included in the analysis, that

was not previously considered, it might be expected that the relationship among species would be affected. These results show that *T. loschalchalerosorum* shares more attributes (e.g. bicipital groove of the humerus, intercondylar area, and popliteal notch of the tibia) with *T. barrerae* than with the other species. Furthermore, considering the remainder of the postcranial elements, *T. aureus* shows more affinity with *T. kirchnerorum* than with the other species (data unpublished and under analysis data from Pérez 2013).

On the other hand, the postcranial elements of the forelimbs and hind limbs of the four species of the genus show an anatomical plan related to the mode of terrestrial life, consistent with what was observed in other rodents and marsupials, for example the posterior extension of the humeral head forming a "peak", the tubercles not surpassing the head, the separation between the trochlea and the capitulum, the flat or just concave articular surface of the radial notch in the ulna, the diaphysis of the radio curved, the extension of the greater trochanter above the femoral head, the posterior or posteromedial position of the third trochanter, and the asymmetry between the lateral and medial condyles, with the lateral wider (Hatt 1932; Sargis 2002a, b; Argot 2003; Candela and Picasso 2008; Flores and Díaz 2009; Olivares 2009; Carrizo and Díaz 2011). However, because the genus *Tympanoctomys* is semi-fossorial and scratch digging, characteristics in their long bones were expected which reflected their digging habit (Elissamburu and Vizcaíno 2004; Morgan and Verzi 2006; Samuels and Van Valkenburgh 2008, 2009; Salton and Sargis 2008; Hopkins and Davis 2009). Previous studies (e.g. Morgan and Verzi 2006; Lessa et al. 2008) indicate that *Tympanoctomys* as well as *Octodon* and *Aconaemys* are capable of building complex burrows, consisting in oblique tunnels that connect the surface with their nests, including several bifurcations and openings, but in *T. aureus* the tunnels are nearly parallel to the ground surface (M.M. Díaz and R.M. Barquez personal observations). Contrary to what were expected in semi-fossorial species, these rodents have slender humerus, radius and ulna; narrow epicondyles of the humerus and short olecranon of the ulna with poorly developed processes.

Almost all indexes analyzed in *Tympanoctomys* have values below those calculated in *Ctenomys*, except for the robustness of the femur where *T. loschalchalerosorum* shows a higher value. Moreover, the results for SMI, HWL, EI and IFA in *T. aureus* has higher values among *Tympanoctomys.* These scores and a lowest value for the robustness of the femur can be related with allometric changes in *T. aureus*, the largest species of the genus. Elissamburu and Vizcaíno, (2004) and Elissamburu and De Santis (2011) analyzed the morphometric variation in other caviomorph rodents to evaluate the fossorial forms in a functional context. Comparing our results, the loadings of the indexes in *Tympanoctomys* are more related to cursorial forms or occasional diggers, like *Dolichotis* or *Microcavia.* Although our analysis is preliminary and serves to quantify what is qualitatively described; in the future deeper studies will be performed including all octodontid taxa.

Lessa et al. (2008), who analyzed and compared certain muscle-skeletal characteristics of Octodontidae, concluded that neither *Octomys* nor *Tympanoctomys* (including

only *T. barrerae*) shows great skeletal adaptations related with digging capacity. The octodontid and ctenomyid rodents, two closely related families, are included within the five extant families of rodents (Geomyidae, Ctenomyidae, Octodontidae, Bathyergidae, and Muridae, including Spalacinae and Rhizomyinae) in which the fossorial and subterranean habits have evolved independently, as a further specialization in close association with the emergence of open environments during mid to late Cenozoic (Lessa et al. 2008). This is especially interesting and encourages the development of studies to learn more the about behavioral and structural adaptations in these families of rodents. Some authors (Elissamburu and Vizcaíno 2004; Morgan and Verzi 2006; Elissamburu and De Santis 2011; Morgan and Álvarez 2013) have studied the adaptations of the forelimbs and hindlimbs, especially the digging capacity of *Ctenomys*, and concluded that the greater development of the medial epicondyle could be an early specialization and one of the main characters by which to recognize the digging fossorial forms. In *Tympanoctomys*, this feature is not observed; it can be related to the fact that this genus occurs in sandy soils then strong modifications of the limbs are not necessary.

Although these results are preliminary, data obtained in this study are consistent with observations made by other authors for other members of the family Octodontidae, and provide information for species that are poorly known or recently described. The family Octodontidae is highly specialized and adapted to living in desert habitats with a wide range of habits in just a few genera, so it is expected that the limbs have modified structures for that purpose. According to our descriptions, there are not too many intrageneric morphological variations regarding to the configuration of the limbs, probably due to phylogenetic proximity, and not related to specific variations in response to different use of substrates or habits. With regard to ecological aspects, just one species (*T. barrerae*) is well known about their burrow system, which is considered as an intermediate level of complexity compared with *Ctenomys* (see Lessa et al. 2008), and something similar was observed by two of the authors (RMB and MMD) in *T. aureus*; nothing is known for the other two species.

Some authors (Upham and Patterson 2012, 2015; Suárez-Villota et al. 2016), through molecular studies, suggested to maintain the four species under the same genus. But Suárez-Villota et al. (2016), in their analysis, do not recognize *T. loschalchalerosorum* as a valid taxon but included within the diversity of *T. barrerae.* As mentioned above, *T. loschalchalerosorum* and *T. barrerae* share several characteristics, but also similarities are observed between *T. aureus* and *T. kirchnerorum* (e.g, shape and orientation of the deltoid crest in the humerus) and *T. aureus* and *T. barrerae* (e.g. depth of intercondylar fossa of the femur). We are currently studying the rest of the postcranial morphology in *Tympanoctomys* like in the other members of the family Octodontidae, in order to understand their evolution in relation to the huge eco-morphological diversity and their origin and time of diversification. Following these proposal, it would be interesting to include information of postcranial morphology as new evidence in comprehensive phylogenetic analysis with all the octodontid members.

Acknowledgements

We thank M. Fernanda López Berrizbeitia for her assistance with the change by Colección Mamíferos Lillo–Universidad Nacional de Tucumán, Ulyses Pardiñas (Centro Nacional Patagónico, Puerto Madryn, Chubut) and Benjamín Bender (IADIZA, Mendoza) for allowing access to the collections. Thanks also to Dr. Emily Oaks who improved the English of the manuscript. This study was founded through a scholarship from CONICET (Consejo Nacional de Investigaciones Científicas y Técnicas).

References

Álvarez A, Moyers Arévalo RL, Verzi DH (2017) Diversification patterns and size evolution in caviomorph rodents. Biological Journal of the Linnean Society 121(4) 907–922. https://doi.org/10.1093/biolinnean/blx026

Argot C (2001) Functional-Adaptive anatomy of the forelimb in the Didelphidae, and the paleobiology of the Paleocene Marsupials *Mayulestes ferox* and *Pucadelphys andinus*. Journal of Morphology 247: 51–79.

Argot C (2002) Functional-Adaptive analysis of the hindlimb anatomy of extant Marsupials and Paleobiology of the Paleocene Marsupials *Mayulestes ferox* and *Pucadelphys andinus*. Journal of Morphology 253: 76–108. https://doi.org/10.1002/jmor.1114

Argot C (2003) Functional-adaptative anatomy of the axial skeleton of some extant marsupials and the paleobiology of the Paleocene marsupials *Mayulestes ferox* and *Pucadelphys andinus*. Journal of Morphology 255: 279–300. https://doi.org/10.1002/jmor.10062

Bacigalupe LD, Iriarte Díaz J, Bozinovic F (2002) Functional morphology and geographic variation in the digging apparatus of cururos (Octodontidae: *Spalacopus cyanus*). Journal of Mammalogy 83(1): 145–152. https://doi.org/10.1644/1545-1542(2002)083<0145:FMAGVI>2.0.CO;2

Barquez R, Flores DA, Díaz MM, Giannini NP, Verzi DH (2002) Análisis filogenético preliminar de los octodóntinos vivientes basado en caracteres morfológicos. Abstract, XVII Jornadas Argentinas de Mastozoología. Mar del Plata, Argentina.

Becerra F, Vassallo AI, Echeverría A, Casinos A (2012) Scaling and adaptations of incisors and cheek ceeth in caviomorph rodents (Rodentia, Hystricognathi). Journal of morphology 73: 1150–1162. https://doi.org/10.1002/jmor.20051

Bezuidenhout AJ, Evans HE (2005) Anatomy of woodchuck *(Marmota monax)*. Special publicación Nº13. American Society of Mammalogists.

Bozinovic F, Contreras LC (1990) Basal rate of metabolism and temperature regulation of two desert herbivorous rodents: *Octomys mimax* and *Tympanoctomys barrerae*. Oecologia 84: 567–570. https://doi.org/10.1007/BF00328175

Candela A, Picasso MBJ (2008) Functional anatomy of the limbs of Erethizontidae (Rodentia, Caviomorpha): Indicators of locomotor behavior in Miocene porcupines. Journal of morphology 269: 552–593. https://doi.org/10.1002/jmor.10606

Carrizo LV, Díaz MM (2011) Descripción del postcráneo de *Rhipidomys austrinus* y *Graomys griseoflavus* (Rodentia, Cricetidae, Sigmodontidae). Iheringia 101(3): 207–219. https://doi.org/10.1590/S0073-47212011000200008

Díaz GB, Ojeda RA, Gallardo MH, Giannoni SM (2000) *Tympanoctomys barrerae*. Mammalian Species 646: 1–4. https://doi.org/10.1644/1545-1410(2000)646<0001:TB>2.0.CO;2

Díaz MM, Verzi DH (2006) Familia Octodontidae. In: Barquez RM, Díaz MM, Ojeda RA (Eds) Mamíferos de Argentina Sistemática y Distribución. Mendoza: SAREM (Sociedad Argentina para el Estudio de los Mamíferos), 231–236.

Díaz MM, Barquez RM, Verzi DH (2015) Genus *Tympanoctomys*. In: Patton JL, Pardiñas UFJ, D'Elía G (Eds) Mammals of South America, Volume 2, Rodents. Chicago, The University of Chicago Press, lL., 1043–1048.

Eisenberg JF (1981) The mammalian radiations. University of Chicago Press, Chicago.

Elissamburu A, Vizcaíno SF (2004) Limb proportions and adaptations in caviomorph rodents (Rodentia: Caviomorpha). Journal of Zoology 262: 145–159. https://doi.org/10.1017/S0952836903004485

Elissamburu A, De Santis L (2011) Forelimb proportions and fossorial adaptations in the scratch-digging rodent *Ctenomys* (Caviomorpha). Journal of Mammalogy 92(3): 683–689. https://doi.org/10.1644/09-MAMM-A-113.1

Evans HE (1993) Miller's Anatomy of the dog, 3rd edition. W.B. Saunders Company.

Flores DA, Díaz MM (2009) Postcranial skeleton of *Glironia venusta* (Didelphimorpha, Didelphidae, Caluromyinae): Description and functional morphology. Zoosystematics and Evolution 85(2): 311-339. https://doi.org/10.1002/zoos.200900009

Gallardo MH, Kirsch JWA (2001) Molecular relationships among Octodontidae (Mammalia: Rodentia: Caviomorpha). Journal of Mammalian Evolution 8: 73–89. https://doi.org/10.1023/A:1011345000786

Gallardo MH, Bickham JW, Honeycutt RL, Ojeda RA, Köhler N (1999) Discovery of tetraploidy in a mammal. Nature 401: 341. https://doi.org/10.1038/43815

Gallardo MH, González CA, Cebrián I (2006) Molecular cytogenetics and allotetraploidy in the red vizcacha rat, *Tympanoctomys barrerae*. Genomics 88: 214–221. https://doi.org/10.1016/j.ygeno.2006.02.010

Gallardo MH, Kausel G, Jiménez A, Bacquet C, González C, Figueroa J, Köhler N, Ojeda RA (2004) Whole genome duplications in South American desert rodents (Octodontidae). Biological Journal of the Linnean Society 82: 443–451. https://doi.org/10.1111/j.1095-8312.2004.00331.x

Gallardo MH, Suárez-Villota YE, Nuñez JJ, Vargas RA, Haro R, Köhler N (2013) Phylogenetic analysis and phylogeography of the tetraploid rodent *Tympanoctomys barrerae* (Octodontidae): insights on its origin and the impact of Quaternary climate changes on population dynamics. Biological Journal of the Linnean Society 108: 453–469. https://doi.org/10.1111/j.1095-8312.2012.02016.x

Gallardo MH, Udrizar Sauthier DE, Ojeda AA, Pardiñas UFJ (2009) Discovery of desert-adapt in Central Patagonia, Argentina. Mammalia 73: 158–161. https://doi.org/10.1515/MAMM.2009.028

Hatt RT (1932) The vertebral columns of ricochetal rodents. Bulletin of the American Museum of Natural History 63: 599–738.

Honeycutt RL, Rowe DL, Gallardo MH (2003) Molecular systematics of the South American caviomorph rodents: relationships among species and genera in the family Octodontidae. Molecular Phylogenetics and Evolution 26: 476–489. https://doi.org/10.1016/S1055-7903(02)00368-8

Hopkins SSB, Davis EB (2009) Quantitative morphological proxies for fossoriality in small mammals. Journal of Mammalogy 90(6): 1449–1460. https://doi.org/10.1644/08-MAMM-A-262R1.1

Horovitz I, Sánchez–Villagra MR (2003) A morphological analysis of marsupial mammal higher-lever phylogenetic relationships. Cladistics 19: 181–212. https://doi.org/10.1111/j.1096-0031.2003.tb00363.x

Lessa EP, Vasallo AI, Verzi DH, Mora MS (2008) Evolution of morphological adaptations for digging in living and extinct ctenomyid and octodontid rodents. The Linnean Society of London, Biological Journal of the Linnean Society 95: 267–283. https://doi.org/10.1111/j.1095-8312.2008.01057.x

Mares MA (1975) South American mammal zoogeography: evidence from convergent evolution in desert rodents. Proceedings of the National Academy of Science USA 72: 1702–1706. https://doi.org/10.1073/pnas.72.5.1702

Mares MA (1993) Desert rodents, seed consumption, and convergence. BioScience 43: 372–379. https://doi.org/10.2307/1312045

Mares MA, Braun JK, Barquez RM, Díaz MM (2000) Two new genera and species of halophytic desert mammals from isolated Salt Flats in Argentina. Occasional Papers, Museum Texas Tech University 203: 1–27.

Morgan CC (2009) Geometric morphometrics of the scapula of South American caviomorph rodents (Rodentia: Hystricognathi): Form, function and phylogeny. M Gallardo ammalian Biology 74: 497–506. https://doi.org/10.1016/j.mambio.2008.09.006

Morgan CC, Álvarez A (2013) The humerus of South American caviomorph rodents: shape, function and size in a phylogenetic context. Journal of Zoology 290(2): 107–116. https://doi.org/10.1111/jzo.12017

Morgan CC, Verzi DH (2006) Morphological diversity of the humerus of the South American subterranean rodent *Ctenomys* (Rodentia, Ctenomyidae). Journal of Mammalogy 87: 1252–1260. https://doi.org/10.1644/06-MAMM-A-033R1.1

Morgan CC, Verzi DH (2011) Carpal-metacarpal specializations for burrowing in South American octodontoid rodents. Journal of Anatomy 219: 167–175. https://doi.org/10.1111/j.1469-7580.2011.01391.x

Ojeda AA (2010) Phylogeography and genetic variation in the South American rodent, *Tympanoctomys barrerae* (Rodentia: Octodontidae). Journal of Mammalogy 91: 302–313. https://doi.org/10.1644/09-MAMM-A-177.1

Ojeda RA, Gonnet JM, Borghi CE, Giannoni SM, Campos CM, Diaz GB (1996) Ecological observations of the red vizcacha rat, *Tympanoctomys barrerae* in desert habitats of Argentina. Mastozoología Neotropical 3: 183–191.

Ojeda AA, Novillo A, Ojeda RA, Roig-Juñent S (2013) Geographical distribution and ecological diversification of South American octodontid rodents. Journal of Zoology 289: 285–293. https://doi.org/10.1111/jzo.12008

Olivares AI (2009) Anatomía, sistemática y evolución de los roedores caviomorfos sudamericanos del grupo *Eumysops ameghino* (Rodentia, Echimyidae). PhD thesis, Facultad de Ciencias Naturales y Museo Universidad Nacional de la Plata, La Plata, Buenos Aires.

Olivares AI, Verzi DH, Vassallo AI (2004) Masticatory morphological diversity and chewing modes in South American caviomorph rodents (family Octodontidae). Journal of Zoology 263: 167–177. https://doi.org/10.1017/S095283690400500X

Pérez MJ (2013) Descripción del postcráneo de *Tympanoctomys loschalchalerosorum* y una comparación intragenérica (Rodentia: Octodontidae). Unpublished undergraduate thesis, Facultad de Ciencias Naturales e Instituto Miguel Lillo, Universidad Nacional de Tucumán, Tucumán, Argentina.

Reig O (1989) Karyotypic repatterning as one triggering factor in cases of explosive speciation. In: Fontdevila A (Ed.) Evolutionary biology of transient unstable populations.Springer Verlag, Berlin, 246–289. https://doi.org/10.1007/978-3-642-74525-6_15

Salton JA, Sargis EJ (2008) Evolutionary Morphology of the Tenrecoidea (Mammalia) Forelimb Skeleton. In: Sargis EJ, Dagosto M (Eds) Mammalian Evolutionary Morphology. Vertebrate Paleobiology and Paleoanthropology. Springer, Netherlands, 51–71.

Samuels J, Van Valkenburgh B (2008) Skeletal Indicators of Locomotor Adaptations in Living and Extinct Rodents. Journal of Morphology 269: 1387–1411. https://doi.org/10.1002/jmor.10662

Samuels J, Van Valkenburgh B (2009) Craniodental Adaptations for Digging in Extinct Burrowing Beavers. Journal of Vertebrate Paleontology 29(1): 254–268. https://doi.org/10.1080/02724634.2009.10010376

Sargis EJ (2001) The grasping behaviour, locomotion and substrate use of the tree shrews *Tupaia minor* and *T. tana* (Mammalia, Scandentia). Journal of Zoology, London 253: 485–490. https://doi.org/10.1017/S0952836901000449

Sargis EJ (2002a) Functional morphology of the forelimb of tupaiids (Mammalia, Scandentia) and its phylogenetic implications. Journal of Morphology 253: 10–42. https://doi.org/10.1002/jmor.1110

Sargis EJ (2002b) Functional morphology of the hindlimb of tupaiids (Mammalia, Scandentia) and its phylogenetic implications. Journal of Morphology 254: 149–185. https://doi.org/10.1002/jmor.10025

Suárez-Villota EI, González-Wevar CA, Gallardo MH, Vásquez RA, Poulin E (2016) Filling phylogenetic gaps and the biogeographic relationships of the Octodontidae (Mammalia: Hystricognathi). Molecular Phylogenetics and Evolution 105: 96–101. https://doi.org/10.1016/j.ympev.2016.08.015

Selthofer R, Nikolié V, Mrčela T, Radié R, Lekšan I, Rudež I, Selthofer K (2006) Morphometric Analysis of the Sternum. Collegium Antropologicum 30(1): 43–47.

Teta P, Pardiñas UFJ, Udrizar Sauthier DE, Gallardo MH (2014) A new species of the tetraploid vizcacha rat *Tympanoctomys* (Caviomorpha, Octodontidae) from Central Patagonia, Argentina. Journal of Mammalogy 95: 60–71. https://doi.org/10.1644/13-MAMM-A-160

Upham NS, Patterson BD (2012) Diversification and biogeography of the Neotropical caviomorph lineage Octodontoidea (Rodentia: Hystricognathi). Molecular and Phylogenetics Evolution 63: 417–429. https://doi.org/10.1016/j.ympev.2012.01.020

Upham NS, Patterson BD (2015) Evolution of caviomorph rodents: a complete phylogeny and timetree. In: Vassallo AI, Antenucci D (Eds) Biology of caviomorph rodents: diversity and evolution. SAREM, series A, Buenos Aires, 63–120.

Vassallo AI, Verzi DH (2001) Patrones craneanos y modalidades de masticación en roedores caviomorfos. Boletín de la Sociedad de Biología de Concepción 72: 139–145.

Verzi DH (2002) Patrones de evolución morfológica en Ctenomyinae (Rodentia, Octodontidae). Mastozoología neotropical 9(2): 309–328.

Verzi DH, Díaz MM, Barquez RM (2015) Family Octodontidae. In: Patton JL, Pardiñas UFJ, D'Elía G (Eds) Mammals of South America. Volume 2, Rodents.University of Chicago Press, Chicago, 1023–1024.

Verzi DH, Olivares AI, Morgan CC, Álvarez A (2016) Contrasting phylogenetic and diversity patterns in octodontoid rodents and a new definition of the family Abrocomidae. Journal of Mammalian Evolution 23: 93–115. https://doi.org/10.1007/s10914-015-9301-1

Appendix

List of specimens analyzed detailing the number of individuals by species in brackets, collection localities, type specimens, and collection numbers are indicated. See materials and methods by collections acronyms.

Ctenomys opimus (4): Jujuy Province, Susques Department: Borde de Ecalón, 31 km al SO de Susques, por ruta 52 y 1 km SE de ruta, 1 (CML 9353). Salta Province, Los Andes Department: Vega Cortadera 1 km W de ruta 53, 3910 m, 2 (CML 7243, 7244); 36 km N San Antonio de Los Cobres, 11,600 ft., 1 (CML 8438).

Tympanoctomys aureus (22): Catamarca Province, Pomán Department: Salar de Pipanaco, 10 km de Pío Brizuela (Est. Río Blanco), km 96 sobre R46, 35 km S de Andalgalá, 3 (CMI 6565, 6818, 6888); en los bordes del Salar Pipanaco, 3 (CMI 6562, 6563, 6564); 5 km del puesto de Pío Brizuela, entrada km 96 sobre R46, 2 (CMI 7188, 7189); a 13 km de la entrada Establecimiento Río Blanco, 4 (CMI 6558, 6559, 6560, 6561); Establecimiento Río Blanco, 28 km S, 9.3 km W Andalgalá, 4 (CML 6137, holotype; 4136, 4137, paratypes; 10110); Pipanaco, Salar Pipanaco, 6 (CMI 6846, 6848, 6849, 6850, 6851, 6856).

Tympanoctomys barrerae (35): La Pampa Province, Limay Mahuida Department: Gran salitral, 6 (CMI 6877, 6878, 6879, 6880, 6882, 6883). Mendoza Province, La Paz Department: 27 km N Desaguadero, 556 m app, 2(CMI 4485, CML 3438), Desaguadero, El Tapón 37 km, 1 (CMI 3314); Lavalle Department: 34 km al N de Desagüadero camino a Arroyito, 1 (CML 10111); Malargüe Department, 6(CMI 7263, 7264, 7266, 7267, 7268, 7269), a 8.5 km camino a Llancanelo, 1(CMI 7098), Camino Llancanelo 7(CMI 7270, 7271, 7272, 7273, 7274, 7275, 7276), Laguna Llancanelo, 2(CMI 7248, 7250); San Rafael Department: 10 km S El Nihuil 2 (CMI 3845, 3846), El Nihuil, 2 (CMI 6290, 6291). San Juan Province, Valle Fértil Department: Parque Provincial Ischigualasto, 4 (CMI 6842, 6843, 6853, 6889). San Luis Province, 1 (CMI 3821).

Tympanoctomys loschalchalerosorum (1): La Rioja Province, Chamical Department: 26 km SW Quimilo, 1 (CML 3695, holotype).

Tympanoctomys kirchnerorum (2): Chubut Province, Sarmiento Department: Ea. La Porfía, 2 (CNP 2503, 2505).